EVALUATION AND CHARACTERIZATION OF NOVEL SIGNAL TRANSDUCTION PATHWAYS IN THE STRIATUM

APPROVED BY SUPERVISORY COMMITTEE

James A. Bibb, Ph.D.
Ege T. Kavalali, Ph.D.
Donald W. Hilgemann, Ph.D.
Donald C. Cooper, Ph.D.

DEDICATION

To my parents, who taught me how to dream and set me free.

ACKNOWLEDGMENTS

More than four years of work, culminating in the production of a doctoral dissertation, does not occur in a vacuum or by the single-handed efforts and sacrifices of the author alone. I would like to thank the members of my Graduate Committee for their support and advice during this challenging process. I would also like to express my deepest gratitude and appreciation to the Fathers of the Medical Scientist Training Program, particularly Drs. Michael Brown and Rodney Ulane, for their unwavering faith in my potential and their seemingly limitless capacity for kindness and empathy.

Needless to say, I owe a tremendous debt of gratitude to my mentor, Dr. James Bibb, for relentlessly pushing me forward, nurturing my growth as a scientist, encouraging free debate between mentor and student, and fostering independent thought. But even beyond these very good reasons, James deserves a lot of credit for all the intangibles that sustained me through this long journey at every turn, even when all seemed lost. Not a day goes by that a scientist is not tested by failure—it is in the blueprint of the scientific quest. James taught me that success is more than the sum of your achievements; it is also a product of how you confront and grow from your daily failures, however crushing or insurmountable they may first appear. These are invaluable life lessons I take with me beyond the lab, into my intended career as a physician scientist and my personal life as a citizen and future husband and father. David Benavides, Chan Nguyen, Ammar Hawasli, Kanehiro Hayashi, and Janice Kansy are other members of the lab who deserve special mention for their friendship and their contributions to my work and my training.

I am also indebted to a few wonderful friends outside the lab, chief among them my best friend and soul mate, Brooke Belyea, whom I met at UT Southwestern. I can't imagine how any of this would have been possible in the absence of Brooke's constant encouragement and boundless patience, her love, her kindness, her humanity.

Finally, I thank my parents for giving me life and the liberty to pursue my happiness, regardless of how far from home that pursuit may take me. I am constantly humbled and overwhelmed by the love and courage it must take to allow one's only

child, at all of eighteen years of age, to move thousands of miles away, across an ocean and two continents, for no better reason than a vague, indefinable idea—his happiness. I can never repay this debt to my parents, only strive to make the best of everything I was given so generously and unconditionally.

My father used to say that earning a Ph.D. is like entering a windowless room in a house full of many such rooms; studying and understanding that particular room down to its smallest detail, from the logic of its furnishings to the proportions of its walls; and once this is done, breaking open a passage out into the next dark and windowless room. I hope that on some level this work represents the opening of such a passage, be it small or large.

EVALUATION AND CHARACTERIZATION OF NOVEL SIGNAL TRANSDUCTION PATHWAYS IN THE STRIATUM

by

BOGACHAN SAHIN

DISSERTATION

Presented to the Faculty of the Graduate School of Biomedical Sciences

The University of Texas Southwestern Medical Center at Dallas

In Partial Fulfillment of the Requirements

For the Degree of

DOCTOR OF PHILOSOPHY

The University of Texas Southwestern Medical Center at Dallas

Dallas, Texas

May, 2008

EVALUATION AND CHARACTERIZATION OF NOVEL SIGNAL TRANSDUCTION PATHWAYS IN THE STRIATUM

Bogachan Sahin, Ph.D.

The University of Texas Southwestern Medical Center at Dallas, 2008

Supervising Professor: James A. Bibb, Ph.D.

In the mammalian central nervous system, protein kinases and protein phosphatases control the function of myriad target proteins in the pre- and postsynaptic compartments, including other protein kinases and phosphatases, neurotransmitter receptors, ion channels, transporters, metabolic enzymes, transcription factors, cytoskeletal elements, and vesicle-docking proteins. Using biochemical and pharmacological approaches, a number of novel striatal signal transduction pathways were evaluated and characterized in the following studies, with emphasis on protein kinase C-mediated signaling. *1*) A known and novel form of mouse *Adk* encoding splice variants of adenosine kinase, the principal enzyme of adenosine metabolism, were cloned from a mouse brain cDNA library and expressed and purified as recombinant proteins with high enzymatic activity. The tissue distribution of adenosine kinase isoform expression was defined. A polyclonal anti-

adenosine kinase antibody was generated for further characterization of the enzyme. *In vitro* protein phosphorylation studies using purified protein kinases and *in vivo* radioimmunoprecipitation assays using the novel antibody for adenosine kinase indicated, however, that this metabolic enzyme is unlikely to be regulated by phosphorylation. *2*) Further studies using a candidate approach demonstrated the regulation of several postsynaptic phosphoproteins by striatal adenosine A_{2A} receptor signaling, including ionotropic glutamate receptor subunits, mitogen-activated protein kinase isoforms, a striatal inhibitor of protein phosphatase 1, a protein phosphatase 1- and actin-binding protein, and the cAMP-response element-binding protein. *3*) In parallel studies, inhibitor-1, a protein phosphatase 1 inhibitor activated by cAMP-dependent protein kinase, was characterized as a novel protein kinase C substrate *in vitro* and *in vivo*. Phosphorylation state-specific antibodies raised against this novel phosphorylation site showed that it is dephosphorylated by protein phosphatase 1 and positively regulated by group I metabotropic glutamate receptors in the striatum. Furthermore, protein kinase C-dependent phosphorylation was shown to reduce the efficiency with which inhibitor-1 serves as a substrate for cAMP-dependent protein kinase *in vitro* and *in vivo*. *4*) Finally, protein kinase C activation was shown to decrease the level of phosphorylation of cyclin-dependent kinase 5 substrates in the striatum, suggesting a possible role for protein kinase C in regulating cyclin-dependent kinase 5 activity.

TABLE OF CONTENTS

PRIOR PUBLICATIONS

1. Sahin, B., and J. A. Bibb. (2004) Protein kinases talk to lipid phosphatases at the synapse. Proc Natl Acad Sci U S A *101(5):1112-3*.
2. Braz, J. C., K. Gregory, A. Pathak, W. Zhao, B. Sahin, R. Klevitsky, T.F. Kimball, J. N. Lorenz, A. C. Nairn, S. B. Liggett, I. Bodi, S. Wang, A. Schwartz, E. G. Lakatta, A. A. DePaoli-Roach, J. Robbins, T. E. Hewett, J. A. Bibb, M. V. Westfall, E. G. Kranias, J. D. Molkentin. (2004) PKC-alpha regulates cardiac contractility and propensity toward heart failure. Nat Med *10(3):248-54.*
3. Sahin B, J. W. Kansy, A. C. Nairn, J. Spychala, S. E. Ealick, A. A. Fienberg, R. W. Greene, J. A. Bibb. (2004) Molecular characterization of recombinant mouse adenosine kinase and evaluation as a target for protein phosphorylation. Eur J Biochem *271(17):3547-55.*
4. Lee, W. M., J. E. Polson, D. S. Carney, B. Sahin, M. Gale, Jr. (2005) Reemergence of hepatitis C virus after 8.5 years in a patient with hypogammaglobulinemia: evidence for an occult viral reservoir. J Infect Dis *192(6):1088-92.*
5. Sahin, B., H. Shu, J. Fernandez, A. El-Armouche, J. D. Molkentin, A. C. Nairn, J.A. Bibb. (2006) Phosphorylation of protein phosphatase inhibitor-1 by protein kinase C. J Biol Chem *281(34):24322-35.*
6. Sahin, B., S. Galdi, J. Hendrick, R. W. Greene, G. L. Snyder, J. A. Bibb. (2007) Evaluation of neuronal phosphoproteins as effectors of caffeine and mediators of striatal adenosine A_{2A} receptor signaling. Brain Res *1129(1): 1-14.*

LIST OF FIGURES

LIST OF ABBREVIATIONS

Ad PKC-α	adenovirus encoding protein kinase C-α
Ad I-1	adenovirus encoding protein phosphatase inhibitor-1
ADP	adenosine 5'-diphosphate
AK	adenosine kinase
AMP	adenosine 5'-monophosphate
AMPA	α-amino-3-hydroxy-5-methyl-4-isoxazole propionic acid
ATP	adenosine 5'-triphosphate
BSA	bovine serum albumin
CalyA	calyculin A
cAMP	3',5'-cyclic adenosine monophosphate (cyclic AMP)
CBB	Coomassie Brilliant Blue
Cdk1	cyclin-dependent kinase 1
Cdk5	cyclin-dependent kinase 5
cGMP	3',5'-cyclic guanosine monophosphate (cyclic GMP)
CK	casein kinase
CREB	cyclic AMP-response element-binding protein
CycA	cyclosporin A
D32	dopamine- and cyclic AMP-regulated phosphoprotein, M_r 32,000
DARPP-32	dopamine- and cyclic AMP-regulated phosphoprotein, M_r 32,000
DHPG	(*S*)-3,5-dihydroxyphenylglycine
DMEM	Dulbecco's modified Eagle's medium
DTT	dithiothreitol
EGTA	ethylene glycol-bis(2-aminoethyl ether)-N,N,N',N'-tetraacetic acid
ERK	extracellular signal-regulated kinase
FBS	fetal bovine serum
FSK	forskolin
FST	fostriecin
GBPI	gut and brain phosphatase inhibitor

GluR1	glutamate receptor 1
GMP	guanosine 5’-monophosphate
hAK	human adenosine kinase
HEPES	N-(2-hydroxyethyl)piperazine-N'-(2-ethanesulfonic acid)
HPLC	high-performance liquid chromatography
I-1	(protein phosphatase) inhibitor-1
IPTG	isopropyl-β-D-thiogalactopyranoside
mAK	mouse adenosine kinase
MALDI-TOF	matrix-assisted laser desorption ionization time-of-flight
MAPK	mitogen-activated protein kinase
MOPS	3-(N-morpholino)propanesulfonic acid
MS	mass spectrometry
MS/MS	tandem mass spectrometry
NMDA	N-methyl-D-aspartate
OKA	okadaic acid
PAGE	polyacrylamide gel electrophoresis
PBS	phosphate-buffered saline
PDBu	phorbol-12,13-dibutyrate
PKA	cyclic AMP-dependent protein kinase
PKC	Ca^{2+}/phospholipid-dependent protein kinase, protein kinase C
PKG	cyclic GMP-dependent protein kinase
PP	protein phosphatase
PTH	phenylthiohydantoin
QqTOF	QSTAR Pulsar I quadrupole time-of-flight
Ro	Ro-32-0432
SAP	shrimp alkaline phosphatase
SDS	sodium dodecyl sulfate
SEM	standard error of the mean
TBS	Tris-buffered saline
TH	tyrosine hydroxylase

CHAPTER 1

A BRIEF OVERVIEW

Intracellular signal transduction refers to the process by which cells perceive physical or chemical stimuli in their environment and mount an appropriate response, such as growth, senescence, migration, differentiation, vesicle release, process elaboration, cell division, or cell death. The cell's ability to integrate and respond to a plethora of environmental information is one of the foundations of multicellularity and reaches an especially impressive level of sophistication in the mammalian central nervous system. Although the vast complexity of neuronal signal transduction pathways may seem daunting, some unifying principles have emerged over the last few decades with regard to the molecular mechanisms underlying the transduction of extracellular signals into intracellular signaling cascades that mediate the cellular response to the original stimulus.

Broadly, all neuronal signal transduction incorporates the following initial elements: *1*) an extracellular stimulus, such as a photon, odorant molecule, neurotransmitter, neuromodulator, neurotrophic factor, cytokine, or steroid hormone; *2*) a cell-surface or intracellular receptor that can be activated by the stimulus with specificity and mobilize downstream effectors; and *3*) an intracellular protein machinery that responds to receptor activation by transducing the extracellular first messenger into an intracellular second messenger (1). Second messengers include cyclic nucleotides, calcium ion, phospholipids, phosphoproteins, and ligand-activated transcription factors, which initiate cascades of biochemical reactions culminating in the execution of the cellular response. This response can be proximal, as in the reversible phosphorylation of an ion channel, receptor, or transporter at the cell surface, or extend to the cell nucleus and result in the differential transcription of target genes.

More than fifty years have passed since the seminal discovery by Krebs and Fischer that the activity of the vital metabolic enzyme, glycogen phosphorylase, is regulated by phosphorylation (2-5). Today, the post-translational regulation of protein function through the reversible phosphorylation of serine, threonine, and tyrosine residues by protein kinases and protein phosphatases represents the most widespread, versatile, and well-studied intracellular signaling mechanism in eukaryotes (6, 7). It is estimated that 2-3% of eukaryotic genes encode protein kinases or protein phosphatases, so perhaps it is not surprising that phosphoproteins account for nearly a third of all proteins in eukaryotic cells (8). The human genome encodes approximately 500 protein kinases, more than two thirds of which catalyze phosphoryl transfer to substrate serine or threonine moieties (9). The signaling cascades associated with a number of protein serine/threonine kinases have garnered considerable attention in the central nervous system. Prominent among these are the protein kinases of the mitogen-activated protein kinase (MAPK) pathway and the second messenger-activated protein kinases, cyclic AMP (cAMP)-dependent protein kinase (PKA), Ca^{2+}/calmodulin-dependent protein kinase II (CaMKII), and Ca^{2+}/phospholipid-dependent protein kinase (protein kinase C, or PKC) (10-17).

In the following studies, several novel signal transduction pathways were evaluated and characterized in the mammalian central nervous system, with a special emphasis on PKC-mediated signaling in the striatum.

CHAPTER 2[†]

MOLECULAR CHARACTERIZATION OF MOUSE ADENOSINE KINASE[‡] AND EVALUATION AS A TARGET FOR PROTEIN PHOSPHORYLATION

2.1. Summary

The regulation of adenosine kinase activity has the potential to control intracellular and interstitial adenosine concentrations. In an effort to study the role of adenosine kinase in adenosine homeostasis in the central nervous system, two isoforms of the enzyme were cloned from a mouse brain cDNA library. Following overexpression in bacterial cells, the corresponding proteins were purified to homogeneity. Both isoforms were enzymatically active and found to possess K_m and V_{max} values in agreement with kinetic parameters described for other forms of adenosine kinase. The distribution of adenosine kinase in discrete brain regions and peripheral tissues was defined. To investigate the possibility that adenosine kinase activity is regulated by protein phosphorylation, a panel of protein serine/threonine kinases was screened for ability to phosphorylate recombinant mouse adenosine kinase *in vitro*. Data from these protein phosphorylation studies suggest that adenosine kinase is most likely not an efficient substrate for cyclic AMP-dependent protein kinase, cyclic GMP-dependent protein kinase, Ca^{2+}/calmodulin-dependent protein kinase II, mitogen-activated protein kinase, casein kinase 1, casein kinase 2, cyclin-dependent kinase 1, or cyclin-dependent kinase 5. Protein kinase C was found to phosphorylate recombinant adenosine kinase efficiently *in vitro*. Further analysis

† Part of this Chapter was published in *The European Journal of Biochemistry*.

‡ Nucleotide sequence data for the long and short isoforms of mouse adenosine kinase are available in the DDBJ/EMBL/GenBank databases under the accession numbers AY540996 and AY540997, respectively.

revealed, however, that phosphorylation by protein kinase C occurred at one or more serine residues in the N-terminal affinity tag used for protein purification. A polyclonal antibody for mouse adenosine kinase was generated to determine whether adenosine kinase occurs as a phosphoprotein *in vivo*. The efficacy and specificity of the antibody were confirmed in immunoblotting, immunofluorescence staining, and immunoprecipitation applications. However, radioimmunoprecipitation assays conducted with this novel antibody failed to detect phospho-adenosine kinase in mouse striatal tissue. These results strongly suggest that adenosine kinase is unlikely to be regulated by phosphorylation in the brain.

2.2. Introduction

Adenosine is a potent biological mediator and a key participant in cellular energy metabolism. In the central nervous system, it mediates well-established neuroprotective, antiepileptic, antinociceptive, locomotor, and somnogenic effects (18-23). In addition to its autonomous actions, this ubiquitous purine nucleoside also represents an important building block for nucleic acids and a wide range of biochemical effectors, including the universal energy currency, ATP; the intracellular second messenger, cAMP; the major metabolic coenzymes, NAD^+, FAD, and acetyl coenzyme A; and the cellular carrier of reducing power, NADPH. Thus, the proper regulation of intracellular and extracellular adenosine levels has broad implications for fundamental aspects of cell biology.

In the central nervous system, extracellular adenosine behaves primarily as a tonic inhibitory neuromodulator that controls neuronal excitability through its interaction with four known subtypes of G protein-coupled receptors, A_1, A_{2A}, A_{2B}, and A_3 (24-26). Adenosine A_1 receptor signaling in the cholinergic arousal centers of the basal forebrain and brainstem reduces global cholinergic tone, facilitating the transition from waking to sleep (27). Adenosine A_{2A} receptors in the striatum are involved in the modulation of locomotor activity and vigilance (28). Caffeine, the most widely used psychomotor stimulant substance in the world, is a well-known antagonist of both adenosine A_1 and A_{2A} receptor subtypes (29). Compared to adenosine A_1 and A_{2A} receptors, the A_{2B} and

A_3-type adenosine receptors have considerably lower ligand affinity (≥ 10 μM) (30-33), suggesting that they function primarily under conditions in which extracellular adenosine levels are elevated beyond the physiological ceiling.

Most adenosine in the central nervous system is generated through the extracellular breakdown of interstitial adenine nucleotides (*i.e.* AMP, cAMP, ADP, and ATP) by 5'-ectonucleotidases (34). Adenosine concentrations increase in this compartment as a result of physiological and pathological influences that raise metabolic demand over metabolic supply, such as fatigue, sleep deprivation, seizure activity, hypoxia, hypoglycemia, and ischemia (35-37). This suggests that adenosine may partly be responsible for relieving metabolic strain on nervous tissue by reducing neuronal activity. Facilitated diffusion of adenosine across the cell membrane via equilibrative nucleoside transporters closely couples baseline adenosine concentrations in the intracellular and extracellular spaces (38). Intracellular adenosine is rapidly directed to a number of metabolic pathways (39), maintaining a net flow of adenosine into the cell under physiological conditions.

Adenosine kinase (AK), a key enzyme of the purine salvage pathway and the most abundant nucleoside kinase in mammals (40, 41), catalyzes the transfer of the γ-phosphate of ATP to the 5'-hydroxyl of the ribose moiety of adenosine, generating ADP and AMP (42-44). Although AK is one of several enzymes responsible for maintaining steady-state adenosine levels in the brain and elsewhere, substantial biochemical and pharmacological evidence indicates that the reaction it catalyzes represents the primary physiological route of adenosine metabolism (45-50). Mice lacking AK ($Adk^{-/-}$ mice) undergo normal embryogenesis, but develop microvesicular hepatic steatosis within four days of birth and die by the end of two weeks with fatty liver (51), underscoring the importance of AK activity in primary and secondary metabolism. The structure of AK has been determined to a resolution of 1.5 Å and consists of one large and one small α/β domain, the latter containing two adenosine binding sites (46). AK has a low K_m with respect to adenosine (40-60 nM) (45), which falls within the physiological range of extracellular adenosine levels (25-250 nM) (52). Consistent with this observation, AK inhibitors are effective pharmacological reagents for increasing interstitial levels of

adenosine (47-50) and have shown some promise in animal models of stroke (53), seizure (54), and pain and inflammation (55). Therefore, AK continues to be the subject of intensive study for the development of neuroprotective and analgesic agents, as well as drugs to treat sleep disorders and enhance vigilance.

Biochemical pathways regulating AK have the potential to modulate extracellular adenosine levels and adenosine receptor signaling. Although the evidence points to a critical role for AK in adenosine homeostasis, the question of whether AK activity itself is regulated remains largely unanswered. Insulin has been shown to induce AK expression in rat lymphocytes (56). Studies in the brain have suggested that AK activity exhibits diurnal variations (57, 58). Animal models of kainic acid-induced epilepsy have been used to demonstrate that seizure susceptibility and severity are increased by postictal astrogliosis, an effect that is mediated by the profound up-regulation of AK expression in the brain as a result of the proliferation of AK-rich glial cells (59, 60). Thus, several lines of evidence from a number of model systems indicate that AK levels are susceptible to regulation, producing physiological or pathological effects expected from equivalent and opposite changes in the levels of extracellular adenosine. In cases that do not involve an increase or decrease in the numbers of AK-expressing cells, the regulation of AK levels likely occurs through the transcriptional and/or translational control of AK expression. However, it remains unclear whether post-translational mechanisms also exist for the regulation of AK activity. A better understanding of AK regulation, with regard to gene expression as well as protein structure and function, may reveal specific signaling pathways that control this enzyme and provide new targets for drug design.

A number of factors could regulate AK at the post-translational level, including protein stability, subcellular localization, regulatory binding partners, and post-translational modifications such as protein phosphorylation. In the following studies, protein phoshorylation was evaluated as a putative mechanism of AK regulation. As discussed in Chapter 1, the reversible phosphorylation of proteins on serine, threonine, and tyrosine residues is the single most common mode of intracellular signal transduction in eukaryotes. To assess the notion that AK is subject to regulation by phosphorylation,

recombinant mouse AK was evaluated as a substrate for a panel of selected protein serine/threonine kinases. The protein kinases tested did not phosphorylate recombinant AK to any significant extent *in vitro*. Moreover, immunoprecipitation of AK from intact mouse brain tissue metabolically labeled with [^{32}P] orthophosphate failed to detect phosphate incorporation by AK *in vivo*. These findings indicate that AK is most likely not regulated by protein kinase-mediated signaling pathways.

2.3. Experimental Procedures

2.3.1. Chemicals and enzymes

All chemicals were from Sigma, except where indicated. Deoxyoligonucleotides were obtained from Integrated DNA Technologies. Protease inhibitors, dithiothreitol (DTT), isopropyl-β-D-thiogalactopyranoside (IPTG), and ATP were from Roche. [γ-^{32}P] ATP was from PerkinElmer Life Sciences. [^{32}P] Orthophosphate and [2,8-^{3}H] adenosine were from Amersham Biosciences. Cyclosporin A was from LC Laboratories. Okadaic acid was from Alexis. Competent bacteria were from Life Technologies. Restriction and DNA-modifying enzymes were from New England Biolabs. The catalytic subunit of cyclic AMP (cAMP)-dependent protein kinase (PKA) purified from bovine heart (61) and protein kinase C (PKC) (a mixture of α, β, and γ isoforms) purified from rat brain (62) were kindly provided by Angus Nairn (Yale University). Cyclic GMP (cGMP), cGMP-dependent protein kinase (PKG), and trypsin were purchased from Promega; MAPK (a mixture of p44 and p42 isoforms), Ca^{2+}/calmodulin-dependent protein kinase II (CaMKII), and calmodulin from Upstate; and casein kinases 1 and 2 (CK1 and CK2) and cyclin-dependent kinase (Cdk1) from New England Biolabs. Cyclin-dependent kinase 5 (Cdk5) and p25-His_6 were affinity-purified by Kanehiro Hayashi (UT Southwestern Medical Center) following co-expression in insect Sf9 cultures using baculovirus vectors (63). Biotinylated thrombin and streptavidin agarose were from Novagen.

2.3.2. Molecular cloning and site-directed mutagenesis

Long and short forms of mouse *Adk* cDNA were amplified by the polymerase chain reaction (PCR) from a mouse brain cDNA library provided by Lisa Monteggia (UT Southwestern Medical Center). Primers were 5'-GGTGCATATGGCAGCTGCGG for the 5' end and 5'-TCCACTCCACAGCCTGAGTT for the 3' end. PCR products were TA-cloned into the bacterial vector pCR II-TOPO (Invitrogen) and sequenced at the DNA Sequencing Core Facility at UT Southwestern Medical Center by automated fluorescent DNA sequencing using primers specific for the T7 and Sp6 promoters. For protein expression, a 5' primer incorporating an *Nde* I restriction site and a 3' primer incorporating a *Bam*H I restriction site were used to subclone mouse *Adk* cDNA into a hybrid bacterial expression vector, pET-16b/28a, generated by Janice Kansy (UT Southwestern Medical Center) by replacing the multiple cloning region of pET-16b with that of pET-28a (Novagen). Primers were 5'-CGTGGGGTGCATATGGCAGCTGCG for the 5' end of long mouse *Adk* cDNA, 5'-GTAGGTGCACATATGACGTCCACC for the 5' end of short mouse *Adk* cDNA, and 5'-ATATAGGATCCTCAGTGGAAGTCTGG for the 3' ends of both cDNA forms. Consensus PKC phosphorylation sites were selected for site-directed mutagenesis using a web-based program for motif prediction (http://scansite.mit.edu). Site-directed mutants were generated at these and other sites using the QuikChange kit (Stratagene) and following the manufacturer's recommendations for mutagenic primer design. Mutations were confirmed by DNA sequencing along both strands, using primers specific for the T7 promoter and T7 terminator.

2.3.3. Generation of recombinant mouse AK protein

Electrocompetent BL21 (DE3) cells were transformed with hybrid pET-16b/28a expression vectors incorporating the long or short form of wild-type or mutant mouse *Adk* cDNA downstream from a vector-encoded hexahistidine affinity tag and thrombin cleavage site. Cultures were grown to log phase and induced with 0.1 mg/ml IPTG at

room temperature for 20 h. Cells were collected by centrifugation at 1,800 × *g* for 30 min and washed in cold Tris-buffered saline (TBS) containing 25 mM Tris-HCl, pH 8.0, and 140 mM NaCl. Following centrifugation at 10,000 × *g* for 15 min, cell pellets were lysed by 3 × French press in a buffer containing 50 mM sodium phosphate, pH 8.0, 300 mM NaCl, and protease inhibitors. Samples were centrifuged at 10,000 × *g* for 30 min and cleared lysates were incubated with a nickel-nitrilotriacetic acid-agarose resin (Qiagen) for 90 min at 4°C. Agarose pellets were collected by centrifugation at 300 × *g* for 5 min and washed 5 × 10 min in a buffer containing 50 mM sodium phosphate, pH 8.0, 300 mM NaCl, 10% glycerol, and protease inhibitors. Bound protein was eluted using a linear gradient of 0 to 500 mM imidazole in the same buffer. The long and short forms of mouse AK (mAK1 and mAK2, respectively) and all site-directed mutants eluted at approximately 150 mM imidazole. Samples were dialyzed overnight in 10 mM Tris-HCl, pH 7.5, and 1 mM DTT, with two changes of buffer. 10 μg of dialyzed protein were analyzed for purity by sodium dodecyl sulfate-polyacrylamide gel electrophoresis (SDS-PAGE) (15% polyacrylamide) and Coomassie Brilliant Blue (CBB) staining. In one set of experiments, the N-terminal hexahistidine affinity tag was removed using biotinylated thrombin according to the manufacturer's recommendations.

2.3.4. AK activity assays

Kinetic analysis of AK activity was performed under empirically defined linear steady-state conditions. Reactions were conducted at 37°C in a final volume of 20 μl. Reaction mixtures contained 50 mM Tris-HCl, pH 7.5, 100 mM KCl, 5 mM $MgCl_2$, 5 mM β-glycerol phosphate, 3 mM ATP, dilutions of [2,8-^{3}H] adenosine with a specific activity of 20-50 Ci/mmol, and recombinant mAK1 or mAK2. Reactions were stopped by incubation at 95°C and spotted on grade DE81 diethylaminoethyl-cellulose discs (Whatman). The discs were washed in 5 mM ammonium formate to remove unphosphorylated adenosine and subjected to liquid scintillation counting.

2.3.5. Immunoblot analysis

Mouse brain and peripheral tissues were rapidly dissected, homogenized by sonication in boiling 1% SDS, and boiled for 5 min. Protein concentrations were determined by the bicinchoninic acid (BCA) protein assay (Pierce) using bovine serum albumin (BSA) as standard. 25 μg of total protein from each sample were subjected to SDS-PAGE (15% polyacrylamide) followed by electrophoretic transfer to nitrocellulose membranes (0.2 μm) (Whatman). The membranes were blocked for 1 h at room temperature in TBS containing 0.1% Tween 20 (TBS-Tween) and 5% dry milk, and blotted with a mouse ascites fluid monoclonal antibody for human AK (1:2000) provided by Jozef Spychala (University of North Carolina at Chapel Hill) (64). In some experiments, a novel polyclonal antibody for mouse AK (1:1000) (see Results) was used to detect immunoprecipitated mouse AK or 100 μg of mouse brain protein. Following incubation with the primary antibody for 1 hr at room temperature, membranes were washed 5 × 10 min in TBS-Tween and incubated for 1 h at room temperature with a horseradish peroxidase-conjugated goat anti-rabbit or goat anti-mouse secondary antibody (1:8000) (Chemicon). All antibodies were diluted in TBS-Tween containing 5% dry milk. Primary antibody dilutions also contained 0.02% NaN_3. Antibody binding was detected by autoradiography using the enhanced chemiluminescence immunoblotting detection system (Amersham Biosciences). Where indicated, results were quantified by densitometry using NIH Image software.

2.3.6. In vitro *protein phosphorylation reactions*

All reactions were conducted at 30°C in a final volume of at least 30 μl containing 10 μM substrate, 100 μM ATP, and 0.2 mCi/ml [γ-^{32}P] ATP, unless otherwise specified. The PKC reaction solution included 20 mM MOPS, pH 7.2, 25 mM β-glycerol phosphate, 1 mM DTT, 1 mM $CaCl_2$, 10 mM $MgCl_2$, 0.1 mg/ml phosphotidylserine, and 0.01 mg/ml diacylglycerol, with the final two components added to the reaction mixture following sonication on ice for 1 min. PKA reactions were conducted in 50 mM HEPES,

pH 7.4, 1 mM EGTA, 10 mM magnesium acetate, and 0.2 mg/ml BSA; PKG reactions in 40 mM Tris-HCl, pH 7.4, 20 mM magnesium acetate, and 3 μM cGMP; MAPK reactions in 50 mM Tris-HCl, pH 7.4, 10 mM $MgCl_2$, and 20 mM EGTA; and Cdk5 reactions in 30 mM MOPS, pH 7.2, and 5 mM $MgCl_2$. For CaMKII, CK1, CK2, and Cdk1, reaction buffers provided by the suppliers were used. As positive controls, reactions were conducted using proteins previously defined as physiological substrates for each protein kinase. Specifically, recombinant protein phosphatase inhibitor-1 (inhibitor-1, or I-1) was used in the PKA, MAPK, Cdk1, and Cdk5 reactions (65, 66); histone H1 (Upstate) in the PKG reaction (67); myelin basic protein (Upstate) in the PKC reaction (68); recombinant tyrosine hydroxylase, courtesy of Paul Fitzpatrick and Colette Daubner (Texas A&M University), in the CaMKII reaction (69); and recombinant dopamine- and cAMP-regulated phosphoprotein, M_r 32,000 (DARPP-32, or D32) in the CK1 and CK2 reactions (70, 71). Recombinant inhibitor-1 and DARPP-32 were generated as previously described (66, 72).

Time-course reactions were performed by removing aliquots of 10 μl from the reaction solution at various time points and adding an equal volume of SDS protein sample buffer to stop the reaction. Kinetic parameters were determined using the results of 4 experiments conducted in duplicate with 1.5 to 20 μM substrate under empirically defined linear steady-state conditions. In all cases, ^{32}P-phosphate incorporation was assessed by SDS-PAGE (15% polyacrylamide) and PhosphorImager analysis. To calculate reaction stoichiometries, radiolabeled reaction products and radioactive standards were quantified by densitometry using ImageQuant software (Amersham Biosciences). Standards consisted of aliquots of 5 μl spotted onto a piece of filter paper from serial dilutions of each reaction mixture (1:100, 1:500, 1:1000), with the moles of phosphate in 5 μl of each dilution defined using the ATP concentration of the original reaction. Division of the signal intensity per mole of substrate (mol^{-1} substrate) by the signal intensity per mole of phosphate (mol^{-1} phosphate) yielded the reaction stoichiometry (mol phosphate/mol substrate).

2.3.7. Two-dimensional phosphopeptide mapping and phosphoamino acid analysis

Dry gel fragments containing ^{32}P-labeled recombinant mouse AK were re-hydrated, washed, and incubated at 37°C for 20 h in 50 mM NH_4HCO_3, pH 8.0, containing 75 ng/ml trypsin. Supernatants containing the tryptic digestion products were lyophilized and the pellets washed up to 4 times with water and once with electrophoresis buffer, pH 3.5 (10% acetic acid, 1% pyridine). For each sample, the pellet resulting from the final round of lyophilization was resuspended in electrophoresis buffer, pH 3.5, and 1/10 of the total volume was set aside for phosphoamino acid analysis. The remainder of the sample was spotted on a microcrystalline cellulose thin-layer chromatography (TLC) plate (Analtech) for one-dimensional electrophoresis. Separation in the second dimension was achieved by ascending chromatography in high-pyridine TLC buffer (37.5% pyridine, 25% butanol, 7.5% acetic acid). Resulting phosphopeptide maps were visualized by autoradiography. Although other phosphoproteins similarly analyzed by phosphopeptide mapping produced discrete spots, ^{32}P-labeled recombinant AK samples consistently showed smearing in the first dimension. After testing a number of different TLC plates, buffer compositions, and electrophoresis conditions, this issue was resolved by the use of polyethyleneimine-cellulose TLC plates (Bodman).

For phosphoamino acid analysis, the aliquots set aside in the previous step were hydrolyzed at 100°C for 1 hr in 6 M HCl under a N_2 atmosphere. The reactions were stopped by a 6-fold dilution in water. Diluted mixtures were lyophilized and pellets were resuspended in electrophoresis buffer, pH 1.9 (8% acetic acid, 2% formic acid) and spotted on microcrystalline cellulose TLC plates along with phospho-serine, phospho-threonine, and phospho-tyrosine standards. Samples were subjected to one-dimensional electrophoretic separation halfway along the plate in electrophoresis buffer, pH 1.9, at which point the plate was transferred to electrophoresis buffer, pH 3.5, and separation was carried to completion in the same dimension. A 1% ninhydrin solution in acetone was sprayed onto the plates to visualize the phosphoamino acid standards. Radiolabeled samples were visualized by autoradiography.

2.3.8. Generation and purification of polyclonal antibodies

Following the isolation of 10-15 ml of pre-immune serum, each of three New Zealand white rabbits was immunized by subcutaneous injection of 1 ml of a 1:1 emulsified mixture of Freund's complete adjuvant and 1 mg of recombinant AK (equal parts mAK1 and mAK2) diluted in 10 mM phosphate-buffered saline, pH 7.4 (PBS). Each animal received a booster injection 2 weeks after immunization, followed by additional booster injections at 4-week intervals. Booster injections were identical in volume and composition to the initial injection, except Freund's complete adjuvant was replaced with Freund's incomplete adjuvant. A test bleed (10-15 ml) was obtained from each animal 2 weeks after the first booster. A larger production bleed (20-30 ml) was obtained 2 weeks after each subsequent booster. Animals were given a total of 10 booster injections before being euthanized. All injections and blood collection were performed by Monya Powell (Animal Resources Center, UT Southwestern Medical Center).

Collected blood was incubated at 37°C for 1 h and placed at 4°C overnight. Serum was isolated from clotted blood by centrifugation at 200 × *g* for 10 min. Immunoblot analysis was performed to evaluate all antisera (1:200) for the ability to detect recombinant mAK1 (50 ng) and endogenous AK in mouse brain lysates (100 μg of total protein). Polyclonal antibodies for mouse AK were purified from high-titer antisera by affinity-column chromatography using an AminoLink resin (Pierce) conjugated to recombinant mouse AK. Peak elution fractions were dialyzed in 10 mM MOPS, pH 7.5, and 154 mM NaCl, and used at a dilution of 1:1000 for immunoblot analysis, or 1:500 for immunohistochemistry.

2.3.9. Immunohistochemistry

To localize regions of AK expression, mouse brain sections were immunohistochemically stained using the novel polyclonal antibody for mouse AK. Briefly, male C57BL/6 mice (8-10 weeks old) were deeply anesthetized with 80 mg

chloral hydrate and perfused transcardially with 200 ml of cold 0.9% NaCl, followed by 500 ml of cold 4% paraformaldehyde in PBS. The brains were rapidly removed, post-fixed with 4% paraformaldehyde in PBS at 4°C overnight, and cryoprotected by treatment with 30% sucrose in PBS for several days at 4°C. Serial sagittal sections of 45 μm thickness were cut using a Leica CM3050 S cryostat, collected in PBS, and stored at 4°C until further analysis. Sections were processed for immunohistochemistry as follows. Following transfer into 40 mM sodium phosphate buffer, pH 7.4, sections were mounted on glass microscope slides, dried for 2 h at room temperature, washed in PBS several times, and blocked in 3% normal donkey serum in PBS containing 0.3% Triton X-100 for 2 h at 4°C. Blocked sections were incubated overnight at 4°C with the polyclonal antibody for mouse AK diluted 1:500 in blocking solution containing 0.1% NaN_3. The next day, sections were washed in PBS several times and incubated for 2 h at room temperature with Cy2-conjugated donkey anti-rabbit immunoglobulin G (Jackson ImmunoResearch Laboratories) diluted 1:200 in PBS. Following incubation with the secondary antibody, sections were washed in PBS several times, dehydrated through a graded series of ethanol solutions, and cover-slipped for visualization using an Olympus BX51 epifluorescence microscope. To verify the specificity of the immunoreactivity, the primary antibody step was omitted in the staining procedure for a subset of alternate sections.

2.3.10. Preparation and incubation of acute striatal slices

Male C57BL/6 mice (8-10 weeks old) were killed by decapitation. The brains were rapidly removed and placed in cold oxygenated Krebs buffer (124 mM NaCl, 4 mM KCl, 26 mM $NaHCO_3$, 1.5 mM $CaCl_2$, 1.25 mM KH_2PO_4, 1.5 mM $MgSO_4$, and 10 mM D-glucose, pH 7.4) within 45 s of euthanasia. Serial coronal sections of 350 μm thickness were prepared using a vibrating blade microtome. Striatal slices were dissected from these sections in cold oxygenated Krebs buffer using a Leica S4E dissecting light microscope. Each slice was transferred to a polypropylene incubation tube containing 2 ml of Krebs buffer and allowed to recover at 30°C under constant oxygenation with 95%

O_2/5% CO_2 for 60 min, with a change of buffer following the first 30 min of recovery. Slices were subsequently treated with drugs as specified for each experiment, transferred to microfuge tubes, snap-frozen on dry ice, and stored at -80°C until further analysis.

In metabolic radiolabeling experiments using [^{32}P] orthophosphate, all tissue manipulation was done in phosphate-free Krebs buffer. After 1 h of recovery, striatal slices were incubated for an additional hour with or without 1.25 mCi/ml [^{32}P] orthophosphate. Metabolic radiolabeling was conducted in the absence or presence of the protein serine/threonine phosphatase inhibitors, okadaic acid (a PP-1 and PP-2A inhibitor) and cyclosporin A (a PP-2B inhibitor).

2.3.11. Immunoprecipitation of AK from the soluble fraction of brain tissue homogenates

Frozen tissue samples were sonicated in boiling 1% SDS, boiled for 5 min, and clarified by centrifugation at 10,000 × *g* for 10 min at 4°C. Following protein concentration determination by the BCA protein assay (Pierce), soluble fractions were diluted 2-fold with NEFTD buffer containing 100 mM NaCl, 5 mM EDTA, 50mM NaF, 50 mM Tris-HCl, pH 7.4, 6% Igepal CA-630 (a non-ionic detergent), and protease inhibitors (Roche). 100-250 μg of diluted soluble protein were incubated overnight at 4°C with 5-20 μg of the polyclonal antibody for mouse AK. The next day, each homogenate-antibody mixture was incubated for 2 h at 4°C with 5 mg of Protein A-Sepharose CL-4B beads (Amersham Biosciences) reconstituted in NEFTD buffer without 6% Igepal CA-630. Following centrifugation at 3000 × *g* for 5 min, supernatants were transferred to fresh tubes and bead pellets were washed several times in a 1:1 mixture of NEFTD buffer and 1% SDS. To release immunoprecipitated protein, washed beads were boiled for 5 min in SDS protein sample buffer and centrifuged at 10,000 × *g* for 10 min. Supernatants were separated by SDS-PAGE (15% polyacrylamide) and either evaluated for ^{32}P-phosphate incorporation by PhosphorImager analysis or transferred to nitrocellulose membranes for immunoblot analysis using the polyclonal antibody for mouse AK. 5 μg of the antibody and 100 μg of soluble mouse brain protein were also blotted as controls.

2.4. Results

2.4.1. Identification of two isoforms of AK expressed in the mouse brain

Two forms of *Adk* cDNA were cloned from a mouse brain cDNA library using primers specific for the 5' and 3' untranslated regions of human *ADK* mRNA (45). One of the two clones was identical to the only full-length sequence reported for mouse *Adk* to date (73). This clone also showed extensive sequence homology with the long isoform of human AK (hAK1) (74). On the other hand, the second clone was homologous to the short isoform of human AK (hAK2) (45) and did not share identity with any previously reported mouse sequence. Therefore, it was predicted that this novel sequence represents the short isoform of mouse AK (mAK2), and the existing sequence corresponds to the long isoform (mAK1).

Mouse and human AK were found to be 89% homologous (Figure 2.1). Non-identical residues between the two species are dispersed throughout the sequence, although residues known to be involved in catalytic activity, such as those responsible for substrate and cation binding, are 100% conserved. Like their human orthologs, mAK1 and mAK2 are completely identical except at their respective N-termini, where the first twenty amino acids of mAK1 (MAAADEPKPKKLKVEAPQA) are replaced by four residues (MTST) in mAK2 (Figure 2.1). This results in a length of 361 and 345 amino acids for mAK1 and mAK2, respectively.

In order to study the function and regulation of mouse AK *in vitro*, both isoforms were subcloned into pET expression vectors encoding an N-terminal hexahistidine tag for affinity purification. Recombinant protein was purified to homogeneity by affinity-column chromatography. SDS-PAGE analysis of the pure fractions indicated an apparent molecular weight of 45 and 43.5 kDa for hexahistidine-tagged recombinant mAK1 and mAK2, respectively (Figure 2.2A). Moreover, *in vitro* AK activity assays showed that the two recombinant proteins were enzymatically active, efficiently catalyzing the phosphorylation of adenosine to AMP (for mAK1, K_m = 20 ± 4 nM; V_{max} = 16 ± 1.6 nmol/min/μg, n = 8) (Figure 2.2B). No significant difference was noted between mAK1

and mAK2 with respect to K_m and V_{max} (data not shown). These kinetic parameters were also in agreement with previously reported values for other forms of AK (45).

2.4.2. Immunoblot analysis of the tissue distribution of AK isoforms

Quantitative immunoblot analysis of AK expression in mouse brain and peripheral tissues using a monoclonal antibody for human AK showed highest levels of AK expression in the liver, followed by kidney, testis, and spleen (Figure 2.3). AK was present at intermediate levels in the brain, with most forebrain structures and the cerebellum showing somewhat higher levels of expression than the midbrain and brainstem. Moreover, in most tissue homogenates, two protein species of different molecular weight were detectable with this antibody. These two closely migrating bands likely represent the long and short isoforms of the enzyme. Many of the tissues included in this analysis also showed a prevalence of one isoform over the other. For instance, in the liver and spleen, the short isoform appears as the predominant AK species, whereas in the testis and kidney, the long isoform is more abundant. Most brain regions, with the exception of the cerebellum, express detectable levels of only the short isoform. In the cerebellum, both isoforms are present at nearly equal levels.

2.4.3. Phosphorylation of recombinant mouse AK by a protein kinase panel

Motif prediction analysis of the mouse AK sequence indicated the presence of putative phosphorylation sites for several protein kinases, including PKA, PKC, CaMKII, CK1, and CK2 (http://scansite.mit.edu). To investigate the possibility that AK activity may be regulated by protein phosphorylation, a panel of these protein kinases and others was tested for ability to phosphorylate recombinant mouse AK *in vitro* (Figure 2.4). PKC was able to phosphorylate mAK1 efficiently. PKA, PKG, MAPK, CK2, or Cdk1 did not detectably phosphorylate mAK1. Faint radiolabeling of mAK1 could be appreciated in reaction mixtures with CaMKII, CK1, and Cdk5. However, maximal reaction stoichiometries were 0.007, 0.008, and 0.003 mol/mol, respectively, precluding

subsequent biochemical analysis. Similar results were obtained when mAK2 was used as the putative protein kinase substrate (data not shown). In contrast, all control substrates were efficiently phosphorylated by their respective protein kinases. At 60 min, inhibitor-1 was phosphorylated to a stoichiometry of 0.99, 0.31, 0.61, and 0.97 mol/mol by PKA, MAPK, Cdk1, and Cdk5, respectively. Consistent with the existence of multiple PKC sites in myelin basic protein (75), the PKC-dependent phosphorylation of this control substrate reached a maximal stoichiometry of 2.35 mol/mol. Histone H1 was phosphorylated to a stoichiometry of 0.32 mol/mol by PKG, tyrosine hydroxylase to a stoichiometry of 0.94 mol/mol by CaMKII, and DARPP-32 to a stoichiometry of 0.49 and 0.92 mol/mol by CK1 and CK2, respectively.

2.4.4. Phosphorylation of recombinant mouse AK by PKC

A time-course protein phosphorylation reaction conducted using an excess of PKC and 10 μM recombinant mouse AK displayed linear conversion of substrate to phosphoprotein over the first 5 min and near-saturation by 20 min, with a maximal stoichiometry greater than 0.3 mol/mol (Figure 2.5A). mAK1 and mAK2 served as equally efficient substrates for PKC *in vitro* (Figure 2.5B). Kinetic analysis of the PKC-dependent phosphorylation of mAK1 revealed a K_m of 6.9 ± 1.1 μM and V_{max} of 68 ± 3 μmole/min/μg for this reaction (Figure 2.5C, n = 8). Similar values were obtained using the short isoform as a substrate (data not shown). A phosphopeptide map of mAK1 preparatively phosphorylated by PKC showed two major spots (Figure 2.6A, left), suggesting the phosphorylation of two mAK1 sites by PKC, or a missed tryptic cleavage resulting in the incomplete digestion of a single phosphopeptide. Phosphoamino acid analysis of the same material indicated that phosphorylation occurs at serine (Figure 2.6A, right). Similar results were obtained with mAK2 (data not shown).

Site-directed mutation of four consensus PKC phosphorylation sites to alanine (Ser48→Ala, Ser85→Ala, Ser272→Ala, and Ser328→Ala) had no effect on the phosphorylation of mAK1 by PKC (Figure 2.6B, *Consensus*). Serine-to-alanine mutants generated at the remaining nine conserved serine residues were also efficient PKC

substrates, although relative to wild-type mAK1, several showed moderate reductions in the maximal stoichiometry of phosphorylation (Figure 2.6B, *Conserved*), suggesting that more than one of these serine residues is phosphorylated by PKC. However, phosphopeptide maps of all mAK1 mutants preparatively phosphorylated by PKC showed two major spots similar to the pattern observed for wild-type phospho-mAK1, (Figure 2.6C), raising the possibility that PKC phosphorylates a non-consensus site at an unconserved serine residue in this protein.

In considering these observations, it was realized that in addition to six histidine residues and a thrombin cleavage site, the N-terminal affinity tag encoded by the expression vector used for generating recombinant mouse AK incorporates five serine residues, constituting a possible PKC target. Indeed, enzymatic removal of the first N-terminal 17 amino acids by thrombin cleavage (MGSSHHHHHHSSGLVPR/GSH, where the thrombin site is indicated by a forward slash) substantially reduced the PKC-dependent phosphorylation of mAK1 (Figure 2.6D). Similarly, mutation of the five N-terminal serine residues in the hexahistidine affinity tag of mAK1 resulted in a fusion protein that was no longer phosphorylated by PKC (Figure 2.6E).

2.4.5. Generation of a polyclonal antibody against mouse AK

These *in vitro* observations indicate that AK does not serve as an efficient substrate for prototypical members of several major classes of protein serine/threonine kinases. However, these findings alone do not rule out the possibility that AK is subject to phosphorylation by protein kinases not directly tested in this screen. If AK does serve as a protein kinase substrate *in vivo*, it should be possible to isolate it as a radiolabeled phosphoprotein by immunoprecipitation from homogenates of intact tissue metabolically labeled with the radioactive precursor, [^{32}P] orthophosphate. In the studies described above, the mouse monoclonal antibody for human AK was used to detect AK expression in discrete brain regions and numerous peripheral tissues by quantitative immunoblot analysis (Figure 2.3). However, attempts to immunoprecipitate AK from mouse brain tissue homogenates using this antibody were not successful (data not shown), possibly

due to the requirement for antigen-antibody interactions at multiple epitopes. Therefore, a rabbit polyclonal antibody was generated against the long and short forms of recombinant mouse AK. (Rabbits were immunized with uncleaved mAK1 and mAK2 bearing the N-terminal hexahistidine tags.) Immunoblot analysis of recombinant mAK1 and total protein from mouse brain homogenates showed that the affinity-purified antibody was highly selective for a doublet corresponding to the two isoforms of AK in the brain (Figure 2.7A). The antibody was also evaluated for immunohistochemical detection of AK in several brain regions (Figure 2.7B). The punctate immunofluorescence staining pattern observed in these tissues was absent from control sections stained with secondary antibody alone (data not shown). Therefore, the staining has the potential to be specific for AK.

AK immunoreactivity was apparent in ubiquitously distributed discrete cell bodies, with little or no staining of cellular processes or white matter tracts. Dense populations of AK-positive cells were appreciated in the striatum, olfactory bulb, and granular layer of the cerebellum. Lower numbers of AK-positive cells were present in the cerebral cortex and hippocampus. The cerebral cortex showed a nearly even distribution of AK-positive cells in all cortical layers. AK immunoreactivity was also dispersed in single cells throughout most of the hippocampus, with a conspicuous dearth of AK-positive cells in the granular cell layer of the dentate gyrus and pyramidal cell layers of the CA1 and CA3 regions.

The polyclonal antibody for mouse AK was next tested for its ability to immunoprecipitate AK from mouse tissue homogenates. Unlike the monoclonal antibody for human AK, the polyclonal antibody for mouse AK was able to immunoprecipitate endogenous AK efficiently from the soluble fraction of mouse brain tissue homogenates (Figure 2.7C). Use of increasing amounts of antibody resulted in the immunoprecipitation of larger quantities of AK, with correspondingly smaller amounts remaining in supernatants. The antibody and total mouse brain protein were blotted separately as visual aids to distinguish immunoprecipitated AK (~45 kDa) from the immunoglobulin G (IgG) heavy chain (~55 kDa) detected by the secondary antibody in immunoblots following immunoprecipitation.

2.4.6. Immunoprecipitation of AK from radiolabeled striatal slices

Following characterization in the applications described above, the polyclonal antibody for mouse AK was used to immunoprecipitate AK from striatal slices radiolabeled with [^{32}P] orthophosphate in the absence or presence of protein serine/threonine phosphatase inhibitors. Although AK was efficiently immunoprecipitated from the homogenates of unlabeled striatal slices (Figure 2.8A), no ^{32}P-phosphate incorporation by immunoprecipitated AK was detectable in homogenates of radiolabeled striatal slices (Figure 2.8B). In contrast, supernatants resulting from the immunoprecipitation of AK from these homogenates contained multiple ^{32}P-labeled phosphoprotein species (data not shown), indicating that efficient metabolic labeling with [^{32}P] orthophosphate had been achieved. These results indicate that AK is not subject to post-translational regulation by serine/threonine phosphorylation in the striatum.

Interestingly, radiolabeled striatal tissue homogenates immunoprecipitated with the polyclonal antibody for mouse AK contained a 55-kDa phosphoprotein whose ^{32}P-phosphate incorporation increased approximately 12-fold as a result of radiolabeling in the presence of protein phosphatase inhibitors (Figure 2.8B, left). To understand whether this protein may be a binding partner for AK *in vivo*, the ^{32}P-labeled gel band was excised and submitted to Yingming Zhao (Protein Chemistry Core Facility, UT Southwestern Medical Center) for protein identification. Mass spectrometry (MS) analysis identified the phosphoprotein as the β subunit of mitochondrial ATP synthase. The ATP synthase complex resides in the inner mitochondrial membrane and catalyzes the formation of ATP from ADP and inorganic phosphate coupled to the movement of protons down a pH gradient into the mitochondrial matrix (76). The β subunit, which is subject to phosphorylation by the protein serine/threonine kinase, protein kinase B (PKB/Akt) (77), forms part of the F_1 motor, the soluble catalytic fragment of ATP synthase closely tethered to the membrane-embedded F_0 complex. Although AK and ATP synthase act upon two closely related precursors in ATP synthesis, namely adenosine and the adenine nucleotide, ADP, there is little evidence to suggest that they function in the same

subcellular compartment. AK is a cytosolic enzyme showing pronounced perinuclear localization in astrocytes and neurons (59). On the other hand, ATP synthase is a mitochondrial protein complex whose β subunit is used commonly as a marker for this compartment. Thus, it is highly unlikely that ATP synthase serves as a binding partner for AK *in vivo*. The immunoprecipitation of its β subunit with the polyclonal antibody for mouse AK probably represents an artifact.

2.5. Discussion

In these studies, the cDNA and deduced amino acid sequences were determined for two isoforms of AK expressed in the mouse brain. To date, the existence of AK splice variants has been described in several mammalian species, namely mouse (51, 59), rat (78), and human (45, 74). A search for multiple forms of AK in other species is likely to generate similar results.

Immunoblot analysis showed that most mouse brain regions express roughly equivalent levels of AK, with midbrain and brainstem structures showing somewhat lower levels than the cerebellum and cortical and subcortical parts of the forebrain. Furthermore, one or the other AK isoform predominates in most tissues, including the brain, where the short isoform is prevalent. The biological significance of this bias remains unknown. Although no difference was observed in enzymatic activity between recombinant mAK1 and mAK2, it is possible that *in vivo* the two molecules are functionally dissimilar in some other important respect, such as neuronal *versus* glial distribution, subcellular localization, transcriptional and/or translational regulation, rate of turnover, or association with heretofore undefined regulatory factors.

The regional and cellular distribution of mouse brain AK expression was elucidated in a previous immunohistochemical study, which reported a generally homogenous pattern of AK immunoreactivity in astrocytes throughout the brain, in addition to pockets of high neuronal expression in the olfactory bulb, striatum, and brainstem (59). The immunofluorescence staining described here for AK expression in a

number of brain regions confirmed these earlier findings at the level of tissue and cell layer distribution. Consistent with the previous study, the novel polyclonal antibody for mouse AK used in this analysis also showed predominant localization of AK expression in broadly distributed discrete cell bodies, with little AK immunoreactivity in cellular processes. However, in the absence of co-staining with antibodies directed against specific cellular markers, the staining shown here necessarily lacks resolution at the level of AK-positive cell types and subcellular compartments. Nonetheless, the noticeable absence of strong AK immunoreactivity in the granular and pyramidal cell layers of the hippocampus is consistent with the earlier observation that most AK expression in the brain is glial. Although these findings largely corroborate the earlier study, the specificity of the immunoreactivity in these stains will formally remain unconfirmed until it is demonstrated that the polyclonal antibody for mouse AK used in this analysis does not stain tissue from *Adk*$^{-/-}$ mice. An alternative approach would be to show that the staining of wild-type tissue is quenched by incubation of the antibody with pure AK protein.

In these studies, AK did not serve as an efficient substrate for representatives of several major classes of protein serine/threonine kinases *in vitro*. Although CaMKII, CK1, and Cdk5 were found to phosphorylate AK weakly, the maximal stoichiometry achieved in these reactions remained below 0.01 mol/mol, precluding further biochemical characterization, such as the identification of phosphorylation sites and the assessment of possible effects of phosphorylation on AK activity. The results also indicated that these reactions are unlikely to occur *in vivo*. Taken together, these findings strongly argue against the regulation of AK by the protein kinases investigated in this study.

On the other hand, it is important to note that the candidate approach used for this screen was by no means exhaustive, and although the protein kinases tested represent most of the principal classes of protein serine/threonine kinases, the possibility remains that other protein kinases target AK. Therefore, a more broad-based strategy was adopted to determine whether AK occurs as a phosphoprotein *in vivo*. A polyclonal antibody was raised against mouse AK for this purpose. However, no ^{32}P-phosphate incorporation by AK was detected in radioimmunoprecipitation assays using this novel

antibody to isolate AK from mouse striatal slices metabolically labeled with [^{32}P] orthophosphate in the absence or presence of a combination of PP-1, PP-2A, and PP-2B inhibitors. These observations strongly suggest that AK is not phosphorylated under basal conditions in the striatum and does not serve as a substrate for protein serine/threonine kinases in this tissue. Strictly speaking, the results do not formally exclude the possibility that AK is regulated by phosphorylation in tissues other than the striatum, or that it serves as a substrate for protein tyrosine kinases and phosphatases under non-basal conditions. A broad-spectrum protein tyrosine phosphatase inhibitor, such as sodium orthovanadate, could be used to evaluate this possibility in future experiments. The insulin-dependent increase in AK levels in rat lymphocytes (56) suggests that phospho-tyrosine signaling pathways may be important for at least one aspect of AK regulation in living cells. The intimate involvement of AK in nucleotide biosynthesis and purine salvage pathways further suggests that AK activity may be under the control of phospho-tyrosine signaling mechanisms, which serve essential functions in the regulation of normal cell growth, division, and differentiation.

In addition to the central observations discussed above, these studies have produced several findings of technical significance. The results reveal a potentially important hazard in the use of pET vector-encoded polyhistidine affinity tags for the purification and study of recombinant PKC substrates. More recently, another group has reported that PKC-α phosphorylates Ser93 of glutathione S-transferase (79), a protein commonly used as a fusion partner to facilitate the investigation of other proteins. These observations underline the risk of artifact inherent in studying recombinant proteins terminally modified with various tag sequences.

With regard to the analysis of phosphoproteins by thin-layer chromatography, it should be noted that the use of polyethyleneimine-cellulose plates was essential to the generation of good phosphopeptide maps using recombinant AK-His_6 phosphorylated by PKC. The smearing observed on microcrystalline cellulose plates during the electrophoresis step could be due to the fact that the PKC phosphorylation site was located within the hexahistidine tag. The presence of six tandem histidine residues in this sequence may have adversely affected the electrophoretic migration of this highly basic

peptide (theoretical pI ≈ 9.6) on microcrystalline cellulose, which is negatively charged at pH 3.5 (80). AK is relatively acidic, with a theoretical pI less than 5.8, so it is reasonable to conclude that it gives rise to a preponderance of negatively charged tryptic peptides that require separation from the basic tag sequence. The impregnation of cellulose with polyethyleneimine introduces a strong anion exchanger into the thin-layer matrix, possibly explaining the better resolution achieved in phosphopeptide maps generated with this kind of TLC plate. These observations may be of interest to other investigators studying AK, PKC, or more generally, recombinant proteins bearing terminal affinity tags.

Figure 2.1: Deduced amino acid sequence alignment of the long and short isoforms of human and mouse AK. Sequences are divided into two domains (yellow and green blocks) based on the crystal structure of hAK2 (46). Yellow blocks constitute the catalytic domain. The regulatory domain (green blocks) folds over the catalytic domain and forms a hydrophobic pocket for adenosine phosphorylation. Residues that make close contacts with adenosine are indicated by red letters. Green letters denote residues that form the ATP/secondary adenosine-binding site. One Mg^{2+} ion is coordinated between the active site and this ATP-binding site by hydrogen-bonding interactions mediated by water and the residues designated by blue letters. Stars indicate non-identical residues.

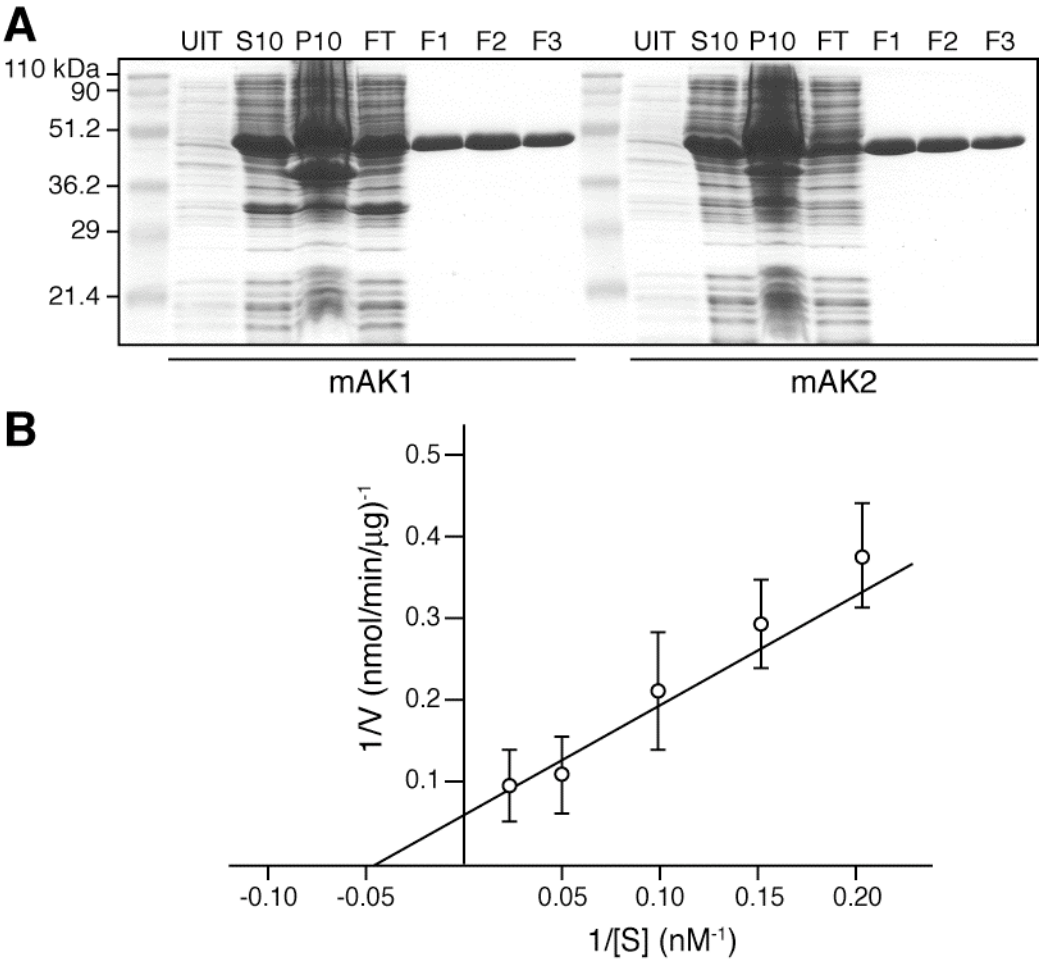

Figure 2.2: Preparation of active recombinant mouse AK. A. Purification of recombinant mAK1 and mAK2 by affinity-column chromatography. The panel shows SDS-PAGE analysis of protein from uninduced bacterial cultures (*UIT*), cell lysate supernatants (*S10*) and pellets (*P10*) resulting from centrifugation at 10,000 × *g*, flow-through fractions (*FT*), and eluted peak fractions (*F1*, *F2*, and *F3*). *B.* Lineweaver-Burk analysis of recombinant mAK1 activity. The data represent means ± S.E.M. for 4 experiments conducted in duplicate under identical linear steady-state conditions.

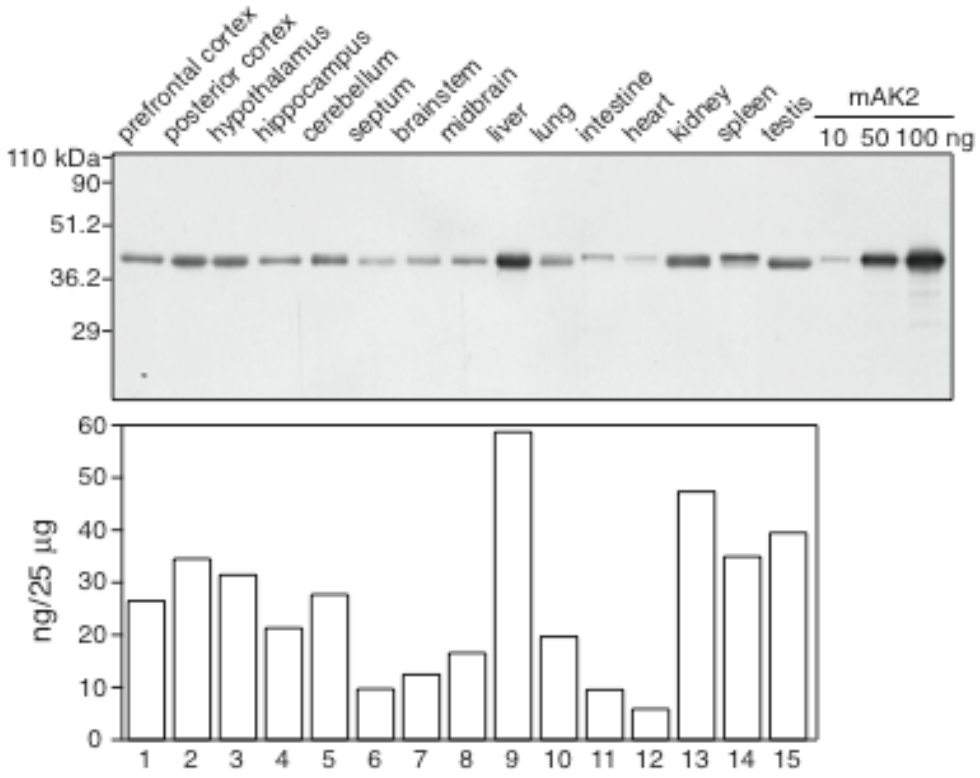

Figure 2.3: Quantitative immunoblot analysis of AK expression in mouse brain and peripheral tissues. The three lanes on the far right were used to blot 10, 50, and 100 ng of recombinant mAK2 for the quantification of relative AK levels shown in the histogram for each tissue examined. Recombinant mAK2 bears an N-terminal hexahistidine affinity tag, resulting in a higher apparent molecular weight than mAK2 found in the sample lanes.

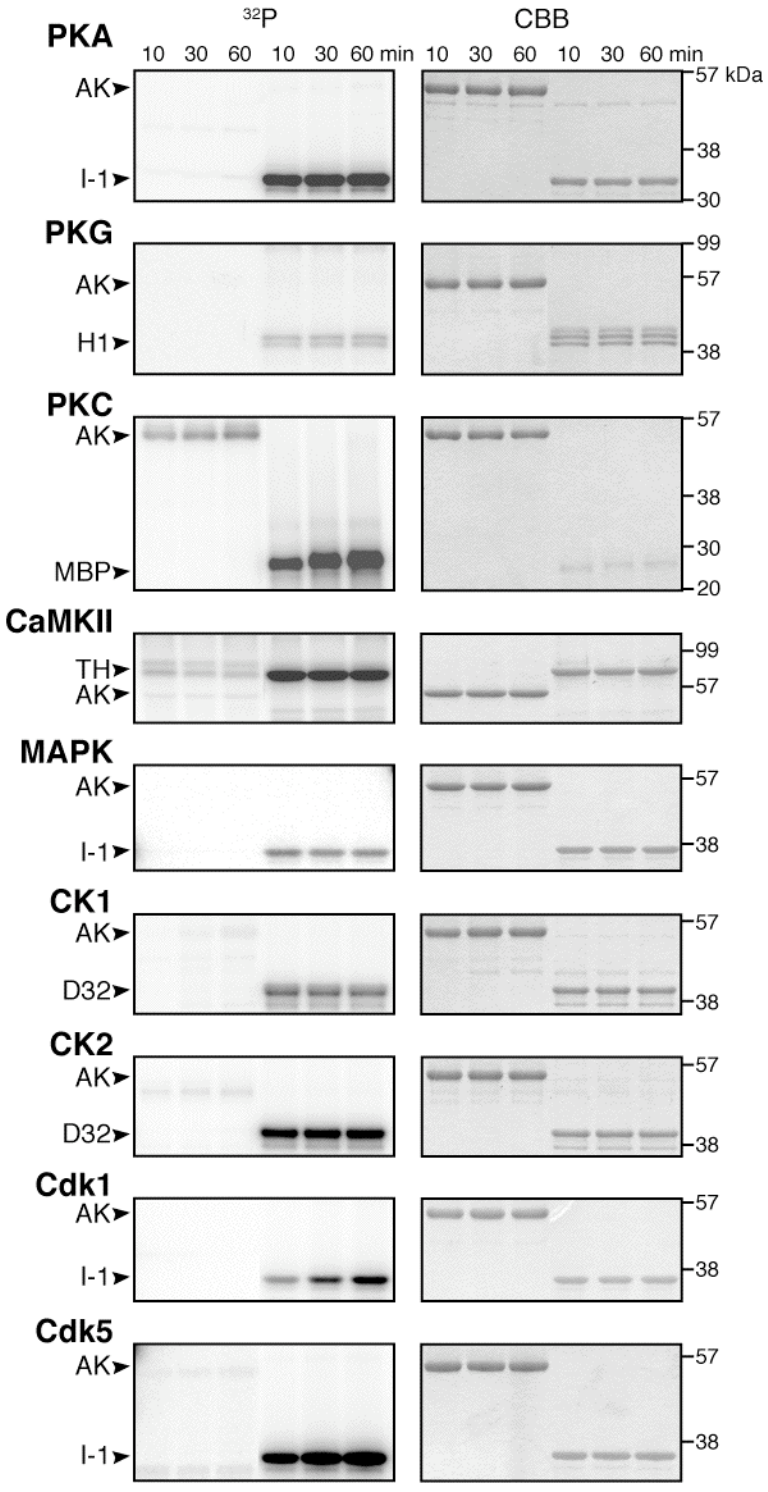
32P
CBB
PKA
10 30 60 10 30 60 min 10 30 60 10 30 60 min
57 kDa
AK
I-1
38
30
PKG
99
AK
57
H1
38
PKC
57
AK
38
MBP
30
20
CaMKII
99
TH
AK
57
MAPK
AK
57
I-1
38
CK1
AK
57
D32
38
CK2
AK
57
D32
38
Cdk1
AK
57
I-1
38
Cdk5
AK
57
I-1
38

Figure 2.4: Evaluation of recombinant mAK1 as substrate for a panel of protein kinases. Phosphorylation of mAK1, inhibitor-1 (*I-1*), myelin basic protein (*MBP*), histone H1 (*H1*), tyrosine hydroxylase (*TH*), and DARPP-32 (*D32*) by PKA, PKG, PKC, CaMKII, MAPK, CK1, CK2, Cdk1, and Cdk5 *in vitro*. The panels show ^{32}P-labeled (left) and CBB-stained (right) reaction mixtures subjected to SDS-PAGE. The multiple histone H1 bands visible by PhosphorImager analysis and CBB stain of the PKG reaction mixture correspond to degradation products of the protein. The two species of higher molecular weight, appearing as ^{32}P-labeled bands above the mAK1 signal in the CaMKII reaction, represent the autophosphorylation of different CaMKII isoforms present in this enzyme preparation. At least one of these CaMKII bands is also present in the tyrosine hydroxylase lanes. The other is likely too close to the more prominent tyrosine hydroxylase band to be visible.

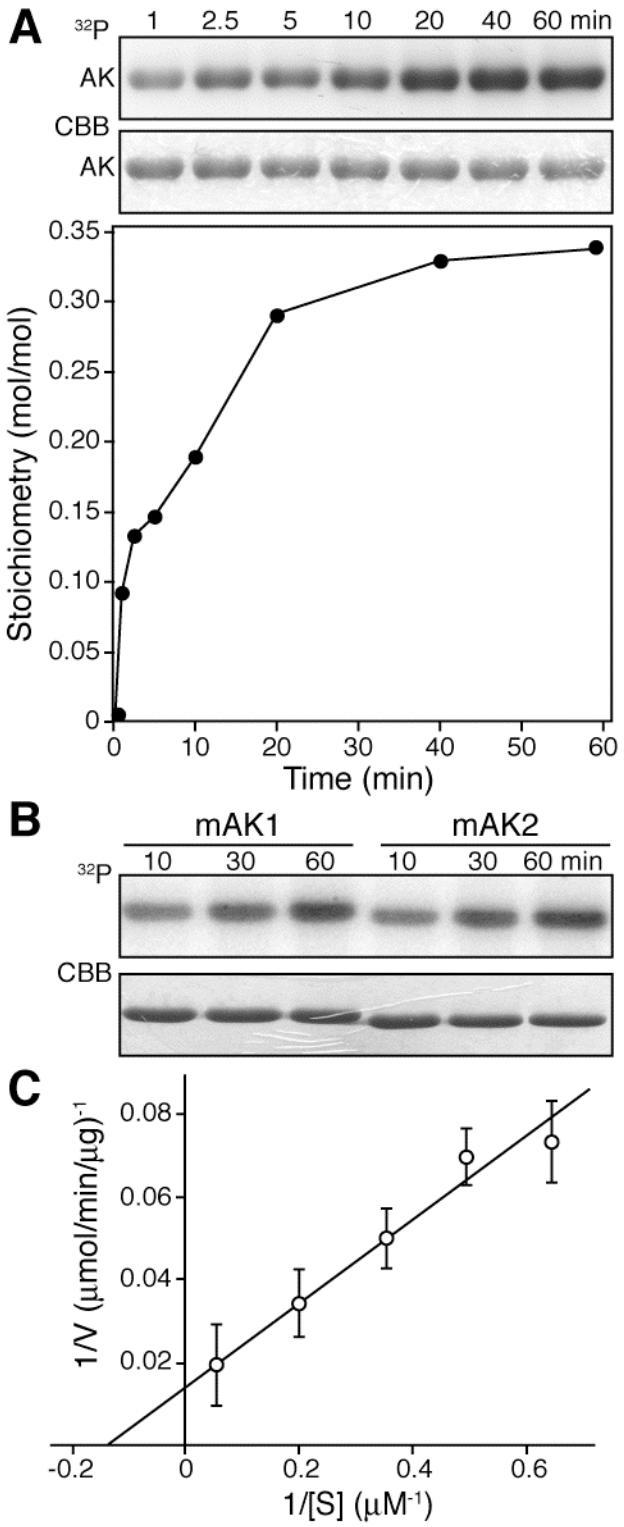
A
32P
1
2.5
5
10
20
40
60 min
AK
CBB
AK
Stoichiometry (mol/mol)
0.35
0.30
0.25
0.20
0.15
0.10
0.05
0
0
10
20
30
40
50
60
Time (min)
B
mAK1
mAK2
10
30
60
10
30
60 min
32P
CBB
C
1/V (μmol/min/μg)-1
0.08
0.06
0.04
0.02
-0.2
0
0.2
0.4
0.6
1/[S] (μM-1)

Figure 2.5: Phosphorylation of recombinant mAK1 and mAK2 by PKC in vitro. *A*. Time-course analysis of the phosphorylation of mAK1 by PKC *in vitro*. The two panels show ^{32}P-labeled (top) and CBB-stained (bottom) mAK1 subjected to SDS-PAGE. Reaction times are indicated along the top. The plot represents phosphate incorporation over time. *B*. Phosphorylation of mAK1 and mAK2 by PKC *in vitro*. The two panels show SDS-PAGE analysis of ^{32}P-labeled (top) and CBB-stained (bottom) mAK1 and mAK2. Reaction times are indicated along the top. *C*. Lineweaver-Burk analysis of the PKC-dependent phosphorylation of mAK1. The data represent means ± S.E.M. for 4 reactions conducted in duplicate under identical linear steady-state conditions.

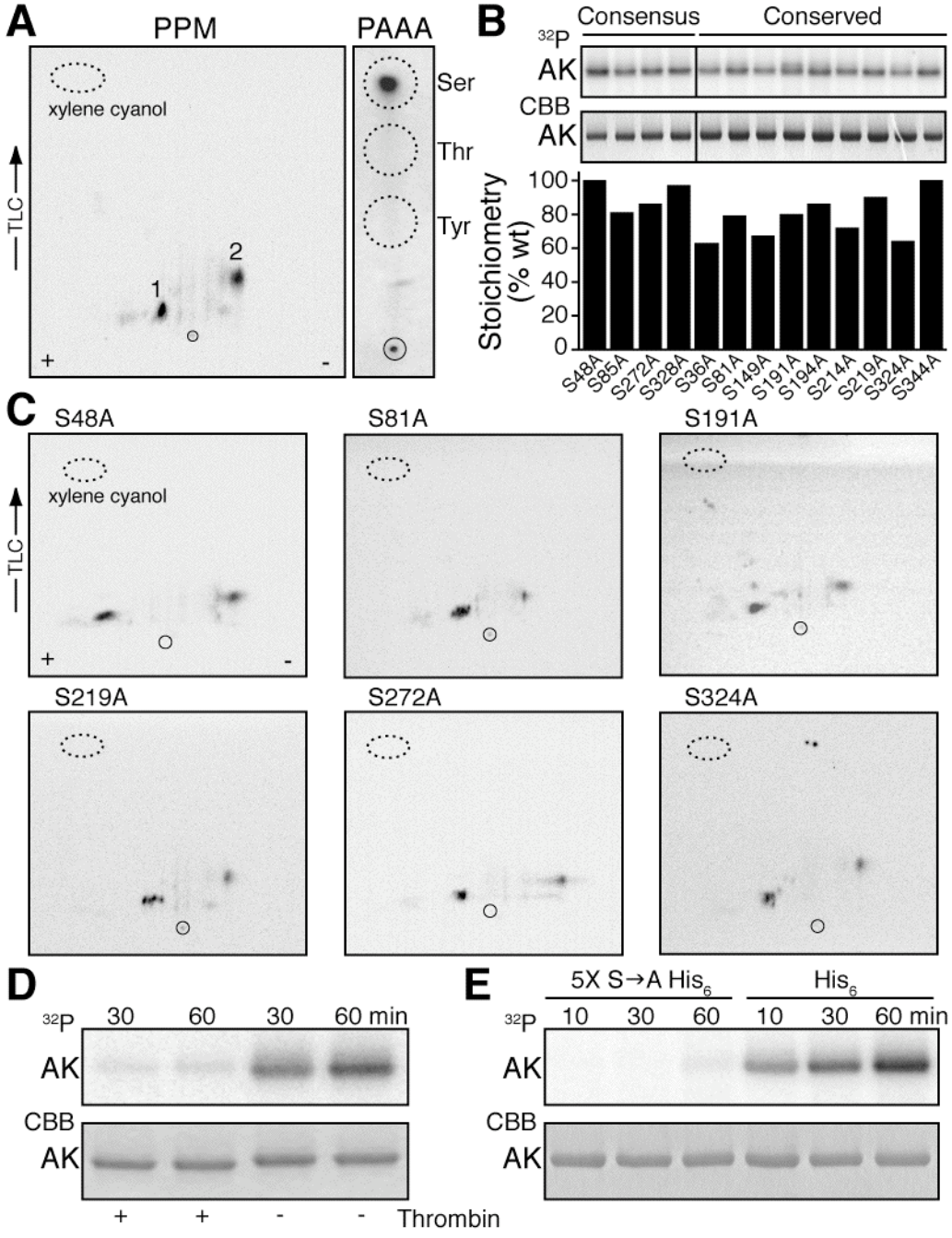
A
PPM
PAAA
xylene cyanol
TLC
1
2
+
-
Ser
Thr
Tyr
B
Consensus
Conserved
32P
AK
CBB
AK
Stoichiometry (% wt)
100
80
60
40
20
0
S48A
S85A
S272A
S328A
S36A
S81A
S149A
S191A
S194A
S214A
S219A
S324A
S344A
C
S48A
S81A
S191A
S219A
S272A
S324A
xylene cyanol
TLC
+
-
D
32P
30
60
30
60 min
AK
CBB
AK
+
+
-
-
Thrombin
E
5X S→A His6
His6
32P
10
30
60
10
30
60 min
AK
CBB
AK

Figure 2.6: Identification of the AK site of PKC-dependent phosphorylation. A. Phosphopeptide mapping (*PPM*) and phosphoamino acid analysis (*PAAA*) of mAK1 preparatively phosphorylated by PKC. The + and – signs on the phosphopeptide map denote electrode polarity, while the upward arrow labeled TLC indicates the direction of ascending chromatography. *B.* Phosphorylation of serine-to-alanine mutants of mAK1 by PKC *in vitro*. The two panels show SDS-PAGE analysis of ^{32}P-labeled (top) and CBB-stained (bottom) mutant mAK1 forms incorporating serine-to-alanine mutations at four consensus PKC phosphorylation sites (*Consensus*, *S48A*, *S85A*, *S272A, S328A*) and nine conserved serine residues (*Conserved, S36A*, *S81A*, *S149A, S191A, S194A, S214A, S219A, S324A, S344A*). The histogram represents the relative stoichiometry of each reaction at 60 min as a percentage of the stoichiometry of the PKC-dependent phosphorylation of wild-type mAK1 (*wt*). *C.* Representative phosphopeptide maps of mutant mAK1 forms phosphorylated by PKC. *D.* The effect of thrombin cleavage on the phosphorylation of mAK1 by PKC. The two panels show SDS-PAGE analysis of ^{32}P-labeled (top) and CBB-stained (bottom) hexahistidine-tagged mAK1 incubated in the presence or absence of thrombin before phosphorylation by PKC. PKC reaction times are indicated along the top. *E.* The effect of serine-to-alanine mutation of the N-terminal hexahistidine affinity tag on the phosphorylation of mAK1 by PKC. The two panels show SDS-PAGE analysis of ^{32}P-labeled (top) and CBB-stained (bottom) mAK1 (*His$_6$*) and a quintuple mutant of mAK1 (*5X S→A His$_6$*) incorporating 5 serine-to-alanine mutations in the N-terminal hexahistidine affinity tag. Reaction times are indicated along the top.

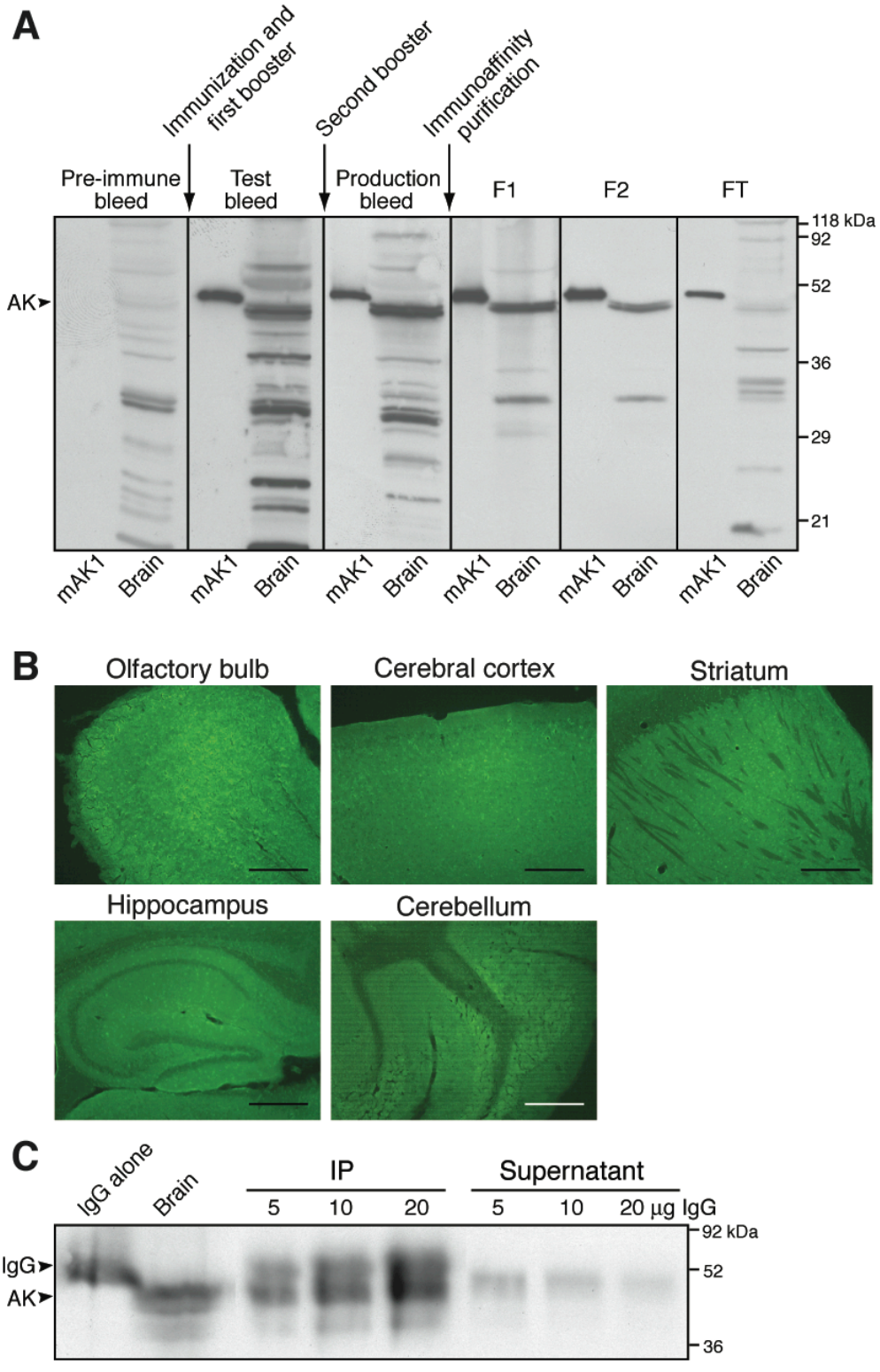
A
Immunization and first booster
Second booster
Immunoaffinity purification
Pre-immune bleed
Test bleed
Production bleed
F1
F2
FT
118 kDa
92
52
36
29
21
AK
mAK1
Brain
B
Olfactory bulb
Cerebral cortex
Striatum
Hippocampus
Cerebellum
C
IgG alone
Brain
IP
Supernatant
5
10
20
5
10
20 µg IgG
92 kDa
52
36
IgG
AK

Figure 2.7: Generation and characterization of a polyclonal antibody for mouse AK. A. Immunoblot analysis of recombinant mAK1 (50 ng) and total mouse brain protein (100 μg) using pre-immune serum from a naïve rabbit, anti-AK antisera isolated from test and first production bleeds from the same animal following immunization, and the first and second eluted peak fractions (*F1* and *F2*) and flow-through fraction (*FT*) resulting from immunoaffinity purification of the polyclonal antibody for mouse AK from the first production bleed. *B.* Immunofluorescence stain of parasagittal sections of mouse olfactory bulb, cerebral cortex, striatum, hippocampus, and cerebellum using the polyclonal antibody for mouse AK. Scale bars, 400 μm. *C.* Immunoblot analysis of AK in Sepharose pellets (*IP*) and supernatants from mouse brain homogenates immunoprecipitated with the indicated amounts of the polyclonal antibody for mouse AK. Immunoblotting was performed using the same antibody. 5 μg of antibody (*IgG alone*) and 100 μg of soluble mouse brain protein were also blotted as controls.

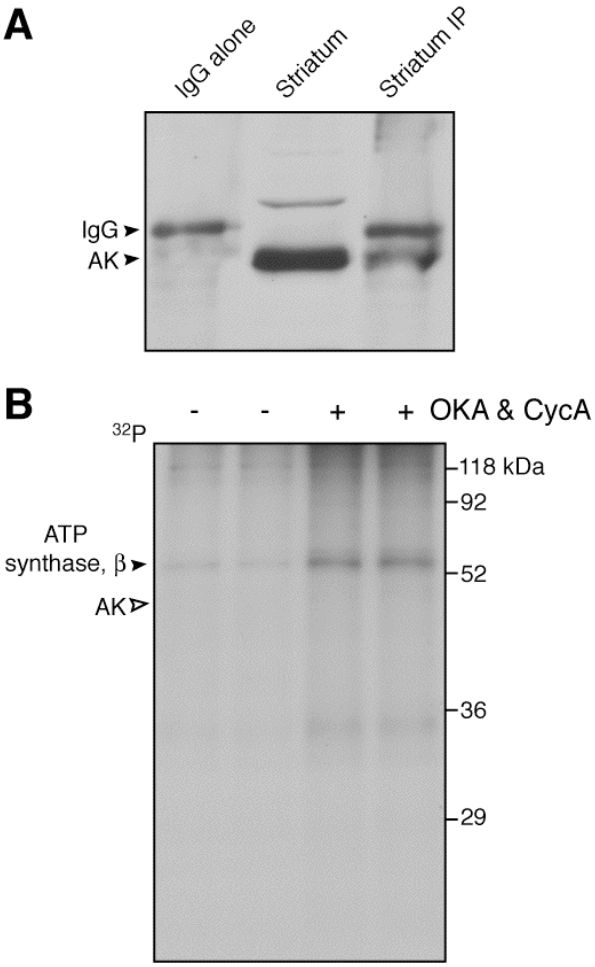

Figure 2.8: Immunoprecipitation of AK from striatal slices radiolabeled with [^{32}P] orthophosphate. A. Immunoblot analysis of soluble mouse striatal protein (*STR*) before and after immunoprecipitation (*IP*) with the polyclonal antibody for mouse AK (*IgG*). Immunoblotting and immunoprecipitation were performed using the same antibody. *B.* Autoradiogram of immunoprecipitates resulting from incubation of the polyclonal antibody for mouse AK with homogenates of striatal slices radiolabeled with [^{32}P] orthophosphate in the absence or presence of okadaic acid (*OKA*, a PP-1 and PP-2A inhibitor, 1 μM, 60 min) and cyclosporin A (*CycA*, a PP-2B inhibitor, 2.5 μM, 60 min). The β subunit of mitochondrial ATP synthase (*filled arrowhead*) and the predicted position of AK (*open arrowhead*) are indicated.

CHAPTER 3†

EVALUATION OF NEURONAL PHOSPHOPROTEINS AS MEDIATORS OF STRIATAL ADENOSINE A_{2A} RECEPTOR SIGNALING

3.1. Summary

Adenosine A_{2A} receptors are predominantly expressed in the dendrites of enkephalin-positive γ-aminobutyric acidergic medium spiny neurons in the striatum, where they are believed to modulate dopaminergic neurotransmission and function in motor control, vigilance, alertness, and arousal. Although the physiological and behavioral corollaries of adenosine A_{2A} receptor signaling have been extensively studied using a combination of pharmacological and genetic tools, relatively little is known about the signal transduction pathways that mediate the diverse biological functions attributed to this adenosine receptor subtype. A candidate approach was taken to search for potential mediators of adenosine A_{2A} receptor signaling in the striatum based on the coupling of these receptors to G proteins that activate adenylate cyclase and increase cAMP formation. Accordingly, a selection of membranal, cytosolic, and nuclear phosphoproteins directly or indirectly regulated by cAMP-dependent protein kinase in the pre- and postsynaptic compartments were evaluated as putative elements of striatal signaling pathways activated by adenosine A_{2A} receptors.

† Part of this Chapter was published in *Brain Research.*

3.2. Introduction

In the central nervous system, the actions of adenosine are mediated by four subtypes of G protein-coupled receptors, namely A_1, A_{2A}, A_{2B}, and A_3 (25). Of these receptor subtypes, adenosine A_1 and A_{2A} receptors are activated in response to the low basal levels of extracellular adenosine found in the mammalian brain under physiological conditions. Therefore, it is believed that in the central nervous system these receptors represent the most relevant sites of action for adenosine and adenosine-like compounds, including caffeine and its major metabolites, which act as adenosine receptor antagonists (81). Adenosine A_1 receptors are coupled to $G\alpha_i$ or $G\alpha_o$ proteins that inhibit adenylate cyclase and reduce cAMP formation (82-84). In contrast, adenosine A_{2A} receptors associate with $G\alpha_s$ or $G\alpha_{olf}$ proteins, which stimulate adenylate cyclase activity and increase cAMP generation (85-88). These receptors also exhibit different regional distributions in the brain. A_1-type adenosine receptors are abundantly expressed throughout the brain, with high levels found in the cerebral cortex, septum, hippocampus, and the basal ganglia, including the striatum (89). In the striatum, many adenosine A_1 receptors are located presynaptically on dopaminergic, glutamatergic, and cholinergic inputs to medium spiny neurons (90-92), where they inhibit neurotransmitter release (93). Some striatal adenosine A_1 receptors may also be present in postsynaptic locations (94, 95). In contrast, adenosine A_{2A} receptors are almost exclusively found in the striatum (96), where they co-localize with dopamine D_2 receptors on the enkephalin-positive, γ-aminobutyric acid (GABA)ergic medium-sized spiny projection neurons of the striatopallidal pathway (97, 98). Although some are expressed presynaptically at glutamatergic nerve terminals, most striatal adenosine A_{2A} receptors are postsynaptic and occur predominantly at excitatory synapses on the dendrites and dendritic spines of GABAergic medium spiny neurons (99, 100). Thus, these receptors may be well positioned to modulate cortical glutamatergic excitatory input to the striatum.

Striatal adenosine A_{2A} receptors are believed to modulate dopaminergic neurotransmission (95, 101-103) and mediate a number of neuronal phenomena, including motor control (104-106), level of arousal (107), and vigilance (108). Although

pharmacological (31, 109) and genetic tools (28, 110, 111) developed in the past twenty years have revealed a wealth of information about the physiological and behavioral consequences of adenosine A_{2A} receptor signaling, relatively little is known about the intracellular signaling cascades that mediate these diverse biological functions. In the following studies, a candidate approach was adopted to identify phosphoprotein targets likely to be regulated by adenosine A_{2A} receptors in the striatum. In keeping with the ability of these receptors to activate adenylate cyclase, the candidate proteins included in this analysis comprised a heterogeneous group of pre- and postsynaptic PKA substrates as well as phosphoproteins indirectly regulated by PKA-mediated signaling.

Specifically, the phosphorylation state of the following PKA substrates was assessed in striatal slices treated with or without an adenosine A_{2A} receptor agonist: in the presynaptic compartment, the rate-limiting enzyme in catecholamine biosynthesis, tyrosine hydroxylase (112), and the synaptic vesicle-associated neuronal protein, synapsin (113, 114); in the postsynaptic compartment, the ionotropic glutamate receptor subunits, N-methyl-D-aspartate (NMDA)-type glutamate receptor 1 (NR1, an obligate NMDA receptor subunit) (115, 116) and glutamate receptor 1 (GluR1, a subunit of the α-amino-3-hydroxy-5-methyl-4-isoxazole propionic acid (AMPA)-type glutamate receptor) (117, 118), the PP-1/actin-binding dendritic protein, spinophilin (119), the striatal PP-1 inhibitor, DARPP-32 (120), and the transcriptional regulator, cAMP-response element-binding protein (CREB) (121). Three additional phosphoproteins indirectly regulated by PKA were also evaluated: the protein serine/threonine kinases, CaMKII and the p44 and p42 isoforms of MAPK (extracellular signal-regulated kinase (ERK) 1 and 2).

PKA activity has been reported to exert profound effects on the function of each of these phosphoproteins. The PKA-dependent phosphorylation of tyrosine hydroxylase at Ser40 (122) stimulates enzymatic activity (123). Synapsin Ser9 phosphorylation by PKA (124) causes synapsin to disassociate from synaptic vesicles (125). The PKA-dependent phosphorylation of NR1 at Ser897 (126) promotes NR1 trafficking from the endoplasmic reticulum to the cell surface (127). There is substantial evidence that PKA-dependent GluR1 phosphorylation at Ser845 potentiates AMPA-type glutamate receptor-mediated currents (128). Spinophilin no longer binds actin when phosphorylated at

Ser94 by PKA (129). Finally, the striatal PP-1 inhibitor, DARPP-32, and the transcription factor, CREB, are activated by PKA-dependent phosphorylation at Thr34 (130) and Ser133 (131), respectively.

As for the non-PKA substrates included in this analysis, there is substantial evidence that both the CaMKII and ERK pathways are under the regulation of PKA-mediated signaling in a number of systems. The autophosphorylation of CaMKII at Thr286 results in Ca^{2+}-independent activation of this protein kinase (132). In the hippocampus, this autophosphorylation event also mediates the translocation of active CaMKII from the cytosol to the postsynaptic density, where phospho-Thr286 CaMKII is dephosphorylated and inactivated by PP-1 (133). In turn, PP-1 activity toward CaMKII in this tissue is negatively regulated by PKA-mediated signaling through protein phosphatase inhibitor-1 (134). A similar PKA-dependent pathway may exist in the striatum. With regard to the ERK pathway, ERK1 and ERK2 are activated by MAPK/ERK kinase (MEK)-dependent dual phosphorylation of Thr202/Tyr204 and Thr183/Tyr185, respectively (135-139). There is evidence that some forms of synaptic plasticity involve the activation of the ERK pathway through PKA-mediated signaling upstream from MEK (140-142).

3.3. Experimental Procedures

3.3.1. Chemicals and enzymes

Forskolin was from LC Laboratories. CGS 21680 was from Sigma. All other reagents were from sources indicated in Chapter 2.

3.3.2. Immunoblot analysis

Frozen striatal tissue samples were sonicated in boiling 1% SDS containing 50 mM NaF and boiled for 5 min. Protein concentrations were determined by the BCA

protein assay (Pierce) using BSA as standard. 100 μg of total protein from each sample were subjected to SDS-PAGE (12.5 or 15% polyacrylamide) followed by electrophoretic transfer to nitrocellulose membranes (0.2 μm) (Whatman). The membranes were processed for immunodetection as described in Chapter 2, using primary antibodies for phospho-Ser40 tyrosine hydroxylase (1:1000) (Chemicon), total tyrosine hydroxylase (1:2000) (Chemicon), phospho-Ser9 synapsin (1:500) (Calbiochem), total synapsin (1:1000) (Cell Signaling), phospho-Ser897 NR1 (1:1000) (Calbiochem), total NR1 (1:2000) (BD Biosciences), phospho-Ser845 GluR1 (1:500) (Upstate), total GluR1 (1:500) (Upstate), phospho-Ser94 spinophilin (1:1000) (129), total spinophilin (1:800) (119), phospho-Thr34 DARPP-32 (1:750) (143), total DARPP-32 (1:8000) (144), phospho-Ser133 CREB (1:1000) (Upstate), total CREB (1:250) (Zymed), phospho-Thr286 CaMKII (1:200) (Santa Cruz), total CaMKII (1:1000) (Santa Cruz), diphospho-Thr202/Tyr204 and Thr183/Tyr185 ERK1 and ERK2 (1:1000) (Cell Signaling), or total ERK1 and ERK2 (1:1000) (Cell Signaling). The antibodies to phospho-Thr34 and total DARPP-32, and phospho-Ser94 and total spinophilin were provided by Paul Greengard (The Rockefeller University). The pharmacological manipulations used in these studies did not alter the total amount of tyrosine hydroxylase, synapsin, GluR1, spinophilin, DARPP-32, CREB, CaMKII, ERK1, or ERK2 in striatal slices. Total NR1 levels decreased in response to forskolin, but not CGS 21680. The biological significance of this decrease is unknown.

3.4. Results

3.4.1. Adenylate cyclase-dependent regulation of selected phosphoproteins in striatal slices

To facilitate the study of signal transduction pathways regulated by striatal adenosine A_{2A} receptors, a candidate approach was taken to screen for physiological phosphoproteins that may be involved in mediating the effects of adenosine in the

striatum. As described above, adenosine A_{2A} receptors are highly enriched in the striatum and couple to G proteins that stimulate adenylate cyclase activity and cAMP generation. Thus, these receptors are likely to regulate the phosphorylation state of proteins in PKA-dependent striatal signaling pathways. In proof-of-principle experiments designed to optimize the use of phosphorylation state-specific antibodies to selected phosphoproteins directly or indirectly regulated by PKA, striatal slices were treated with or without the adenylate cyclase activator, forskolin, and assessed for phosphoprotein levels (Figure 3.1). Incubation with forskolin resulted in the increased phosphorylation of PKA sites in the presynaptic proteins, tyrosine hydroxylase and synapsin. Forskolin also induced the up-regulation of PKA sites in the postsynaptic proteins, NR1, GluR1, spinophilin, DARPP-32, and CREB. For three additional targets, phosphorylation sites not directly phosphorylated by PKA were also tested. Forskolin caused an increase in the level of MEK-dependent phosphorylation of ERK1 and ERK2 at Thr202/Tyr204 and Thr183/Tyr185, respectively. On the other hand, no significant change in the autophosphorylation of CaMKII at Thr286 was detected in response to forskolin.

3.4.2. Regulation of selected phosphoproteins by an adenosine A_{2A} receptor agonist in the striatum

With the exception of phospho-Thr286 CaMKII, adenylate cyclase activation reproducibly increased the levels of all pre- and postsynaptic phosphoproteins evaluated. Levels of these phosphoproteins were next assessed in striatal slices treated with the selective adenosine A_{2A} receptor agonist, CGS 21680. To characterize the relative responsiveness of each putative target to adenosine A_{2A} receptor activation by CGS 21680, a series of time-course and dose response experiments were conducted, in which striatal slices were incubated with 0-5 μM CGS 21680 for 0-30 min and assessed for levels of phospho-Ser40 tyrosine hydroxylase, phospho-Ser9 synapsin, phospho-Ser897 NR1, phospho-Ser845 GluR1, phospho-Ser94 spinophilin, phospho-Thr34 DARPP-32,

phospho-Ser133 CREB, diphospho-Thr202/Tyr204 ERK1, and diphospho-Thr183/Tyr185 ERK2 (Figure 3.2).

In order of decreasing responsiveness to adenosine A_{2A} receptor stimulation, levels of the following phosphoproteins were optimally elevated by the indicated treatment with CGS 21680:

1. Phospho-Ser897 NR1 by 1 μM CGS 21680 for 5 min;
2. Diphospho-Thr202/Tyr204 ERK1 by 1 μM CGS 21680 for 10 min;
3. Diphospho-Thr183/Tyr185 ERK2 by 1 μM CGS 21680 for 10 min;
4. Phospho-Thr34 DARPP-32 by 1 μM CGS 21680 for 15 min;
5. Phospho-Ser94 spinophilin by 2 μM CGS 21680 for 15 min;
6. Phospho-Ser845 GluR1 by 5 μM CGS 21680 for 10 min, and;
7. Phospho-Ser133 CREB by 5 μM CGS 21680 for 15 min.

Consistent with the postsynaptic localization of adenosine A_{2A} receptors, CGS 21680 had no effect on the phosphorylation of tyrosine hydroxylase at Ser40, a presynaptic PKA substrate. In these experiments, the antibody for phospho-Ser9 synapsin did not generate interpretable immunoblots (data not shown), but it is suspected that adenosine A_{2A} receptor activation does not alter the phosphorylation level of synapsin at Ser9 due to the presynaptic location of this protein.

3.5. Discussion

These results illustrate the feasibility of a more extensive candidate screen for the identification of additional phosphoprotein effectors in striatal adenosine A_{2A} receptor signaling pathways. However, this approach is inherently limited by the availability and quality of phosphorylation state-specific antibodies for candidate phosphoproteins. A viable alternative to the candidate approach is provided by proteomics. Proteomic analysis has been used successfully in this laboratory to identify novel Cdk5 substrates,

such as the microtubule-binding protein, stathmin (145). With regard to the present line of research, proteomic analysis holds the potential to reveal the involvement of unknown or poorly characterized phosphoproteins in adenosine A_{2A} receptor-mediated effects. By circumventing the assumption that all biochemical signaling pathways relevant to adenosine A_{2A} receptor signaling require the direct or indirect actions of PKA, it also offers the possibility of bringing to light previously unsuspected targets. Indeed, some of the salient signaling events regulated by adenosine A_{2A} receptors in the striatum may be PKA-independent (146). On the other hand, it is important to bear in mind that a proteomic approach would require high-throughput mass spectrometry technology in order to process the large sample sizes likely to be generated by time-course and dose response analyses. Therefore, it may be of limited use for defining the pharmacological parameters required by each target protein to respond optimally to adenosine A_{2A} receptor activation.

This is in contrast to the immunodetection method used in the present study. The findings point to the potential utility of the immunodetection approach for studying the relative responsiveness of different targets to differential adenosine A_{2A} receptor stimulation. As described above, the phosphoproteins examined differed considerably in the extent to which they were up-regulated in response to a given dose of CGS 21680 administered for a given length of time. This observation may have biological significance with respect to the strength and duration of the adenosine stimulus required by each target for optimal phosphorylation under physiological conditions. Based on these results, one could conjecture, for instance, that a process with potentially long-range consequences, such as the up-regulation of CREB-dependent gene expression, does not readily lend itself to modulation by levels of adenosine that normally suffice to regulate a more acute phenomenon like excitatory neurotransmission. By the same speculative token, adenosine A_{2A} receptor activation in the striatum may differently regulate glutamatergic transmission mediated by NMDA- *versus* AMPA-type glutamate receptors. Interestingly, doses of CGS 21680 that increased NR1, but not GluR1, phosphorylation in these experiments have been reported to modulate the conductance of NMDA, but not AMPA, receptors in the striatum (147, 148).

Studies by others have already shown that the PKA-dependent phosphorylation of DARPP-32 and spinophilin is directly regulated by adenosine A_{2A} receptor activation in the striatum (149, 150). However, the evidence in the literature is more indirect with regard to a link between the other phosphoproteins evaluated in this study and adenosine A_{2A} receptors in the striatum.

Although a growing body of evidence indicates that striatal adenosine A_{2A} receptors modulate NMDA receptor-mediated glutamatergic neurotransmission in this tissue (147, 148, 151-155), there is no definitive evidence that these effects are dependent on NR1 phosphorylation at Ser897. Adenosine A_{2A} receptors acting in a PKA-dependent fashion have been reported to potentiate the effects of metabotropic glutamate receptor 5 activation on NMDA-evoked responses in the striatum (156), and more recently, activation of group I metabotropic glutamate receptors has been shown to increase striatal levels of phospho-Ser897 NR1 (157). Thus, the findings described here constitute the first direct indication that NR1 phosphorylation at Ser897 is regulated by adenosine A_{2A} receptor signaling in the striatum.

As for GluR1, it has been reported recently that dopamine D_2 receptors negatively regulate phospho-Ser845 GluR1 levels in the striatum in a PKA/DARPP-32-dependent manner (158). The same study also showed that tonic activation of adenosine A_{2A} receptors by endogenous adenosine is required for the dopamine D_2 receptor antagonist-evoked increase in GluR1 phosphorylation at this PKA/PP-1 site. However, the authors did not evaluate the effect of adenosine A_{2A} receptor signaling alone on Ser845 phosphorylation.

Interestingly, the core promoter of the adenosine A_{2A} receptor gene may be regulated by phospho-Ser133 CREB through an adenosine A_{2A} receptor- and PKA-dependent mechanism in the striatum (159). In light of the results described here, adenosine A_{2A} receptors may therefore directly regulate their own expression by stimulating the phosphorylation and activation of CREB.

Finally, adenosine A_{2A} receptors regulate ERK activity in peripheral tissues and transformed cell lines (160-162). Moreover, in primary striatal cultures, ERK1 and ERK2 may be activated by adenosine A_{2A} receptors through a MEK- and PKA-dependent

pathway (163). However, a direct relationship between adenosine A_{2A} receptors and ERK activation has not been shown in the striatum, or the central nervous system at large. These results are the first demonstration that ERK1 and ERK2 are phosphorylated, and presumably activated, in the striatum in response to adenosine A_{2A} receptor activation. Notably, diphospho-ERK levels were among the most sensitive to stimulation with CGS 21680.

Consistent with the findings here, adenosine A_{2A} receptor-dependent regulation has not been reported for phospho-Ser9 synapsin, phospho-Ser40 tyrosine hydroxylase, or phospho-Thr286 CaMKII.

In conclusion, the present analysis confirms or extends what is currently known about the relationship between the above phosphoproteins and striatal adenosine A_{2A} receptors. Future investigations could address the biochemical, physiological, and behavioral consequences of the observed effects and assess the influence of adenosine A_1 and dopamine D_2 receptor signaling on these pathways using a combination of immunodetection and proteomic analysis.

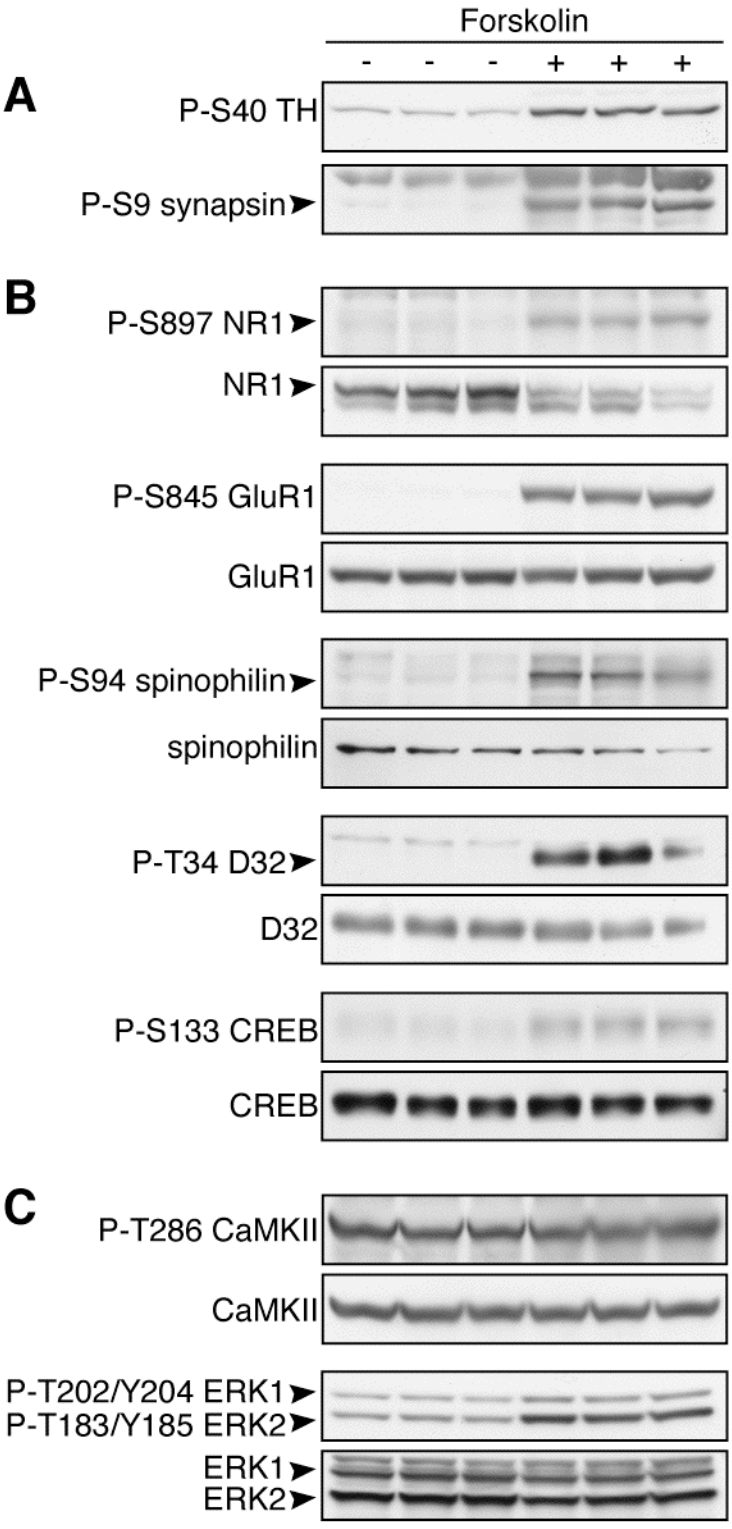
Forskolin
- - - + + +
A
P-S40 TH
P-S9 synapsin
B
P-S897 NR1
NR1
P-S845 GluR1
GluR1
P-S94 spinophilin
spinophilin
P-T34 D32
D32
P-S133 CREB
CREB
C
P-T286 CaMKII
CaMKII
P-T202/Y204 ERK1
P-T183/Y185 ERK2
ERK1
ERK2

Figure 3.1: Regulation of selected phosphoproteins by the adenylate cyclase activator, forskolin, in striatal slices. Immunoblot analysis of *A.* phospho-Ser40 tyrosine hydroxylase (*TH*), phospho-Ser9 synapsin; *B.* phospho-Ser897 NR1, phospho-Ser845 GluR1, phospho-Ser94 spinophilin, phospho-Thr34 DARPP-32 (*D32*), phospho-Ser133 CREB; and *C.* phospho-Thr286 CaMKII, diphospho-Thr202/Tyr204 ERK1, and diphospho-Thr183/Tyr185 ERK2 levels in striatal slices treated with or without forskolin (10 μM, 10 min). Immunoblots of total protein levels are also included for all phosphoproteins except synapsin and tyrosine hydroxylase.

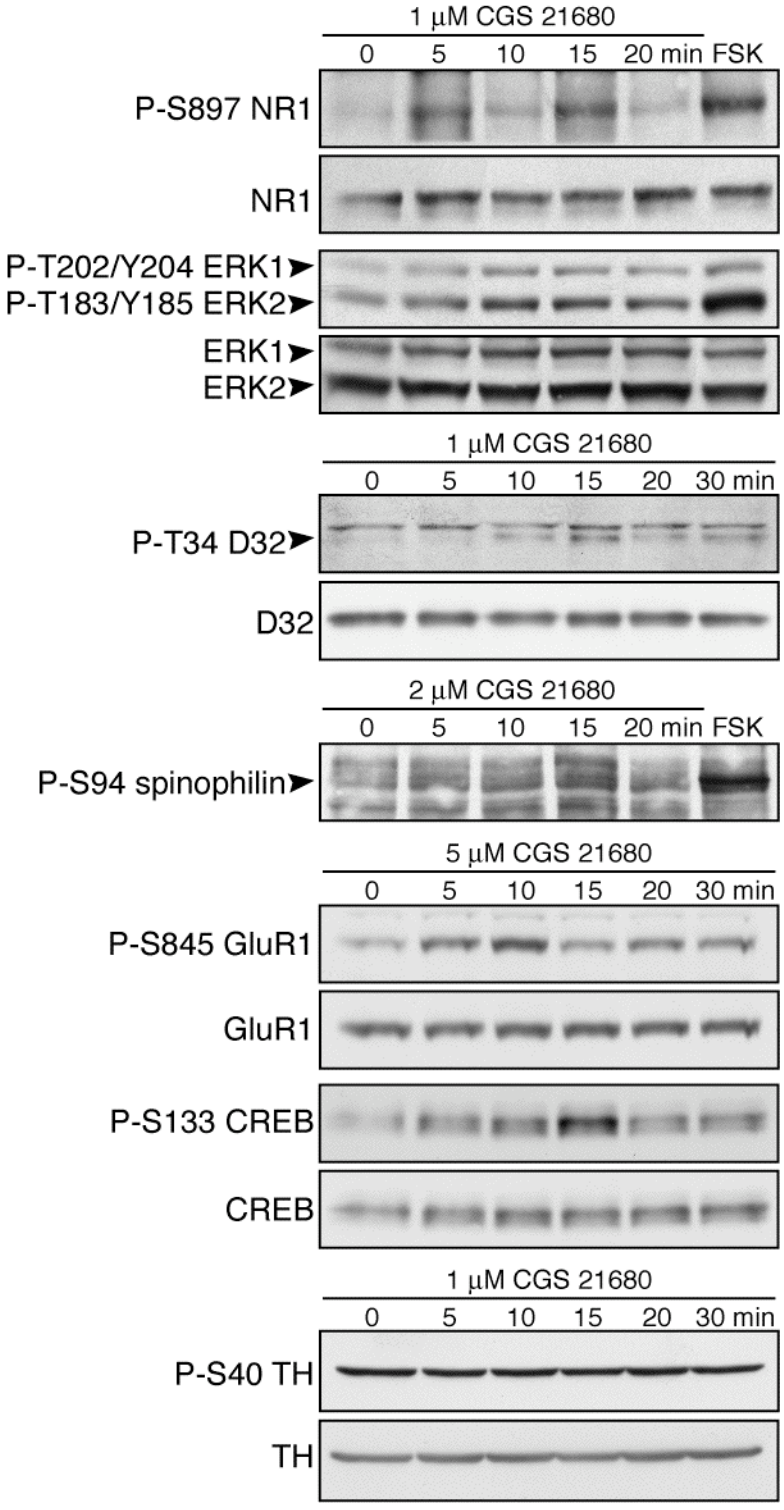
1 μM CGS 21680
0 5 10 15 20 min FSK
P-S897 NR1
NR1
P-T202/Y204 ERK1
P-T183/Y185 ERK2
ERK1
ERK2
1 μM CGS 21680
0 5 10 15 20 30 min
P-T34 D32
D32
2 μM CGS 21680
0 5 10 15 20 min FSK
P-S94 spinophilin
5 μM CGS 21680
0 5 10 15 20 30 min
P-S845 GluR1
GluR1
P-S133 CREB
CREB
1 μM CGS 21680
0 5 10 15 20 30 min
P-S40 TH
TH

Figure 3.2: Regulation of selected phosphoproteins by the adenosine A_{2A} receptor agonist, CGS 21680, in striatal slices. Immunoblot analysis of phospho-Ser897 NR1, diphospho-Thr202/Tyr204 ERK1, diphospho-Thr183/Tyr185 ERK2, phospho-Thr34 DARPP-32 (*D32*), phospho-Ser94 spinophilin, phospho-Ser845 GluR1, phospho-Ser133 CREB, and phospho-Ser40 tyrosine hydroxylase (*TH*) levels in striatal slices treated with CGS 21680 (0-5 μM, 0-30 min). Immunoblots of total protein levels are also shown for all phosphoproteins except spinophilin. In some experiments, control slices were treated with forskolin (*FSK*, 10 μM, 10 min).

CHAPTER 4†

PHOSPHORYLATION OF PROTEIN PHOSPHATASE INHIBITOR-1 BY PROTEIN KINASE C

4.1. Summary

Protein phosphatase inhibitor-1 is a small, unstructured protein that becomes a potent and selective inhibitor of protein phosphatase 1 when phosphorylated by cAMP-dependent protein kinase at Thr35. The following studies indicate that inhibitor-1 is phosphorylated by protein kinase C at Ser65 *in vitro*. Moreover, the use of phosphorylation state-specific antibodies showed that protein kinase C phosphorylates inhibitor-1 at Ser65 in cultured cells and intact striatal brain tissue. Selective pharmacological inhibition of protein phosphatase activity suggested that phospho-Ser65 inhibitor-1 is likely dephosphorylated by protein phosphatase 1 *in vivo*. Under basal conditions, phosphorylation of inhibitor-1 at Ser65 was undetectable in the striatum. However, activation of group I metabotropic glutamate receptors uncovered dynamic regulation of phospho-Ser65 inhibitor-1 in this tissue. Phosphomimetic mutation of Ser65 to Asp did not convert inhibitor-1 into a protein phosphatase 1 inhibitor. On the other hand, *in vitro* and *in vivo* experiments suggested that phospho-Ser65 inhibitor-1 is a less efficient substrate of cAMP-dependent protein kinase. These observations are consistent with earlier studies regarding the function of inhibitor-1 phosphorylation at Ser67 by cyclin-dependent kinase 5 and underscore the possibility that phosphorylation in this region of inhibitor-1 by multiple protein kinases may serve as an integrative

† Parts of this Chapter were published in *Nature Medicine* and *The Journal of Biological Chemistry*.

signaling mechanism that governs the responsiveness of inhibitor-1 to cAMP-dependent protein kinase activation.

4.2. Introduction

Intracellular signal transduction in eukaryotic organisms relies on the precise regulation of protein phosphorylation by protein kinases and protein phosphatases. These enzymes are broadly classified based on their specificity for serine/threonine or tyrosine residues. Approximately equal numbers of protein tyrosine kinases and phosphatases are encoded by most eukaryotic genomes (164, 165). In contrast, merely a handful of protein serine/threonine phosphatases appear to be required for reversing the actions of a much larger cohort of protein serine/threonine kinases (9, 166, 167), raising the question of how protein serine/threonine phosphatase specificity is achieved. To counter this numerical disparity, protein serine/threonine phosphatases rely on a rich array of regulatory subunits that control the localization, activity, and substrate specificity of protein phosphatase catalytic subunits. In the case of protein phosphatase 1 (PP-1), one of the major eukaryotic protein serine/threonine phosphatases, nearly 60 actual and putative regulator proteins have been identified to date (168, 169). Most of these regulators are involved in the targeting of PP-1 to specific subcellular locations, while several modulate its catalytic activity.

Historically, protein phosphatase inhibitor-1 was the first such endogenous molecule found to regulate protein phosphatase activity *in vivo* (170). This 19 kDa protein has a highly conserved primary sequence in vertebrates ranging from fish to mammals (171, 172). It largely lacks elements of secondary structure (173), possibly explaining why it is unusually stable to heat, acid, detergents, and organic solvents (174). Phosphorylation at Thr35 by PKA converts the inactive protein into a selective and highly potent inhibitor of the catalytic subunit of PP-1 ($IC_{50} \approx 1$ nM) (170, 175). This site is dephosphorylated by the type 2 protein phosphatases, PP-2A and PP-2B (Ca^{2+}/calmodulin-dependent protein phosphatase, or calcineurin) (176-178). PP-2B

activity predominates in the presence of high intracellular Ca^{2+}, placing inhibitor-1 regulation under the opposing influences of cAMP and Ca^{2+} signaling. Downstream from inhibitor-1, a mechanism for signal amplification is provided by the substrate specificity of PP-1. PP-1 dephosphorylates a broad spectrum of phosphoproteins targeted by an array of protein kinases, including PKA as well as others (176). Thus, the inhibition of PP-1 by phospho-Thr35 inhibitor-1 results in the amplification of PKA-dependent signaling cascades and has the potential to impose cAMP regulation upon the phosphorylation state of cellular substrates phosphorylated by other protein kinases.

Inhibitor-1 is highly expressed in the brain, adipose tissue, kidney, and skeletal muscle (179), with lower levels occurring in the heart and lung (171). It has been shown to play a particularly important role as a PP-1 inhibitor in excitable tissues like brain and cardiac muscle, where it has emerged as a key player in models of synaptic plasticity (178, 180) and cardiomyocyte contractility (181-183), respectively. Within the brain, inhibitor-1 is especially enriched in the cortex, striatum, and dentate gyrus of the hippocampal formation (184). In the heart, nearly 80% of inhibitor-1 is found in the sarcoplasmic reticulum (185), consistent with a role for inhibitor-1 in the regulation of PP-1 substrates associated with this compartment in cardiomyocytes.

Protein phosphatase regulatory subunits like inhibitor-1 can be regulated by multiple protein kinases and phosphatases, thus serving as potential points of integration for disparate signal transduction cascades. For instance, DARPP-32, a homologous PP-1 inhibitor highly enriched in the striatum, is phosphorylated at different serine/threonine residues by PKA (130), CK1 and CK2 (186, 187), and Cdk5 (188). Consistent with this notion, inhibitor-1 isolated from rabbit skeletal muscle in earlier studies was found to be heavily phosphorylated at Ser67 (189). This residue was later characterized as a site of phosphorylation by MAPK, Cdk1, and Cdk5 *in vitro*, with Cdk5 accounting for all phosphorylation in the brain (190). The same study found that phospho-Ser67 inhibitor-1 does not inhibit PP-1, but rather serves as a moderately less efficient substrate for PKA at Thr35. More recently, it was suggested that inhibitor-1 may be phosphorylated by PKC in cardiac muscle, where phospho-Ser67 inhibitor-1 was implicated in modulating the contractile response by regulating the activity of the SERCA-2 pump in a PKC-dependent

fashion (191). However, the precise interaction between PKC and inhibitor-1 in this novel signaling pathway has not yet been delineated and is the focus of the present study.

The following studies show that inhibitor-1 is phosphorylated by PKC at Ser65 *in vitro* and in intact brain tissue. Under basal conditions inhibitor-1 is maintained in a dephosphorylated state at this site by tonic PP-1 activity. However, activation of $G\alpha_q$-coupled glutamate receptors results in a net increase in phospho-Ser65 inhibitor-1 levels. Furthermore, phosphorylation at Ser65 converts inhibitor-1 into a less efficient substrate for PKA at Thr35. Together, these findings suggest a role for inhibitor-1 as an integrator of the PKA and PKC pathways in the regulation of PP-1 activity in brain and other tissues.

4.3. Experimental Procedures

4.3.1. Chemicals and enzymes

Shrimp alkaline phosphatase (SAP), and endoproteinase Lys-C were from Promega. PP-1 was purchased from Upstate. Phosphorylase *b* kinase was from Sigma. Phosphorylase *b* was from Calzyme. Cell culture reagents were purchased from Invitrogen. Peptides and phosphopeptides were synthesized by Haydn Ball (Protein Chemistry Technology Center, UT Southwestern Medical Center). Phorbol-12,13-dibutyrate (PDBu), Ro-32-0432, and fostriecin were from Calbiochem. Calyculin A was from LC Laboratories. (*S*)-3,5-dihydroxyphenylglycine (DHPG) was from Tocris. Roscovitine was from Calbiochem and Laurent Meijer (Centre National de la Recherche Scientifique, Roscoff, France). All other reagents were from sources indicated in Chapter 2.

4.3.2. Site-directed mutagenesis

The pET-15b expression vector incorporating the cDNA for rat inhibitor-1-His_6 (190) served as a template for site-directed mutagenesis using PCR. Mutants containing single or multiple amino acid substitutions were generated as described in Chapter 2.

4.3.3. Purification of inhibitor-1

Recombinant inhibitor-1 was generated as previously described (190). Chemically competent BL21 (DE3) cells were transformed with pET-15b expression vectors encoding wild-type or mutant rat inhibitor-1. Cultures were grown to log phase, induced with IPTG at 37°C for 2h, and lysed by French press. Cleared lysates were incubated with a nickel-nitrilotriacetic acid-agarose resin (Qiagen). Bound protein was eluted from the resin using a linear gradient of 0 to 500 mM imidazole. All forms of inhibitor-1 eluted at approximately 150 mM imidazole. Samples were dialyzed overnight in 10 mM HEPES, pH 7.4, with two changes of buffer. 10 μg of dialyzed protein were analyzed for purity by SDS-PAGE (15% polyacrylamide) and CBB staining.

4.3.4. In vitro *protein phosphorylation reactions*

All reactions were conducted as described in Chapter 2. In some experiments, preparative phosphorylation of inhibitor-1 by a protein kinase was followed by re-purification of phospho-inhibitor-1 prior to use in a subsequent assay. For these studies, inhibitor-1 was re-purified from *in vitro* protein phosphorylation reaction mixtures by the addition of trichloroacetic acid to 20% in the presence of 0.5 mg/ml BSA, followed by re-suspension of the precipitate in 1 M Tris-HCl, pH 8.0, and overnight dialysis into 10 mM HEPES, pH 7.4, with two changes of buffer. Dephospho-inhibitor-1 was prepared identically except for the use of heat-inactivated protein kinase in the preparative phosphorylation step.

4.3.5. Two-dimensional phosphopeptide mapping

Microcrystalline cellulose TLC plates (Analtech) were used for phosphopeptide mapping. Otherwise, phosphopeptide maps were generated as described in Chapter 2.

4.3.6. PP-1 inhibition assays

The PP-1 substrate, phosphorylase *a*, was generated for these assays by preparative phosphorylation of 30 mg of phosphorylase *b* at 30°C for 60 min in a final volume of 3 ml containing 2.15 mg of phosphorylase *b* kinase, 200 μM ATP, 1.7 mCi/ml [γ-^{32}P] ATP, 100 mM Tris-HCl, pH 8.2, 100 mM β-glycerol phosphate, 0.1 mM $CaCl_2$, and 10 mM magnesium acetate. The reaction was stopped by the addition of an equal volume of 90% saturated $(NH_4)_2SO_4$. Following incubation on ice for 20 min, the mixture was centrifuged at 15,000 × *g* for 15 min. The pellet was resuspended in 45% saturated $(NH_4)_2SO_4$ in wash buffer containing 50 mM Tris-HCl, pH 7.0, 0.1 mM EGTA, and 0.1% β-mercaptoethanol, incubated on ice for 30 min, and centrifuged at 15,000 × *g* for 15 min. The pellet was resuspended in wash buffer and dialyzed for 36 h in 10 mM Tris-HCl, pH 7.5, 0.1 mM EGTA, and 10% glycerol, with 6 changes of buffer. Following dialysis, ^{32}P-phosphorylase *a* was analyzed by the BCA protein assay and Cerenkov counting, and dephosphorylated by PP-1 under linear conditions (130), in the absence or presence of recombinant wild-type inhibitor-1 and site-directed inhibitor-1 mutants re-purified by trichloroacetic acid precipitation from preparative protein phosphorylation reactions conducted with or without PKA. Protein dephosphorylation reactions were conducted at 30°C in a final volume of 30 μl containing 10 μM ^{32}P-phosphorylase *a*, 1 μg/ml PP-1, 50 mM Tris-HCl, pH 7.0, 0.01% BRIJ, 0.1% β-mercaptoethanol, 0.3 mg/ml BSA, 0.1 mM EGTA, 5 mM caffeine, and 0-1 μM inhibitor-1. Reactions were stopped by the addition of 100 μl of 10% trichloroacetic acid. Following centrifugation at 15,000 × *g* for 3 min, supernatants and pellets were analyzed by Cerenkov counting.

4.3.7. Phosphorylation site identification by MS

In one set of experiments, inhibitor-1 from *in vitro* protein phosphorylation reaction mixtures with and without PKC was subjected to SDS-PAGE and in-gel digestion with trypsin. Dried digest mixtures were re-dissolved in 20 μL of 5% formic acid and loaded onto a POROS R2 reversed-phase column (Applied Biosystems) for purification. After being washed with 5% formic acid, peptides were eluted directly into a nanoelectrospray needle (Proxeon Biosystems) with 1 μl of either 50% methanol/1% $NH_3 \cdot H_2O$ for precursor ion scanning in negative ion mode, or 50% methanol/1% acetic acid for tandem mass spectrometry (MS/MS) in positive ion mode. MS analysis was performed on a QSTAR Pulsar I quadrupole time-of-flight (QqTOF) tandem mass spectrometer (Applied Biosystems/MDS SCIEX) equipped with a nanoelectrospray ion source (MDS Proteomics, Odense, Denmark). For precursor ion scanning, the instrument was set in negative ion mode to detect the PO_3^- fragment ion at m/z -79. After data acquisition, the instrument was switched to positive ion mode, and the phosphopeptide sequence and site of phosphorylation were determined by nanoelectrospray-QqTOF MS/MS. In the MS/MS scan mode, the precursor ion was selected in the quadrupole (Q1) and fragmented in the collision cell (q2), using argon as the collision gas. This analysis was performed by Hongjun Shu (Alliance for Cellular Signaling, UT Southwestern Medical Center).

In parallel studies conducted by Joseph Fernandez (Protein/DNA Technology Center, The Rockefeller University), ^{32}P-labeled phospho-inhibitor-1, resulting from phosphorylation by PKC in the presence of [γ-^{32}P] ATP, was subjected to SDS-PAGE and digested with endoproteinase Lys-C. The digest mixture was fractionated by reversed-phase HPLC on a C_{18} column (Vydac, 1.0 mm ID × 150 mm) and collected fractions screened for radioactivity. The fraction containing the radiolabel was subjected to MALDI-TOF analysis. To confirm phosphorylation, a small aliquot of the fraction was treated with SAP in 50 mM NH_4HCO_3 at 37°C for 30 min and analyzed by MALDI-TOF. The remainder of the fraction was dried and the phosphorylation site modified with 1-propanethiol to produce S-propylcysteine after β-elimination of the phosphate. This

modification results in a net mass shift of -21 Da, generating a derivative that is stable to Edman degradation chemistry and elutes after phenylthiohydantoin (PTH)-leucine. The reaction was performed by incubating the phosphopeptide with 10 μl of 1 M NaOH, 3 μl of saturated $Ba(OH)_2$, and 15 μl of 0.5 M 1-propanethiol at 37°C for 2 h. Edman degradation was performed after the modified peptide was analyzed by MALDI-TOF to confirm the completion of the reaction.

4.3.8. Generation of phosphorylation state-specific antibodies

Polyclonal phosphorylation state-specific antibodies for phospho-Ser65 and diphospho-Ser65/Ser67 inhibitor-1 were generated and affinity-purified as previously described (192), using synthetic phosphopeptides encompassing residues 61-69 of mouse and rat inhibitor-1. Briefly, four New Zealand white rabbits were each immunized with 1 ml of a 1:1 emulsified mixture of Freund's complete adjuvant and 300 μg of one of two inhibitor-1 phosphopeptides, incorporating either phospho-Ser65 alone, or phospho-Ser65 and phospho-Ser67, diluted in PBS. Booster injections contained Freund's incomplete adjuvant and 150 μg of phosphopeptide in the same volume. All injections and blood collection were performed by Monya Powell (Animal Resources Center, UT Southwestern Medical Center), following the schedule described in Chapter 2. Phosphorylation state-specific antibodies were purified from the resulting anti-sera using a SulfoLink resin (Pierce) conjugated to the corresponding phosphopeptide antigens. Purified antibodies were evaluated for specificity by immunoblot analysis of dephospho- and phospho-inhibitor-1 standards (50 ng). Three forms of phospho-inhibitor-1 were generated by preparative phosphorylation of inhibitor-1 at Ser65, Ser67, or Ser65 and Ser67 using PKC and/or Cdk5. The reactions with PKC achieved a final stoichiometry of 0.35 mol/mol at Ser65, while the Cdk5 reactions reached a stoichiometry of 1 mol/mol at Ser67. Diphospho-Ser65/Ser67 inhibitor-1 was generated by phosphorylating inhibitor-1 sequentially with PKC and then with Cdk5. The inhibitor-1 phosphopeptides used in these studies, KSTLpSMSPR, phosphorylated at the second serine residue, and KSTLpSMpSPR, phosphorylated at the second and third serine residues, were

synthesized by Haydn Ball (Protein Chemistry Technology Center, UT Southwestern Medical Center).

4.3.9. Infection of cultured cells with replication-deficient adenoviruses

The replication-deficient adenoviruses encoding rat inhibitor-1 (182) and constitutively active PKC-α (193) were kindly provided by Thomas Eschenhagen (University Hospital Hamburg-Eppendorf, Hamburg, Germany) and Jeffery Molkentin (University of Cincinnati, Children's Hospital Medical Center), respectively. PC12 rat pheochromocytoma cells, courtesy of Eric Nestler (UT Southwestern Medical Center), were cultured in Dulbecco's modified Eagle's medium (DMEM) containing 5% fetal bovine serum (FBS) and 10% horse serum in either 60 mm plates for eventual immunoblot analysis or 2-well glass slides (Lab-Tek II CC2 Chamber Slide System, Nalge Nunc International) for eventual immunocytochemical staining. After 24 h, the culture medium was changed and cells were infected with a selected adenovirus at a multiplicity of infection of 100 plaque-forming units for 2 h at 37°C in a humidified 5% CO_2 incubator. Infected cells were cultured for an additional 24 h before being harvested for immunoblot analysis or processed for immunocytochemistry.

N2a mouse neuroblastoma cells, a gift from Susanne Mumby (UT Southwestern Medical Center), were cultured in DMEM containing 10% FBS and infected with the adenovirus encoding inhibitor-1. Subsequently, cells were cultured for 24 h and treated with 1 μM PDBu for 10 min following incubation in the presence or absence of 1 μM Ro-32-0432 for 1 h. After drug treatment, cells were collected in phosphate-buffered saline using a cell scraper. Following centrifugation, cell pellets were rapidly frozen on dry ice and stored at -80°C until assayed.

4.3.10. Preparation and incubation of acute striatal slices

All striatal slice pharmacology studies were conducted as described in previous Chapters, using drugs as specified for each experiment.

4.3.11. Immunoblot analysis of cell and tissue homogenates

Frozen cell pellets and striatal tissue samples were processed for immunoblot analysis as described in Chapter 3. 100 μg of total protein from each sample were subjected to SDS-PAGE (15% polyacrylamide) followed by electrophoretic transfer to nitrocellulose membranes (0.2 μm) (Whatman). The membranes were immunoblotted as described in Chapter 2, using primary antibodies for phospho-Ser65 inhibitor-1 (1:500) (see Results), phospho-Ser67 inhibitor-1 (1:5000) (190), diphospho-Ser65/Ser67 inhibitor-1 (1:500) (see Results), total inhibitor-1 (1:4000) (184), phospho-Thr34 DARPP-32/phospho-Thr35 inhibitor-1 (1:750) (143), total DARPP-32 (1:8000) (144), phospho-Ser831 GluR1 (1:500) (Upstate), total GluR1 (1:500) (Upstate), PKC (α, β, γ) (1:500) (Upstate), or β-actin (1:500,000) (Abcam). For the detection of phospho-Thr35 inhibitor-1, membranes were blocked for 1 h at room temperature in TBS-Tween containing 5% BSA and incubated overnight at 4°C with a primary antibody dilution in the same solution. For quantification, apparent phosphoprotein levels were adjusted to reflect relative levels of total protein loaded per lane. The pharmacological manipulations used in these studies did not alter the total amount of inhibitor-1, DARPP-32, or GluR1 in cells or striatal slices.

4.3.12. Immunocytochemistry

To localize subcellular regions of PKC and inhibitor-1 expression, PC12 cells cultured in 2-well glass slides and acutely infected with a selected adenoviral vector were incubated in the absence or presence of 5 μM PDBu for 10 min and processed for immunocytochemistry. Briefly, cells were washed in PBS several times and fixed with 4% paraformaldehyde in PBS for 10 min at room temperature. Fixed cells were washed in PBS and blocked in 0.25% cold water fish gelatin in PBS containing 0.04% saponin for 1 h at room temperature. After being washed in PBS, cells were incubated for 1 h at room temperature with the antibody for PKC (α, β, γ), total inhibitor-1, or diphospho-Ser65/Ser67 inhibitor-1 diluted 1:100 in blocking solution containing 0.01% NaN_3.

Following incubation with the primary antibody, cells were washed in PBS several times and incubated for 30 min at room temperature with Cy2-conjugated goat anti-rabbit immunoglobulin G (Jackson ImmunoResearch Laboratories) diluted 1:1000 in blocking solution. Sections were washed several times in PBS and once in water, allowed to dry at room temperature after removal of chambers, and cover-slipped for visualization using an Olympus BX51 epifluorescence microscope. To verify the specificity of the immunoreactivity, the primary antibody step was omitted in the staining procedure for a subset of control cells.

4.3.13. Statistical analysis

Differences between data groups were evaluated for significance using a Student's *t* test of unpaired data (± standard error of the mean).

4.4. Results

4.4.1. Identification of Ser65 as the site of inhibitor-1 phosphorylation by PKC

Inhibitor-1 serves as an efficient substrate for PKC *in vitro* (Figure 4.1). A time-course protein phosphorylation reaction conducted in the presence of excess PKC over the course of 2 h displayed linear conversion of inhibitor-1 to phospho-inhibitor-1 in the first 10 min and near-saturation by 60 min, with a final stoichiometry greater than 0.6 mol/mol. Previous evidence implicated Ser67 of inhibitor-1 as a possible site of phosphorylation by PKC (191). Indeed, mutation of this serine residue to alanine resulted in a partial reduction (~30%) in the ability of PKC to phosphorylate inhibitor-1 *in vitro* (Figure 4.2A). Since this mutation alone was insufficient to eliminate PKC-dependent phosphorylation entirely, it was conjectured that Ser67 is one of multiple inhibitor-1 sites phosphorylated by PKC. However, a phosphorylation state-specific antibody against phospho-Ser67 inhibitor-1 failed to detect any phosphorylation of this

residue by PKC *in vitro* (Figure 4.2B). In contrast, the same antibody was able to detect MAPK-dependent phosphorylation of inhibitor-1 at Ser67, as expected (190). These findings suggested that Ser67 of inhibitor-1 is not a PKC target, although mutation of this residue adversely affects phosphorylation of another, heretofore unidentified, residue by PKC, raising the possibility that Ser67 may be near the PKC site.

To further characterize the PKC-dependent phosphorylation of inhibitor-1 *in vitro* and evaluate whether the inhibitor-1 PKC site is close to Ser67, various phosphorylated forms of inhibitor-1 were analyzed by phosphopeptide mapping (Figure 4.2C). Cdk5 phosphorylates inhibitor-1 at Ser67 (190) and Ser6, a residue near the N-terminal PP-1 binding motif (James Bibb, unpublished observation). Accordingly, a phosphopeptide map of inhibitor-1 preparatively phosphorylated by Cdk5 in the presence of [γ-^{32}P] ATP showed two major spots (*1* and *2*), likely corresponding to the two phosphopeptides encompassing phospho-Ser6 and phospho-Ser67 (Figure 4.2C, top panel). In contrast, a phosphopeptide map of inhibitor-1 preparatively phosphorylated by PKC contained only one predominant spot (Figure 4.2C, middle panel). This single spot appeared to migrate in the same fashion as spot 2 of the first phosphopeptide map, suggesting that the PKC site may be identical to or occur on the same tryptic inhibitor-1 peptide as one of the two Cdk5 sites. A phosphopeptide map of Ser6→Ala inhibitor-1 phosphorylated by Cdk5 lacked spot 1 entirely, but not spot 2 (Figure 4.2C, bottom panel), indicating that spot 2 represents phospho-Ser67. These results lend further weight to the notion that PKC phosphorylates a target residue in the immediate vicinity of Ser67.

Two different approaches were used to directly identify the site of PKC-dependent phosphorylation. First, inhibitor-1 from *in vitro* protein phosphorylation reactions conducted with and without PKC was digested with trypsin and analyzed by nanoelectrospray-QqTOF MS/MS. Based on the generation of a PO_3^- fragment ion at m/z -79, a single phosphopeptide candidate was isolated by the quadrupole and fragmented in the collision cell. Spectral analysis of the collision fragments identified the phosphopeptide as STLpSMSPR, phosphorylated at the second serine residue (Figure 4.3A), which corresponds to Ser65 of inhibitor-1. This analysis was conducted by Hongjun Shu (Alliance for Cellular Signaling, UT Southwestern Medical Center).

This finding was reproduced by a second approach, in which inhibitor-1 preparatively phosphorylated by PKC in the presence of [γ-^{32}P] ATP was digested with endoproteinase Lys-C, and proteolytic fragments were subjected to MALDI-TOF MS analysis and Edman degradation sequencing. Specifically, the digest mixture was fractionated by reversed-phase HPLC and collected fractions screened for radioactivity. Counts were found primarily in a single fraction, which produced a predominant mass of 1371.2, corresponding to the sequence STLSMSPRQRK +80 Da (Figure 4.3B, top panel) and indicating the presence of a phosphorylation site. A small portion of the fraction was treated with SAP, and a mass of 1291.6 was observed (Figure 4.3B, middle panel), confirming the peptide was phosphorylated. The remainder of the fraction was dried and the phosphorylation site modified with 1-propanethiol to produce a stable derivative to Edman degradation chemistry. A mass of 1349.4 was observed after MALDI-TOF MS analysis (Figure 4.3B, bottom panel), corresponding to the expected mass shift of -21 Da and indicating a complete reaction. Edman degradation was performed on the derivatized fraction. PTH-S-propylcysteine was observed in cycle 4 (data not shown), indicating that the fourth N-terminal residue, corresponding to Ser65 of inhibitor-1, is the site of phosphorylation. This analysis was performed by Joseph Fernandez (Protein/DNA Technology Center, The Rockefeller University).

These findings were confirmed by site-directed mutagenesis of Ser65 to alanine (Figure 4.3C). Unlike wild-type inhibitor-1 or the Ser67→Ala mutant, Ser65→Ala inhibitor-1 did not serve as a PKC substrate to any detectable extent, consistent with the conclusion that this residue is the only site of phosphorylation by PKC. The proximity of this PKC site to Ser67 (within two positions in the N-terminal direction) may help explain the adverse effect of the Ser67→Ala mutation on the ability of PKC to phosphorylate inhibitor-1 at the nearby Ser65 residue.

4.4.2. Generation of phosphorylation state-specific antibodies for phospho-Ser65 inhibitor-1

To further study the phosphorylation of inhibitor-1 by PKC *in vitro* and *in vivo*, two phosphorylation state-specific antibodies were generated in order to detect inhibitor-1 when it is either singly phosphorylated at Ser65, or doubly phosphorylated at Ser65 and Ser67 (Figure 4.4). Immunoblot analysis of recombinant inhibitor-1 phosphorylated *in vitro* using purified PKC, Cdk5, or PKC and Cdk5 showed that the two novel antibodies, like the previously characterized antibody for phospho-Ser67 inhibitor-1, do not detect dephospho-inhibitor-1. Moreover, each antibody is highly selective for the form of phospho-inhibitor-1 against which it was raised.

The antibody for phospho-Ser65 inhibitor-1 detected inhibitor-1 only when it was phosphorylated by PKC (Figure 4.4**,** first panel). Interestingly, Cdk5-dependent phosphorylation of inhibitor-1 that had already been phosphorylated by PKC eliminated the ability of the antibody to detect phospho-Ser65, presumably due to steric hindrance from the additional phosphate group transferred to the nearby Ser67 residue by Cdk5. Thus, this antibody was found to have a high degree of specificity for inhibitor-1 singly phosphorylated at Ser65.

The antibody for diphospho-Ser65/Ser67 inhibitor-1 selectively detected inhibitor-1 phosphorylated by PKC and Cdk5 (Figure 4.4**,** third panel). Cdk5-dependent phosphorylation alone was not detectable with this antibody. On the other hand, the antibody did detect inhibitor-1 phosphorylated by PKC alone, although 6-fold less efficiently than it detected inhibitor-1 serially phosphorylated by PKC and Cdk5. Hence, this antibody was found to be highly selective for diphospho-Ser65/Ser67 inhibitor-1, with little (phospho-Ser65) or no (phospho-Ser67) detection of phospho-inhibitor-1 species phosphorylated singly at one of these residues.

The previously characterized antibody for phospho-Ser67 inhibitor-1 was also highly selective for its target (Figure 4.4**,** second panel). It did not detect dephospho-inhibitor-1 or inhibitor-1 phosphorylated by PKC. The apparent ability of the antibody to partially detect inhibitor-1 serially phosphorylated by PKC and Cdk5 was likely

attributable to the incomplete phosphorylation of Ser65 in the diphospho-Ser65/Ser67 inhibitor-1 standard used in this screen. During the generation of this doubly phosphorylated form of inhibitor-1, a final stoichiometry of 0.35 mol/mol was achieved in the preparative protein phosphorylation reaction with PKC, while the subsequent reaction with Cdk5 reached a stoichiometry of 1.0 mol/mol. As a result, a heterogeneous product mixture was produced, containing 35% diphospho-Ser65/Ser67 and 65% phospho-Ser67 inhibitor-1. The antibody for phospho-Ser67 inhibitor-1 detected this mixture 63% as efficiently as it detected inhibitor-1 phosphorylated by Cdk5 alone. The relative signal intensity of 63% can be explained by the abundance of phospho-Ser67 inhibitor-1 (65%) in the sample and the inability of the antibody for phospho-Ser67 inhibitor-1 to detect inhibitor-1 doubly phosphorylated at Ser65 and Ser67. It is reasonable to conclude from these findings that the antibody for phospho-Ser67 inhibitor-1 is highly specific for inhibitor-1 phosphorylated at Ser67 and does not detect its target when the nearby Ser65 residue is also phosphorylated, possibly due to the same steric factors mentioned above for the antibody for phospho-Ser65 inhibitor-1.

In addition to illustrating the specificity of these antibodies for the forms of inhibitor-1 they were generated to detect, these findings further confirm that PKC phosphorylates inhibitor-1 at Ser65 *in vitro*.

4.4.3. Phosphorylation of inhibitor-1 by exogenous PKC-α in PC12 cells

To determine whether inhibitor-1 can be phosphorylated by PKC in living cells, recombinant inhibitor-1 and a constitutively active form of PKC-α were overexpressed in PC12 rat pheochromocytoma cells using adenoviral vectors. Acute infection of PC12 cells with the adenovirus encoding constitutively active PKC-α (Ad PKC-α) resulted in a 10-fold increase in the expression of PKC-α in these cells, as determined by immunoblot analysis (Figure 4.5A, top panel). Infection with the adenovirus encoding inhibitor-1 (Ad I-1) led to a 2.5-fold increase in the level of inhibitor-1 protein expression (Figure 4.5A, second panel).

No phosphorylation of inhibitor-1 at Ser65 was detectable with the antibody for phospho-Ser65 inhibitor-1 in cells infected with Ad I-1 or co-infected with Ad I-1 and Ad PKC-α (Figure 4.5A, third panel). However, when the same blot was re-probed with the antibody for diphospho-Ser65/Ser67 inhibitor-1, dual phosphorylation of inhibitor-1 at Ser65 and Ser67 was readily detected in cells co-infected with Ad I-1 and Ad PKC-α (Figure 4.5A, fourth panel). Basal levels of diphospho-Ser65/Ser67 inhibitor-1 remained undetectable in cells infected with Ad I-1 alone. This result illustrates that PKC-α is able to phosphorylate inhibitor-1 at Ser65 in living cells and further suggests that this phosphorylation occurs in the context of phosphorylation at the nearby Ser67 residue.

In these experiments, levels of phospho-Ser67 inhibitor-1 increased in cells as result of infection with Ad I-1, but remained unaltered by co-infection with Ad PKC-α (Figure 4.5A, fifth panel).

4.4.4. Regulation of phospho-Ser65 inhibitor-1 by a phorbol ester and a specific PKC inhibitor in N2a cells and striatal slices

To assess the phosphorylation of inhibitor-1 by endogenous PKC activity in another cell line, N2a mouse neuroblastoma cells acutely infected with Ad I-1 were treated with the PKC-activating phorbol ester, PDBu, in the absence or presence of the specific PKC inhibitor, Ro-32-0432. Treatment of infected N2a cells with PDBu resulted in an increase in the phosphorylation of inhibitor-1 at Ser65 that was detected by the antibody for diphospho-Ser65/Ser67 inhibitor-1 (Figure 4.5B, second panel), but not the antibody for phospho-Ser65 inhibitor-1 (Figure 4.5B, first panel). This increase in phosphorylation was reversed by pretreatment of the cells with Ro-32-0432, suggesting that the effect of PDBu is PKC-dependent. Treatment with PDBu or Ro-32-0432 did not alter the levels of phospho-Ser67 inhibitor-1 in these cells (Figure 4.5B, third panel). These results demonstrate that activation of endogenous PKCs in living cells results in the net phosphorylation of inhibitor-1 at Ser65, also in the context of phosphorylation at Ser67.

Phosphorylation of inhibitor-1 by PKC was next assessed in mouse striatal tissue, where inhibitor-1 is highly expressed. As in PC12 cells infected with Ad PKC-α and N2a cells treated with PDBu, phosphorylation of inhibitor-1 at Ser65 was detectable in PDBu-treated striatal slices using the antibody for diphospho-Ser65/Ser67 inhibitor-1 (Figure 4.6A), but not the antibody for phospho-Ser65 inhibitor-1 (data not shown). These results strongly argue that phospho-Ser65 inhibitor-1 either does not occur *in vivo* in the absence of Ser67 phosphorylation, or does not persist long enough for detection. Therefore, all subsequent experiments to detect phosphorylation of inhibitor-1 at Ser65 were conducted using the antibody for diphospho-Ser65/Ser67 inhibitor-1.

Using this dual site-specific antibody, virtually no phosphorylation of inhibitor-1 at Ser65 was detected in striatal slices under basal conditions (Figure 4.6A, 0 min and 0 μM PDBu). However, treatment with PDBu resulted in a time- and dose-dependent increase in the phosphorylation of inhibitor-1 at Ser65 in this tissue (Figure 4.6A). The optimal PDBu concentration and incubation time for maximal phosphorylation of Ser65 were defined as 5 μM PDBu for 15 min (n = 4). Pretreatment of striatal slices with the PKC inhibitor, Ro-32-0432, reduced the level of maximal phosphorylation by 88 ± 3% (n = 5) (Figure 4.6B, left), indicating that PDBu-induced phosphorylation of inhibitor-1 at Ser65 in the striatum is dependent on PKC activity. A similar reduction (73 ± 6%, n = 5) was observed with a known PKC target, Ser831 of the AMPA-type glutamate receptor subunit, GluR1 (Figure 4.6B, right).

4.4.5. Regulation of phospho-Ser65 inhibitor-1 by protein phosphatase inhibitors and DHPG in striatal slices

Phospho-Ser67 inhibitor-1 is dephosphorylated by PP-2A and PP-2B in the striatum (190). To characterize the dephosphorylation of phospho-Ser65 inhibitor-1 in the same tissue, striatal slices were treated with a panel of selective protein phosphatase inhibitors (Figure 4.7A). The PP-2B inhibitor, cyclosporin A, and PP-2A inhibitor, fostriecin, had no significant effect on diphospho-Ser65/Ser67 inhibitor-1 levels. Okadaic acid inhibits PP-1 and PP-2A differentially in a dose-dependent manner (194).

At a concentration of 0.2 μM, it inhibits 80% of PP-2A activity and 5% of PP-1 activity, whereas at 1 μM, it inhibits 95% of PP-2A activity and 35% of PP-1 activity. Thus, the higher dose is 7-fold more effective at inhibiting PP-1, but only 1.2-fold more effective at inhibiting PP-2A. 0.2 μM okadaic acid, which predominantly inhibits PP-2A, caused a small, but significant, increase in the levels of diphospho-Ser65/Ser67 inhibitor-1 in striatal slices. On the other hand, treatment with 1 μM okadaic acid resulted in a more substantial increase that was comparable to the maximal effect of PDBu and was 4.6-fold larger than the increase caused by the lower dose of okadaic acid. This difference, together with the failure of fostriecin to cause a change in diphospho-Ser65/Ser67 inhibitor-1 levels, suggests that PP-1 is likely the major protein phosphatase that dephosphorylates phospho-Ser65 inhibitor-1 in the striatum. Treatment with calyculin A, which equally inhibits most PP-1 and PP-2A activity at 1 μM (194), caused an increase in diphospho-Ser65/Ser67 inhibitor-1 levels that was comparable to the increase due to the high dose of okadaic acid, consistent with a role for PP-1 in the dephosphorylation of phospho-Ser65 inhibitor-1. Pretreatment of striatal slices with the PKC inhibitor, Ro-32-0432, attenuated the effects of okadaic acid (1 μM) and calyculin A by 64 ± 2% and 71 ± 3%, respectively, indicating that PKC activity is required for the increase in phosphorylation of Ser65 as a result of PP-1 inhibition.

Glutamatergic innervation from the cerebral cortex and thalamus, together with dopaminergic innervation from the substantia nigra, accounts for the majority of afferent inputs to the striatum (195). To determine whether PKC-dependent phosphorylation of inhibitor-1 in this structure is regulated by $G\alpha_q$-coupled glutamate receptors, diphospho-Ser65/Ser67 inhibitor-1 levels were assessed in striatal slices treated with DHPG, a group I metabotropic glutamate receptor agonist. DHPG treatment alone had no effect on the levels of diphospho-Ser65/Ser67 inhibitor-1 (data not shown). As discussed in the previous section, diphospho-Ser65/Ser67 inhibitor-1 levels are virtually undetectable in unstimulated striatal slices. This is likely a result of tonic PP-1 activity at Ser65. To improve the probability of detecting regulation of this site by group I metabotropic glutamate receptor activation, striatal slices were briefly incubated with 0.5 μM calyculin A, resulting in a modest, but detectable, increase in diphospho-Ser65/Ser67 inhibitor-1

levels (Figure 4.7B, control). Subsequent treatment with DHPG caused a further, significant elevation in phosphorylation, suggesting that under conditions of reduced PP-1 activity, the phosphorylation state of inhibitor-1 at Ser65 may be regulated by glutamatergic neurotransmission via $G\alpha_q$-coupled glutamate receptors in the striatum (Figure 4.7B).

4.4.6. Analysis of the effect of phospho-Ser65 upon the ability of inhibitor-1 to serve as a PP-1 inhibitor and PKA substrate

Unlike phospho-Thr35 inhibitor-1, phospho-Ser67 inhibitor-1 does not serve as an inhibitor of PP-1; however, phosphorylation at Ser67 turns inhibitor-1 into a slightly poorer PKA substrate, thereby reducing the efficiency with which it can be converted into a PP-1 inhibitor (190). To assess the effect of phosphorylation at Ser65 on the ability of inhibitor-1 to inhibit PP-1 or serve as a substrate for PKA, recombinant inhibitor-1 was preparatively phosphorylated with PKC. However, these reactions achieved stoichiometries no greater than 0.35 mol/mol, possibly due to product inhibition, the instability of enzyme-lipid complexes in aqueous solution, and/or the labile nature of purified PKC preparations stored frozen over long periods. Therefore, the predicted phosphomimetic inhibitor-1 mutants, Ser65→Asp, Ser67→Asp, and Ser65+Ser67→Asp, were generated in order to simulate constitutive phosphorylation of inhibitor-1 at Ser65 and/or Ser67.

Wild-type and Ser65+Ser67→Asp inhibitor-1 from *in vitro* protein phosphorylation reactions conducted with and without PKA were evaluated for their ability to inhibit PP-1 *in vitro* (Figure 4.8). In the absence of phosphorylation at Thr35, wild-type or Ser65+Ser67→Asp inhibitor-1 did not inhibit the activity of PP-1 at any of the concentrations tested (0-1 μM). On the other hand, phospho-Thr35 forms of wild-type and Ser65+Ser67→Asp inhibitor-1 inhibited PP-1 activity with equal potency (IC_{50} ≈ 6.0 nM). Identical results were derived using dephospho- and phospho-Thr35 forms of Ser65→Asp and Ser67→Asp inhibitor-1 (data not shown). These results suggest that phosphorylation of Ser65, alone or together with Ser67, neither converts inhibitor-1 into a

PP-1 inhibitor, nor exerts any significant effect on the inhibitory activity of phospho-Thr35 inhibitor-1 toward PP-1.

Next, the ability of phosphomimetic inhibitor-1 mutants to serve as a substrate for PKA under linear conditions was evaluated (Figure 4.9A). Wild-type and Ser67→Asp inhibitor-1 were phosphorylated by PKA with similar efficiency. However, mutation of Ser65 to aspartate resulted in a 42.3 ± 4.1% reduction in the initial rate of phosphate incorporation by PKA. The initial reaction rate was further reduced (55.6 ± 2.5%) by mutation of both Ser65 and Ser67 to aspartate. Thus, while the Ser67→Asp mutation by itself was not sufficient to alter the ability of inhibitor-1 to serve as a PKA substrate, it had a small, but significant, inhibitory effect when Ser65 was also mutated.

To better understand the mechanism by which these phosphomimetic mutations reduce the ability of inhibitor-1 to be phosphorylated by PKA, apparent K_m and k_{cat} values were determined for the PKA-dependent phosphorylation of wild-type and Ser65+Ser67→Asp inhibitor-1. The mutation of both Ser65 and Ser67 to aspartate did not alter the apparent K_m of the reaction, but decreased the k_{cat} value from 0.45 ± 0.07 s^{-1} to 0.20 ± 0.01 s^{-1} (n = 4), suggesting that phosphomimetic mutation of these serine residues does not alter the binding affinity of inhibitor-1 for PKA, but reduces the turnover number, resulting in a significant decrease in catalytic efficiency (k_{cat}/K_m) from (7.6 ± 0.2) × 10^4 $M^{-1}s^{-1}$ to (3.5 ± 0.1) × 10^4 $M^{-1}s^{-1}$ ($p < 0.001$, Student's unpaired t test, n = 4) (Figure 4.9B).

The possibility that PKC-dependent phosphorylation of inhibitor-1 at Ser65 reduces the ability of inhibitor-1 to serve as a PKA substrate at Thr35 was evaluated *in vivo* by treatment of striatal slices with the adenylate cyclase activator, forskolin, following incubation in the absence or presence of PDBu. Pretreatment with PDBu attenuated the increase in levels of phospho-Thr35 inhibitor-1 in striatal slices treated with forskolin (Figure 4.9C, left). In contrast, PDBu had no significant effect on the elevation of phospho-Thr34 DARPP-32 levels resulting from forskolin treatment of the same slices (Figure 4.9C, right), suggesting that the activation of PKC in striatal slices specifically alters the ability of inhibitor-1 to be phosphorylated by PKA.

4.4.7. Analysis of the effect of phospho-Ser65 and phospho-Ser67 on Cdk5- and PKC-dependent phosphorylation of inhibitor-1, respectively

As described above, the single site-specific antibodies for phospho-Ser65 and phospho-Ser67 inhibitor-1 do not detect phosphorylation at these sites when both Ser65 and Ser67 are phosphorylated. This is likely due to steric hindrance exerted on antigen-antibody binding by the presence of a large, negatively charged phosphate group at a nearby position. Steric factors may also impinge on enzyme-substrate interactions. Therefore, the effect of phospho-Ser65 on the Cdk5-dependent phosphorylation of inhibitor-1 was assessed by evaluating the ability of Cdk5 to phosphorylate inhibitor-1 from *in vitro* protein phosphorylation reactions conducted in the absence or presence of PKC (Figure 4.10A, left). Similarly, PKC was evaluated for its ability to phosphorylate inhibitor-1 from *in vitro* protein phosphorylation reactions conducted with or without Cdk5 (Figure 4.10A, right). Prior phosphorylation of Ser65 by PKC (0.7 mol/mol) did not have a significant effect on the final stoichiometry of inhibitor-1 phosphorylation by Cdk5. In contrast, prior phosphorylation of inhibitor-1 by Cdk5 (1.8 mol/mol) resulted in a 91 ± 6% decrease in the final stoichiometry of phosphorylation of Ser65 by PKC. Similar results were obtained when PKC and Cdk5 were used to phosphorylate the phosphomimetic inhibitor-1 mutants, Ser67→Asp and Ser65→Asp, respectively (Figure 4.10B).

Conducted in the presence of excess enzyme over the course of 90 min, these protein phosphorylation reactions are unlikely to represent the phosphorylation of inhibitor-1 under physiological conditions. *In vivo*, inhibitor-1 phosphorylation by PKC or Cdk5 probably does not proceed to completion or achieve equilibrium at substoichiometric levels of phosphate incorporation. In this regard, determination of initial *in vitro* reaction rates is likely to be more informative than stoichiometric analysis of the full time-course of each reaction. Therefore, the effect of phospho-Ser67 on the initial rate of inhibitor-1 phosphorylation by PKC was also evaluated. Phospho-Ser67 inhibitor-1 was phosphorylated by PKC with an initial reaction rate that was 8-fold lower than that of dephospho-inhibitor-1 (Figure 4.10C). Thus, under linear steady-state

conditions, phospho-Ser67 inhibitor-1 served as a much less efficient PKC substrate, suggesting that this form of inhibitor-1 is unlikely to serve as a PKC substrate *in vivo*.

4.4.8. Investigation of the mechanism by which phospho-Ser65 occurs only in the context of phospho-Ser67 inhibitor-1 in vivo

As described in previous sections, PKC-dependent phosphorylation of inhibitor-1 at Ser65 in cultured cells and intact striatal tissue was detected by the antibody for diphospho-Ser65/Ser67 inhibitor-1, but not the antibody for phospho-Ser65 inhibitor-1. Phospho-Ser65 would be expected to occur only in the presence of phospho-Ser67 if inhibitor-1 were fully phosphorylated at Ser67 *in vivo*. However, the stoichiometry of phosphorylation of inhibitor-1 at Ser67 is only 0.34 mol/mol under basal conditions in the striatum (190). In the absence of full phosphorylation at Ser67, these findings suggest that either *1)* only phospho-Ser67 inhibitor-1 is phosphorylated by PKC *in vivo*, while dephospho-inhibitor-1 is not, or *2)* phospho-Ser65 alone does not persist long enough for detection, possibly due to *i.* rapid dephosphorylation by PP-1, or *ii.* rapid phosphorylation of Ser67 by Cdk5. Each of these possibilities is considered in turn below.

1. The first possibility predicts that compared to dephospho-inhibitor-1, phospho-Ser67 inhibitor-1 would serve as an equally efficient, if not better, PKC substrate *in vitro*. However, in protein phosphorylation reactions conducted with PKC under linear steady-state conditions, dephospho-inhibitor-1 was phosphorylated 8-fold more efficiently than phospho-Ser67 inhibitor-1 (Figure 4.10C), indicating that all else being equal the latter is probably not a preferred PKC substrate *in vivo*.

While the PKC-dependent phosphorylation of phospho-Ser67 inhibitor-1 may be kinetically unfavorable *in vitro*, it remains possible that inside the cell PKC is enabled by an unknown mechanism to phosphorylate phospho-Ser67 inhibitor-1 rather than dephospho-inhibitor-1. For example, a regulatory protein may convert phospho-Ser67 inhibitor-1 into a more efficient PKC substrate, or subcellular localization may selectively direct activated PKC to phospho-Ser67 inhibitor-1 while precluding contact with dephospho-inhibitor-1. To evaluate the possibility that active PKC co-localizes with

phospho-Ser67 inhibitor-1 in PC12 cells, uninfected controls and cells acutely infected with Ad I-1 or Ad PKC-α were incubated in the absence or presence of PDBu and immunocytochemically stained for PKC (α, β, γ), total inhibitor-1, or diphospho-Ser65/Ser67 inhibitor-1 (Figure 4.11). To determine background levels of immunoreactivity, a set of control cells were stained using secondary antibody alone (data not shown). Endogenous levels of PKC and inhibitor-1 protein expression in PC12 cells were too low to be detected by this method (Figure 4.11A and B, top panels). Overexpression of PKC and inhibitor-1 by acute infection of PC12 cells with adenoviral vectors enhanced detection, but resulted in a diffuse cytosolic staining pattern (Figure 4.11A and B, bottom panels), making it difficult to draw conclusions about the subcellular localization of endogenous or exogenous forms of PKC or inhibitor-1. Although uninformative by this measure, these results did illustrate the potential utility of the antibody for diphospho-Ser65/Ser67 inhibitor-1 as a marker for PKC-dependent phosphorylation in cultured cells (Figure 4.11C, lower right panel).

These findings do not provide conclusive evidence for phospho-Ser67 inhibitor-1 phosphorylation by PKC *in vitro* or *in vivo*.

2-i. It is possible that phosphorylation of inhibitor-1 at Ser65 alone is not detected *in vivo* because phospho-Ser65 is rapidly dephosphorylated by PP-1 unless it is protected by phospho-Ser67. This explanation predicts that inhibition of PP-1 activity would allow *in vivo* detection of phospho-Ser65 inhibitor-1 using the single site-specific antibody. However, in striatal slices treated with the PP-1 inhibitors, okadaic acid or calyculin A, in the absence or presence of PDBu, this antibody repeatedly failed to detect phosphorylation of inhibitor-1 at Ser65 alone (data not shown). It is important to bear in mind that okadaic acid and calyculin A potently inhibit PP-2A at doses that also inhibit PP-1, causing an increase in phospho-Ser67 inhibitor-1 levels in the striatum (190). Therefore it is conceivable that while PP-1 inhibition allows phospho-Ser65 to persist longer, concomitant inhibition of PP-2A results in the phosphorylation of Ser67 to a stoichiometry of ~1 mol/mol, precluding the detection of phospho-Ser65 by itself.

2-ii. The *in vitro* evidence presented in the previous section suggests that dephospho- and phospho-Ser65 inhibitor-1 may be equally efficient Cdk5 substrates

(Figure 4.10A and B, left panels). Thus, it is possible that PKC-dependent phosphorylation of Ser65 is undetectable by itself *in vivo* because it is rapidly followed by phosphorylation of Ser67 by Cdk5. This conjecture was tested in striatal slices by evaluating the ability of the Cdk5 inhibitor, roscovitine, to allow detection of phospho-Ser65 by itself (Figure 4.12). However, treatment with roscovitine in the absence or presence of PDBu did not result in the detectable generation of phospho-Ser65 inhibitor-1 in this tissue (Figure 4.12, first panel). As expected, roscovitine decreased phospho-Ser67 and diphospho-Ser65/Ser67 inhibitor-1 levels (Figure 4.12, second and third panels). Significantly, the PDBu-induced elevation in phospho-Ser831 GluR1 levels was unaltered by pretreatment of striatal slices with roscovitine (Figure 4.12, fourth panel), suggesting that the effect of roscovitine on the levels of diphospho-Ser65/Ser67 inhibitor-1 is due to a decrease in Ser67 phosphorylation and does not extend to PKC substrates other than inhibitor-1.

Interestingly, PDBu caused a decrease in phospho-Ser67 inhibitor-1 levels and appeared to exert an additive effect when applied with roscovitine (Figure 4.12, third panel). This finding, together with the failure of roscovitine to unmask the presence of phospho-Ser65 inhibitor-1 in striatal slices, appears to lend support to the first possibility, considered above, that only phospho-Ser67 inhibitor-1 serves as a PKC substrate *in vivo*, while dephospho-inhibitor-1 does not. Accordingly, when phospho-Ser67 inhibitor-1 is phosphorylated by PKC at Ser65, it is converted into the diphospho-Ser65/Ser67 form and removed from the pool of phospho-Ser67 inhibitor-1 detectable with the antibody for this phosphorylation site. This results in an apparent, though not necessarily actual, decrease in the levels of phospho-Ser67 inhibitor-1. While this interpretation appears plausible, treatment with PDBu or overexpression of active PKC-α did not have the same effect on phospho-Ser67 inhibitor-1 levels in cultured cells (Figure 4.5A, fifth panel; Figure 4.5B, third panel). Moreover, striatal levels of phospho-Thr75 DARPP-32, a Cdk5 substrate not phosphorylated by PKC, were also decreased by treatment with PDBu (see Chapter 5), indicating that the effect of PDBu on phospho-Ser67 inhibitor-1 levels in the striatum represents, at least in part, an actual decrease in Ser67 phosphorylation, and not entirely an artifact of poor antibody binding under steric hindrance from a nearby

phosphorylation site. The effect of PDBu and PKC activity on Cdk5 substrates will be explored further in Chapter 5.

These results do not shed light on the sequence by which Ser65 and Ser67 are phosphorylated *in vivo*. Although the failure of roscovitine to reveal the occurrence of phospho-Ser65 inhibitor-1 in striatal slices seems to argue against the rapid Cdk5-dependent phosphorylation of phospho-Ser65 inhibitor-1 at Ser67, the results do not rule out the possibility that phospho-Ser65 inhibitor-1, generated as a result of simultaneous PKC activation and Cdk5 inhibition in these experiments, was nonetheless rapidly dephosphorylated by PP-1 and therefore not detected by immunoblot analysis.

4.5. Discussion

PKC phosphorylates protein phosphatase inhibitor-1 at Ser65 *in vitro* and in cultured cells and striatal brain tissue. To monitor inhibitor-1 phosphorylation by PKC, antibodies were generated that detect inhibitor-1 when it is either singly phosphorylated at Ser65 or doubly phosphorylated at Ser65 and Ser67. Only the diphospho-form was detectable *in vivo*. Pharmacological studies showed that phospho-Ser65 inhibitor-1 is likely dephosphorylated by PP-1 and up-regulated in response to the activation of group I metabotropic glutamate receptors in the striatum. Interestingly, pre-incubation with a PP-1 inhibitor was required for treatment of striatal slices with DHPG to result in increased disphospho-Ser65/Ser67 inhibitor-1 levels, suggesting that glutamatergic neurotransmission must coincide with PP-1 inhibition for Ser65 to become phosphorylated *in vivo*.

Consistent with earlier studies of Cdk5-dependent phosphorylation in this region of inhibitor-1 (190) and its homolog, DARPP-32 (188), *in vitro* PP-1 inhibition assays indicated that phosphorylation at Ser65 and/or Ser67 likely has no effect on the inhibitory activity of phospho-Thr35 inhibitor-1. Further *in vitro* experiments suggested that phosphorylation of Ser65, either alone or together with Ser67, reduces the efficiency of inhibitor-1 phosphorylation by PKA at Thr35. This effect was also observed in intact

striatal tissue, where PKC activation specifically attenuated the increase in phospho-Thr35 inhibitor-1 levels in response to activation of adenylate cyclase. Thus, the ability of inhibitor-1 to be converted into a PP-1 inhibitor may be regulated by the PKC-dependent phosphorylation of Ser65. This novel signaling pathway, involving the first endogenous inhibitor found to regulate protein phosphatase activity *in vivo*, exemplifies the diversity of protein phosphatase regulation mechanisms arising from the differential modulation of protein phosphatase regulatory subunits.

Cdk5-dependent phosphorylation of inhibitor-1 at Ser67 has a modest negative effect on the ability of PKA to phosphorylate Thr35 of inhibitor-1 (190). This is in contrast to the inhibitor-1 homolog, DARPP-32, in which Cdk5-dependent phosphorylation of Thr75 results in a complete block of DARPP-32 phosphorylation by PKA at the homologous Thr34 residue (188). This functional difference between inhibitor-1 and DARPP-32 with respect to Cdk5-dependent phosphorylation leaves the significance of inhibitor-1 phosphorylation at Ser67 somewhat unclear. The present results indicate that phospho-Ser65- and diphospho-Ser65/Ser67-mimetic mutants of inhibitor-1 have a much greater effect on PKA-dependent phosphorylation of Thr35 than the phospho-Ser67-mimetic mutation alone. The *in vivo* evidence also shows that phospho-Ser65 likely occurs only in the context of phospho-Ser67 inhibitor-1. Thus, the function of phospho-Ser67 may be to facilitate and/or protect the PKC-dependent phosphorylation of inhibitor-1 at Ser65, a pathway that counters the activation of inhibitor-1 by PKA.

Opposing actions of PKA and PKC have been reported to regulate a number of physiological processes in excitable tissues, including cardiac contraction, cellular tolerance to ethanol, synaptic transmission, neurite outgrowth, and Hebbian synaptic plasticity (196-200). These cases of opposite regulation often involve the phosphorylation of distinct serine/threonine residues by PKA and PKC on a single type of effector molecule, such as nicotinic acetylcholine receptors at the neuromuscular junction (201-203), and GABA type A receptors (204, 205) and NMDA-type glutamate receptors in the central nervous system (126). Recently it was shown that PKA and PKC conversely regulate inhibitor-1 function in cardiac muscle, where PKC-dependent

phosphorylation of inhibitor-1 may render it unable to associate with, and therefore inhibit, PP-1 (191). The present results demonstrate the differential regulation of inhibitor-1 by PKA and PKC in the brain, where inhibitor-1 may be less readily activated by PKA to become a PP-1 inhibitor if it is already phosphorylated by PKC. Both of these PKC-mediated mechanisms of inhibitor-1 regulation would be predicted to result in the net disinhibition of PP-1 activity and may represent synergistic components of the same general process by which PKA and PKC oppositely regulate PP-1 activity through inhibitor-1 phosphorylation.

Inhibitor-1 is the second PP-1 inhibitor shown to be under the opposing influence of PKA and PKC, after the recently discovered gut and brain phosphatase inhibitor (GBPI) (206). GBPI belongs to a growing family of PKC-activated PP-1 inhibitors (207), but unlike other members of this family, it is also regulated by PKA. Interestingly, PKA-dependent phosphorylation of GBPI reverses the activating effect of phosphorylation by PKC. Based on the present study, inhibitor-1 regulation by these two protein kinases represents the converse scenario involving the PKA-mediated activation and PKC-mediated inactivation of a PP-1 inhibitor. Thus, inhibitor-1 and GBPI may be well positioned in biochemical terms to play an integrative role at junctions between the PKA and PKC pathways.

Counter-regulation of PP-1 inhibitors by PKA and PKC is not a universal of property of these small, heat-stable molecules. Like inhibitor-1, DARPP-32 is activated by PKA in the striatum to become a potent PP-1 inhibitor, but in these studies, it was not directly phosphorylated by PKC *in vitro* (data not shown). Consistent with this result, PKC activation failed to attenuate the PKA-dependent phosphorylation of DARPP-32 in striatal slices. These observations suggest a role for PKC in regulating access by PKA to inhibitor-1, but not to other PP-1 inhibitors, such as DARPP-32, further demonstrating the complexity of the network of signaling cascades regulating PP-1 activity *in vivo*.

These studies focused on the regulation of inhibitor-1 by PKC in the striatum, where inhibitor-1 has been implicated in the mediation of cocaine reward (208). PKC-dependent phosphorylation of inhibitor-1 was also observed in hippocampal slices (data not shown). Inhibitor-1 is highly expressed in the hippocampus (184). Moreover, several

of the demonstrable functions of inhibitor-1 in the central nervous system are associated with this brain region (178, 180, 209). With the notable exception of the liver in some species, inhibitor-1 is also expressed to various levels in many peripheral tissues, such as heart, kidney, and skeletal muscle (171, 179). As noted previously, in the heart, levels of inhibitor-1 expression and phosphorylation regulate cardiac contractility and predisposition to heart failure (181, 182, 185, 191). It will be interesting to learn how PKC-dependent phosphorylation affects the function of inhibitor-1 in brain regions like the cortex and hippocampus, and peripheral tissues outside cardiac muscle.

Regarding the mechanism by which PKC activation results in the generation of diphospho-Ser65/Ser67 inhibitor-1, but no detectable levels of phospho-Ser65 inhibitor-1, the case for phospho-Ser67 inhibitor-1 serving as a preferred PKC substrate *in vivo* is at best weak. On the one hand, the *in vitro* evidence does not support it. On the other, the immunocytochemical analysis of PC12 cells proved inconclusive, so the argument for subcellular co-localization of PKC and phospho-Ser67 inhibitor-1 remains unsubstantiated. Of all the evidence presented, only the PDBu-induced decrease in phospho-Ser67 inhibitor-1 levels in the striatum seems consistent with the notion that PKC phosphorylates phospho-Ser67 inhibitor-1 *in vivo*, generating diphospho-Ser65/Ser67 inhibitor-1, which is not detected by the antibody for phospho-Ser67 inhibitor-1 and therefore represents a virtual loss of phosphorylation at Ser67. While this explanation is well within the realm of possibility, the PDBu-induced decrease in striatal phospho-Ser67 inhibitor-1 levels may be explained in large part by another mechanism investigated in Chapter 5.

Nonetheless, assuming that inhibitor-1 is phosphorylated at Ser65 only when Ser67 is already phosphorylated, and that at least part of the PDBu-dependent decrease in Ser67 phosphorylation in the striatum represents a virtual reduction due to steric hindrance exerted by phospho-Ser65 on antibody binding, why was no such reduction observed in cultured cells as a result of PKC overexpression or activation? One possibility is that PC12 and N2a cells acutely infected with Ad I-1 express unusually high basal levels of phospho-Ser67 inhibitor-1 so that the conversion of a fraction of these large pools into diphospho-Ser65/Ser67 inhibitor-1 is not detected as a loss of Ser67

phosphorylation. A related explanation is that striatal neurons are unusually responsive to PDBu, perhaps because they express PDBu-sensitive PKC isozymes not normally found in PC12 or N2a cells, resulting in the loss of a significant percentage of striatal phospho-Ser67 inhibitor-1 to immunodetection due to the robust PDBu-induced phosphorylation of Ser65. To evaluate these possibilities, recombinant dephospho- and phospho-inhibitor-1 standards could be used to determine the molar concentrations of total, phospho-Ser67, and diphospho-Ser65/Ser67 inhibitor-1 in cultured cells and striatal tissue treated with or without PDBu. Comparison of the *in vivo* stoichiometry of phospho-Ser67 *versus* diphospho-Ser65/Ser67 inhibitor-1 under basal and stimulated conditions may shed further light on the nature of the relationship between the two sites. An indirect initial estimate based on the detection of a recombinant phospho-Ser65 inhibitor-1 standard by the antibody for diphospho-Ser65/Ser67 inhibitor-1 placed the maximal *in vivo* stoichiometry of diphospho-Ser65/Ser67 inhibitor-1 at 0.56 mol/mol (Figure 4.4, third panel; Figure 4.12, third panel), nearly twice the basal *in vivo* stoichiometry of 0.34 mol/mol reported for phospho-Ser67 inhibitor-1 (190). A similar result based on the use of a recombinant diphospho-Ser65/Ser67 inhibitor-1 standard for quantification would be conclusive evidence that Ser65 can be phosphorylated in the absence of phospho-Ser67 *in vivo*, although it would not exclude the possibility that at least some Ser65 phosphorylation is directed toward phospho-Ser67 inhibitor-1.

The possibility that phospho-Ser67 is required for Ser65 phosphorylation could be more directly assessed by evaluating Ser67→Ala inhibitor-1 as a substrate for PKC *in vivo*. Ideally, wild-type and Ser67→Ala inhibitor-1 would be overexpressed by transfection or acute viral infection of primary striatal cultures from mice lacking inhibitor-1 (*Ppp1r1a*$^{-/-}$ mice). Following treatment with PDBu, cultured cells would be assessed for inhibitor-1 phosphorylation at Ser65 and Ser67 using the three phosphorylation state-specific antibodies available for the two sites. If phospho-Ser67 were necessary for Ser65 phosphorylation *in vivo*, no phosphorylation of Ser67→Ala inhibitor-1 at phospho-Ser65 would be detected with the antibody for phospho-Ser65 or diphospho-Ser65/Ser67 inhibitor-1. Recombinant wild-type and Ser67→Ala inhibitor-1 preparatively phosphorylated by PKC *in vitro* would serve as controls for the ability of

the antibodies to detect phospho-Ser65 in the context of the serine-to-alanine mutation at position 67. As an alternative to primary striatal cultures from *Ppp1r1a*$^{-/-}$ mice, one could use a cell line that does not express measurable amounts of inhibitor-1, such as HEK293T (210). An absolute requirement for phospho-Ser67 *in vivo* would be expected to result in the complete elimination of inhibitor-1 phosphorylation at Ser65 by the Ser67→Ala mutation. A mere reduction in diphospho-Ser65/Ser67 inhibitor-1 levels due to the Ser67→Ala mutation would not be conclusive because it could be attributed to the fact that compared to wild-type inhibitor-1, Ser67→Ala inhibitor-1 is a less efficient PKC substrate *in vitro*.

Although the possibility of phospho-Ser67 preceding and facilitating the phosphorylation of Ser65 has not been formally ruled out, the present results are probably more consistent with a model in which phosphorylation of Ser67 follows phospho-Ser65 and protects it from rapid dephosphorylation by PP-1. Compared to dephospho-inhibitor-1, phospho-Ser65 inhibitor-1 was phosphorylated equally well by Cdk5 *in vitro*, whereas phospho-Ser67 inhibitor-1 served as a much poorer PKC substrate both under linear steady-state conditions and in the presence of excess enzyme. Kinetic analysis of the Cdk5-dependent phosphorylation of phospho-Ser65 inhibitor-1 could be used to confirm that this form of inhibitor-1 is an efficient Cdk5 substrate *in vitro*. The notion that phospho-Ser67 protects phospho-Ser65 from PP-1-dependent dephosphorylation could also be easily tested by evaluating the ability of PP-1 to dephosphorylate ^{32}P-phospho-Ser65 in the context of wild-type *versus* Ser67→Asp inhibitor-1. Alternatively, diphospho-Ser65/Ser67 inhibitor-1 radiolabeled at phospho-Ser65 could be used.

Be that as it may, the *in vivo* evidence for this hypothesis is largely incomplete. One of its predictions is an increase in Ser67 phosphorylation as a result of the PKC-dependent phosphorylation of Ser65. On the contrary, PKC activation *in vivo* resulted in either no change or a decrease in apparent phospho-Ser67 inhibitor-1 levels. However, given the inability of the antibody for phospho-Ser67 inhibitor-1 to recognize its target in the presence of phospho-Ser65, an undetectable increase in phospho-Ser67 inhibitor-1 levels as an indirect result of PKC activation cannot be ruled out on the basis of these results.

Another prediction posed by this hypothesis is that the combination of PKC activation and Cdk5 inhibition *in vivo* should generate detectable levels of inhibitor-1 phosphorylated only at Ser65. However, no detectable phospho-Ser65 inhibitor-1 was generated in striatal slices treated with roscovitine and PDBu combined. This may be due to the rapid PP-1-dependent dephosphorylation of phospho-Ser65 inhibitor-1 in the absence of phospho-Ser67. The same experiments conducted in the presence of PP-1 inhibitors may help clarify this issue. It is important to bear in mind that most pharmacological PP-1 inhibitors, such as okadaic acid and calyculin A, also inhibit PP-2A and will therefore raise phospho-Ser67 inhibitor-1 levels. This may present a potential complication for these studies. However, the positive effect of PP-2A inhibition on phospho-Ser67 inhibitor-1 levels should be countered by the inhibitory effect of roscovitine. Thus, the combined use of PP-1 inhibitors and roscovitine may open a rare pharmacological window for phospho-Ser65 inhibitor-1 to persist long enough in the tissue for subsequent immunodetection. Such an observation would lend considerable weight to the notion that Ser67 phosphorylation follows and protects phospho-Ser65 *in vivo*.

The phosphorylation of a protein at two neighboring, if not directly adjacent, amino acid residues is not without precedent. MEK phosphorylates ERK1 at Thr202 and Tyr204, and ERK2 at Thr183 and Tyr185 (135, 136, 139). Myosin light chain is phosphorylated at Thr18 and Ser19 by myosin light chain kinase (211, 212). The insulin receptor tyrosine kinase activation domain is subject to autophosphorylation at Tyr1146, Tyr1150, and Tyr1151 (213). Phospholamban, which is a PKA substrate at Ser16 and CaMKII substrate at Thr17 (214), and the NR1 subunit of the NMDA-type glutamate receptor, which is phosphorylated at Ser896 and Ser897 by PKC and PKA, respectively (126), are well-characterized examples of proteins that serve as substrates for different protein kinases at two neighboring residues. Some of the steric limitations inherent in the use of phosphorylation state-specific antibodies for studying phosphoproteins that are targets of multiple protein kinases at neighboring phosphorylation sites are illustrated by the cases of phospholamban (215) and protein phosphatase inhibitor-1.

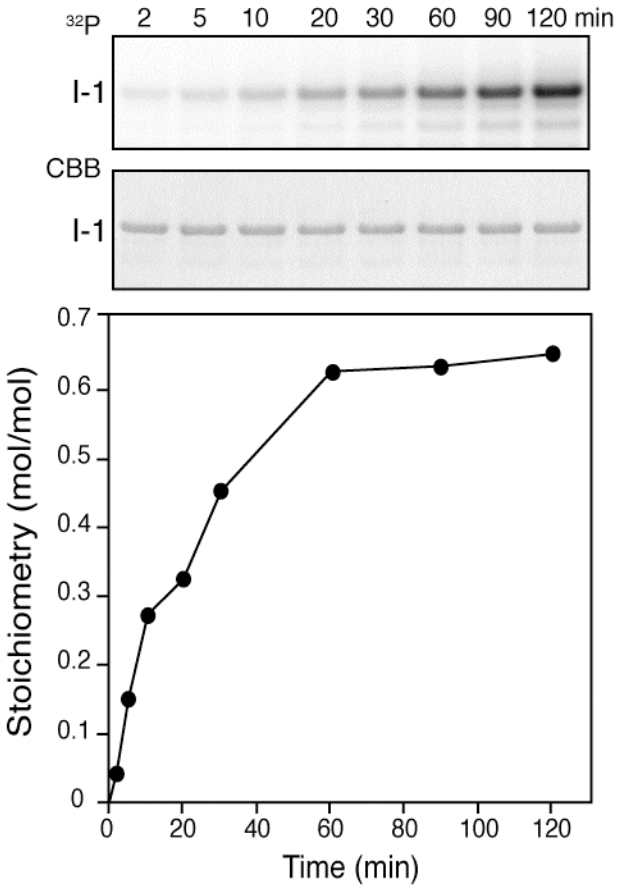

Figure 4.1: Time-course analysis of inhibitor-1 phosphorylation by PKC in vitro. The two panels depict ^{32}P-labeled (top) and CBB-stained (bottom) recombinant inhibitor-1 (*I-1*) subjected to SDS-PAGE. Reaction times are indicated along the top. The plot represents phosphate incorporation over time.

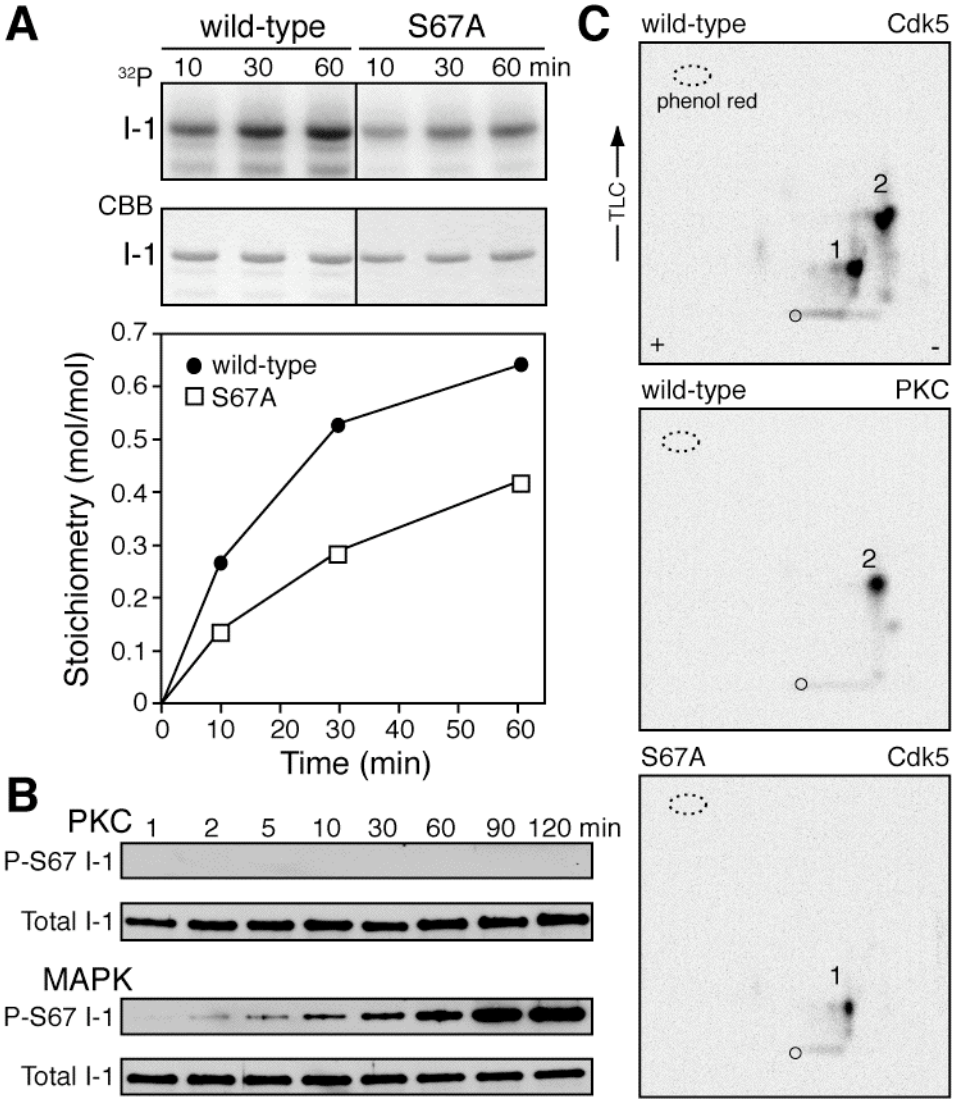
A
wild-type
S67A
32P 10 30 60 10 30 60 min
I-1
CBB
I-1
Stoichiometry (mol/mol)
wild-type
S67A
Time (min)
B
PKC 1 2 5 10 30 60 90 120 min
P-S67 I-1
Total I-1
MAPK
P-S67 I-1
Total I-1
C
wild-type Cdk5
phenol red
TLC
wild-type PKC
S67A Cdk5

Figure 4.2: Evaluation of Ser67 as the inhibitor-1 site of PKC-dependent phosphorylation. *A.* Time-course analysis of the phosphorylation of wild-type *versus* Ser67→Ala (*S67A*) inhibitor-1 (*I-1*) by PKC *in vitro*. The two panels show ^{32}P-labeled (top) and CBB-stained (bottom) wild-type and Ser67→Ala inhibitor-1 subjected to SDS-PAGE. Reaction times are indicated along the top. The plot represents phosphate incorporation over time. *B.* Immunoblot analysis of inhibitor-1 phosphorylated by PKC or MAPK using an antibody specific for phospho-Ser67 (top panels) or total inhibitor-1 (bottom panels). 50 ng of protein are loaded per lane. *C.* Phosphopeptide mapping analysis of wild-type inhibitor-1 preparatively phosphorylated by Cdk5 and PKC, and Ser67→Ala (*S67A*) inhibitor-1 preparatively phosphorylated by Cdk5. The + and – signs on the top phosphopeptide map denote electrode polarity, while the upward arrow labeled TLC indicates the direction of ascending chromatography.

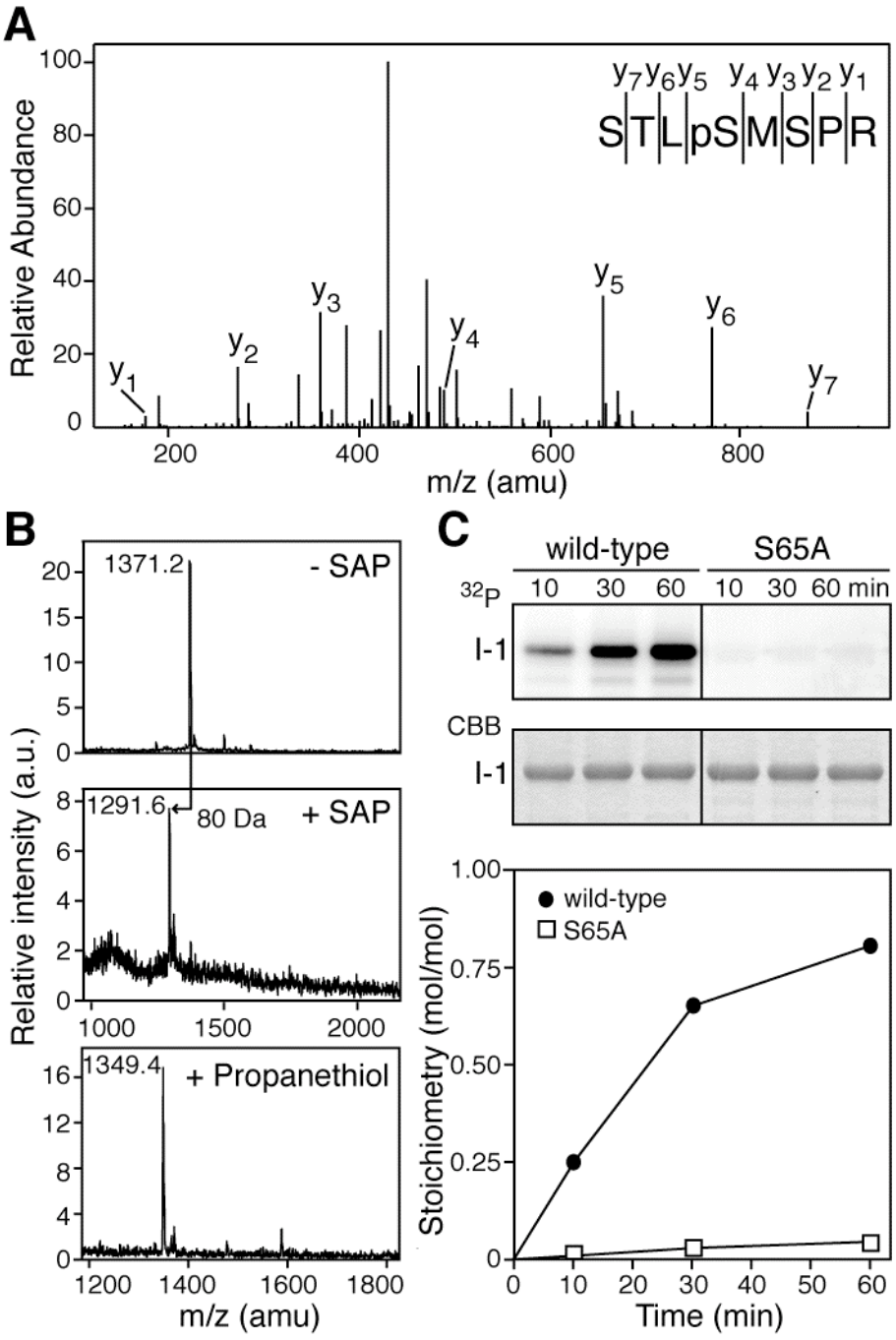
A
Relative Abundance
m/z (amu)
y7 y6 y5 y4 y3 y2 y1
S T L pS M S P R
y1
y2
y3
y4
y5
y6
y7
B
Relative intensity (a.u.)
1371.2
- SAP
1291.6
80 Da
+ SAP
1349.4
+ Propanethiol
m/z (amu)
C
wild-type
S65A
32P
10 30 60 10 30 60 min
I-1
CBB
I-1
wild-type
S65A
Stoichiometry (mol/mol)
Time (min)

Figure 4.3. Identification of Ser65 as the inhibitor-1 site of PKC-dependent phosphorylation. *A*. Nanoelectrospray-QqTOF MS/MS analysis of peptides resulting from tryptic digestion of inhibitor-1 phosphorylated by PKC. The product spectrum shown was generated by fragmentation of the singly charged tryptic peptide, STLpSMSPR (phospho-serine denoted by pS). Each peak of the y-ion series is denoted on the peptide sequence by a vertical line between two amino acids where the peptide bond was broken to generate the indicated y-ion. *B*. MALDI-TOF MS analysis of the ^{32}P-labeled phosphopeptide resulting from phosphorylation of inhibitor-1 by PKC in the presence of [γ-^{32}P] ATP, digestion with endoproteinase Lys-C, fractionation by reversed-phase HPLC, and isolation of the fraction containing radioactivity. The peak corresponding to the phosphopeptide (top spectrum) was shifted -80 Da by SAP treatment (middle spectrum) and -21 Da by propanethiol derivatization (bottom spectrum) prior to Edman amino acid microsequencing. *C*. Confirmation of Ser65 as the inhibitor-1 (*I-1*) site of PKC-dependent phosphorylation by site-directed mutagenesis. Results of *in vitro* protein phosphorylation reactions conducted with PKC and wild-type *versus* Ser65→Ala (*S65A*) inhibitor-1 are shown. The two panels show SDS-PAGE analysis of ^{32}P-labeled (top) and CBB-stained (bottom) wild-type and Ser65→Ala inhibitor-1. Reaction times are indicated along the top. The plot represents phosphate incorporation as a function of time.

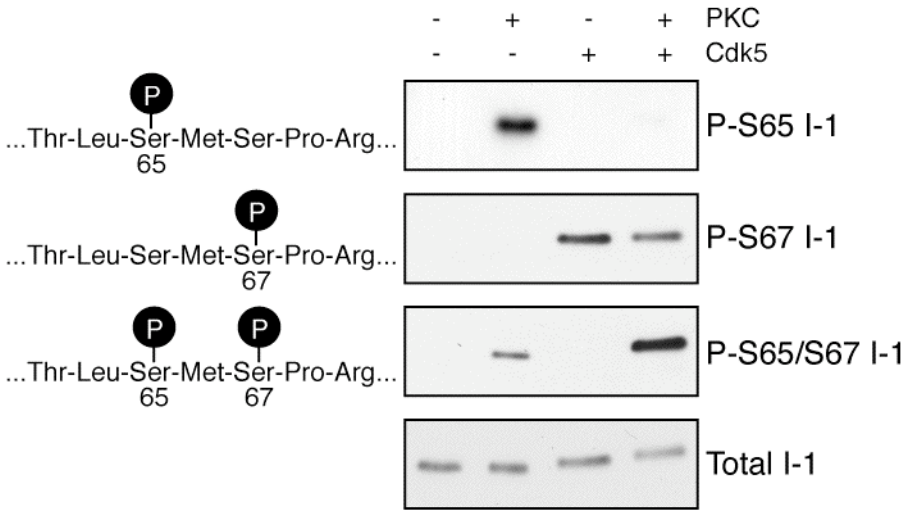

Figure 4.4: Generation of phosphorylation state-specific antibodies against phospho-Ser65 inhibitor-1. Immunoblot analysis of dephospho-inhibitor-1 (*I-1*) and inhibitor-1 phosphorylated by PKC, Cdk5, or PKC and Cdk5, using an antibody for phospho-Ser65 (top panel), phospho-Ser67 (second panel), diphospho-Ser65/Ser67 (third panel), or total inhibitor-1 (bottom panel). The phosphorylation state of inhibitor-1 detected by each phosphorylation state-specific antibody is represented schematically next to the corresponding immunoblot.

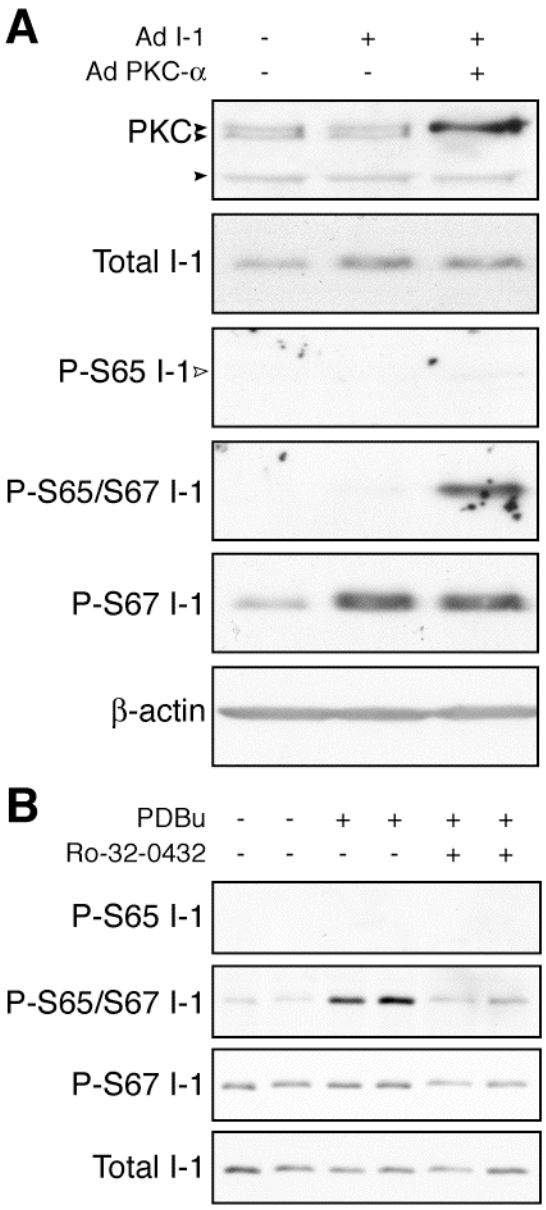
A
Ad I-1 - + +
Ad PKC-α - - +
PKC
Total I-1
P-S65 I-1
P-S65/S67 I-1
P-S67 I-1
β-actin
B
PDBu - - + + + +
Ro-32-0432 - - - - + +
P-S65 I-1
P-S65/S67 I-1
P-S67 I-1
Total I-1

Figure 4.5: PKC-dependent phosphorylation of inhibitor-1 in cultured cells. A. Immunoblot analysis of PKC (top panel); total, phospho-Ser65, phospho-Ser67, and diphospho-Ser65/Ser67 inhibitor-1 (*I-1*) (middle panels); and β-actin (bottom panel) in PC12 cells infected with the indicated adenoviruses. In order from top to bottom, the filled arrowheads next to the PKC immunoblot indicate the three Ca^{2+}-dependent PKC isoforms, α, β, and γ. The open arrowhead next to the immunoblot for phospho-Ser65 inhibitor-1 shows the predicted position of inhibitor-1 on the membrane. *B.* Immunoblot analysis of phospho-Ser65 (top panel), diphospho-Ser65/Ser67 (second panel), phospho-Ser67 (third panel), and total inhibitor-1 (bottom panel) levels in N2a cells infected with Ad I-1 and incubated in the absence or presence of the PKC inhibitor, Ro-32-0432 (1 μM, 60 min), before being treated with PDBu (5 μM, 10 min).

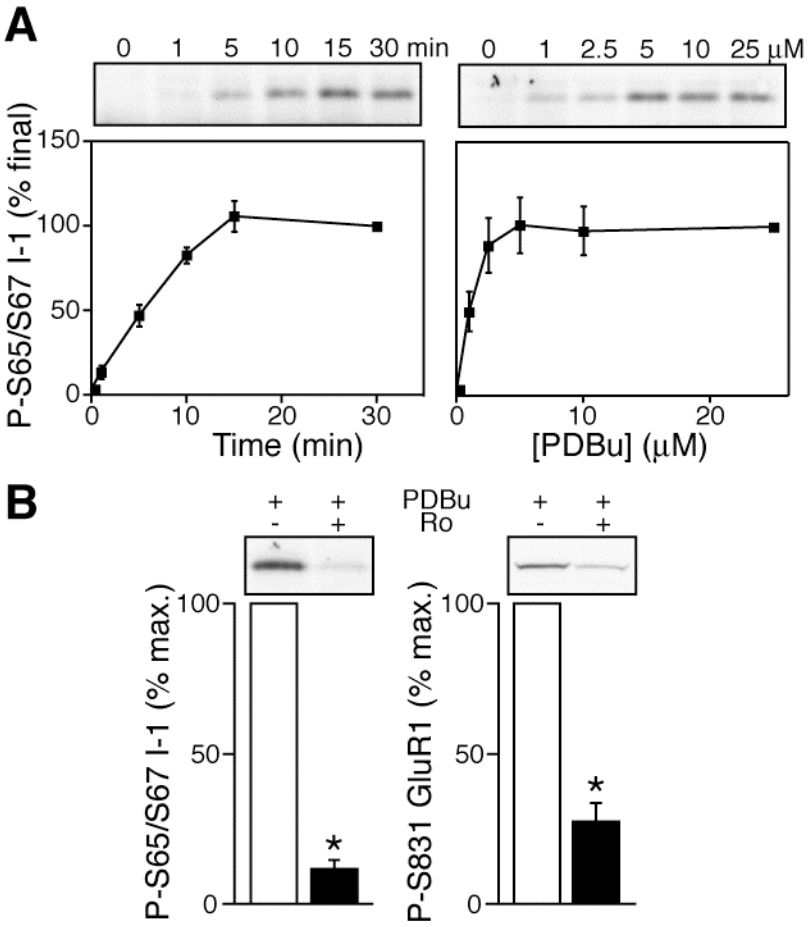

Figure 4.6: Regulation of diphospho-Ser65/Ser67 inhibitor-1 levels by pharmacological manipulation of PKC activity in striatal slices. *A*. Time-course and PDBu dose response curves of diphospho-Ser65/Ser67 inhibitor-1 (*I-1*) levels determined by quantitative immunoblot analysis of striatal slices treated with 5 μM PDBu for 0-30 min (left), or with 0-25 μM PDBu for 15 min (right). The data represent means ± S.E.M. for 4 time-course and 4 dose response experiments. *B*. Quantitative immunoblot analysis of diphospho-Ser65/Ser67 inhibitor-1 (left) and phospho-Ser831 GluR1 (right) levels in striatal slices treated with PDBu (5 μM, 15 min) following incubation in the absence or presence of the PKC inhibitor, Ro-32-0432 (*Ro*, 5 μM, 60 min). *, $p < 0.01$, Student's unpaired *t* test, n = 5.

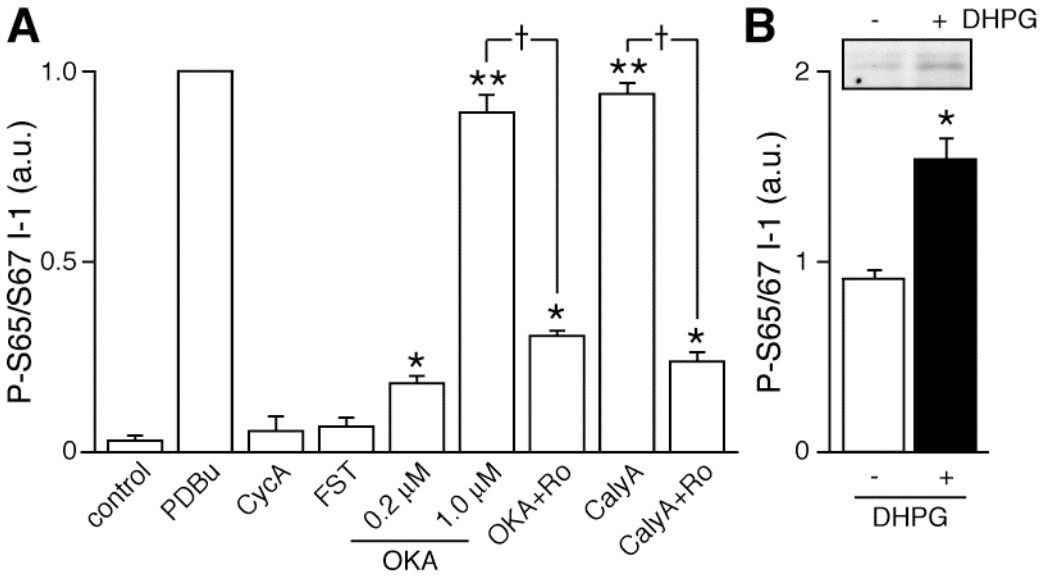
A
P-S65/S67 I-1 (a.u.)
1.0
0.5
0
control
PDBu
CycA
FST
0.2 µM
1.0 µM
OKA
OKA+Ro
CalyA
CalyA+Ro
B
- + DHPG
P-S65/67 I-1 (a.u.)
2
1
0
- +
DHPG

Figure 4.7: Regulation of diphospho-Ser65/Ser67 inhibitor-1 levels by protein phosphatase inhibitors and DHPG in striatal slices. A. Quantification of diphospho-Ser65/Ser67 inhibitor-1 (*I-1*) levels in striatal slices incubated in the absence or presence of PDBu (5 μM, 15 min), cyclosporin A (*CycA*, a PP-2B inhibitor, 2.5 μM, 60 min), fostriecin (*FST*, a PP-2A inhibitor, 0.5 μM, 60 min), 0.2 μM okadaic acid (*OKA*, predominantly a PP-2A inhibitor, 60 min), 1 μM okadaic acid (a PP-1 and PP-2A inhibitor, 60 min), calyculin A (*CalyA*, a PP-1 and PP-2A inhibitor, 1 μM, 60 min), and Ro-32-0432 (*Ro*, 5 μM, 60 min). Slices co-incubated with Ro-32-0432 and a protein phosphatase inhibitor were pre-treated with Ro-32-0432 for 60 min before being incubated for an additional 60 min with okadaic acid (1 μM) or calyculin A in the presence of Ro-32-0432. Diphospho-Ser65/Ser67 inhibitor-1 levels are normalized to the mean value obtained from slices treated with PDBu. *, $p < 0.01$ compared to untreated control slices, Student's unpaired *t* test, n = 4. **, $p < 0.001$ compared to untreated control slices, Student's unpaired *t* test, n = 4. †, $p < 0.01$, Student's unpaired *t* test, n = 4. *B*. Quantitative immunoblot analysis of diphospho-Ser65/Ser67 inhibitor-1 levels in striatal slices treated with or without the group I metabotropic glutamate receptor agonist, DHPG (50 μM, 5 min), following incubation in the presence of calyculin A (0.5 μM, 30 min). *, $p < 0.01$, Student's unpaired *t* test, n = 4.

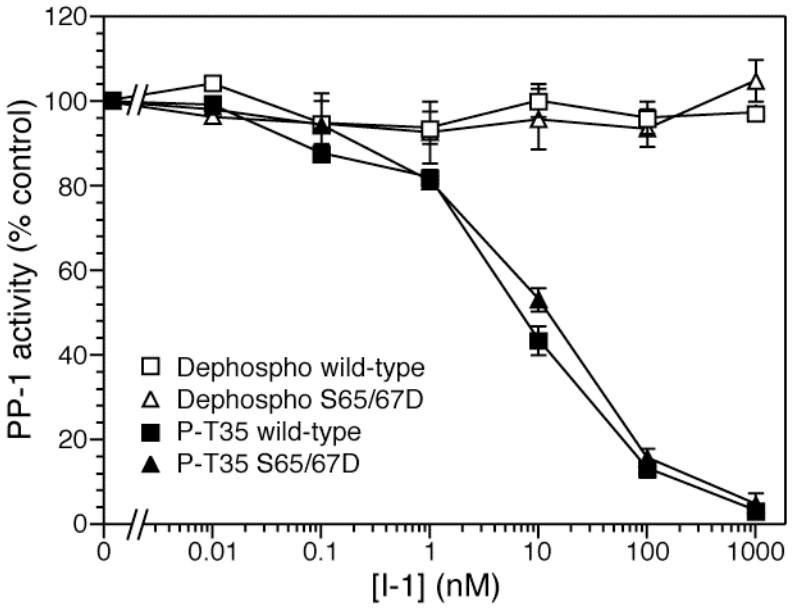

Figure 4.8: Comparison of PP-1 inhibition by dephospho- and phospho-Thr35 forms of wild-type and Ser65+Ser67→Asp inhibitor-1. PP-1 inhibition was analyzed using 0-1 μM wild-type (*open squares*), Ser65+Ser67→Asp (*S65/67D*) (*open triangles*), phospho-Thr35 wild-type (*filled squares*), and phospho-Thr35 Ser65+Ser67→Asp (*filled triangles*) inhibitor-1 (*I-1*). Data represent means ± S.E.M. for 4 experiments conducted in duplicate.

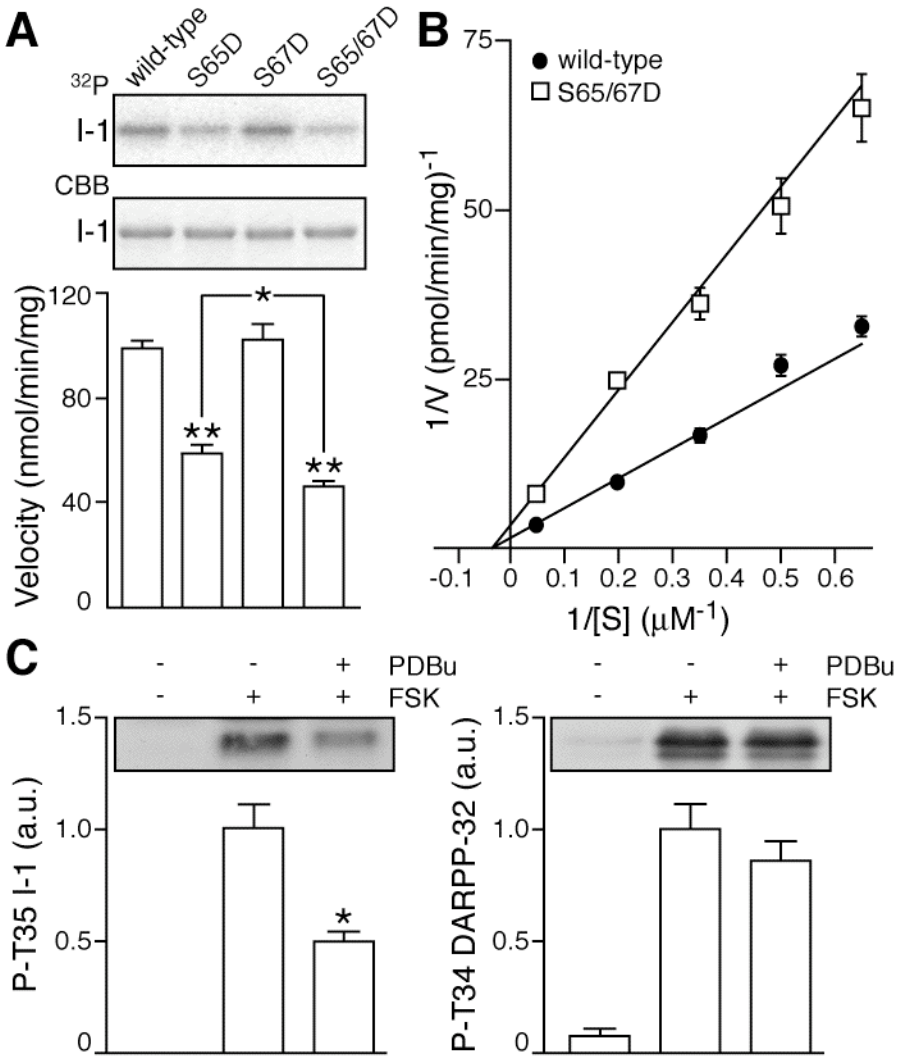
A
wild-type
S65D
S67D
S65/67D
32P
I-1
CBB
I-1
Velocity (nmol/min/mg)
120
80
40
0
*
**
**
B
75
50
25
wild-type
S65/67D
1/V (pmol/min/mg)-1
-0.1
0
0.1
0.2
0.3
0.4
0.5
0.6
1/[S] (μM-1)
C
PDBu
FSK
P-T35 I-1 (a.u.)
1.5
1.0
0.5
0
*
P-T34 DARPP-32 (a.u.)

Figure 4.9: Effect of phosphorylation of inhibitor-1 at Ser65 on the ability of PKA to phosphorylate inhibitor-1. *A. In vitro* phosphorylation of wild-type inhibitor-1 *versus* serine-to-aspartate mutants of inhibitor-1 (*S65D*, *S67D*, *S65/67D*) by PKA under linear conditions. The two panels show SDS-PAGE analysis of ^{32}P-labeled (top) and CBB-stained (bottom) wild-type and mutant inhibitor-1 forms from 1 of 4 experiments conducted in duplicate. The initial rate of phosphate incorporation is plotted for each substrate. *, $p < 0.01$, Student's unpaired *t* test. **, $p < 0.001$ compared to wild-type inhibitor-1, Student's unpaired *t* test. *B.* Lineweaver-Burk analysis of the PKA-dependent phosphorylation of wild-type *versus* Ser65+Ser67→Asp (*S65/67D*) inhibitor-1. The plot represents the results of 4 reactions conducted under identical linear conditions using duplicate samples. *C.* Quantitative immunoblot analysis of phospho-Thr35 inhibitor-1 (left) and phospho-Thr34 DARPP-32 (right) levels in striatal slices treated with the adenylate cyclase activator, forskolin (*FSK*, 10 μM, 10 min), following incubation in the absence or presence of PDBu (5 μM, 10 min). *, $p < 0.01$, Student's unpaired *t* test, n = 5.

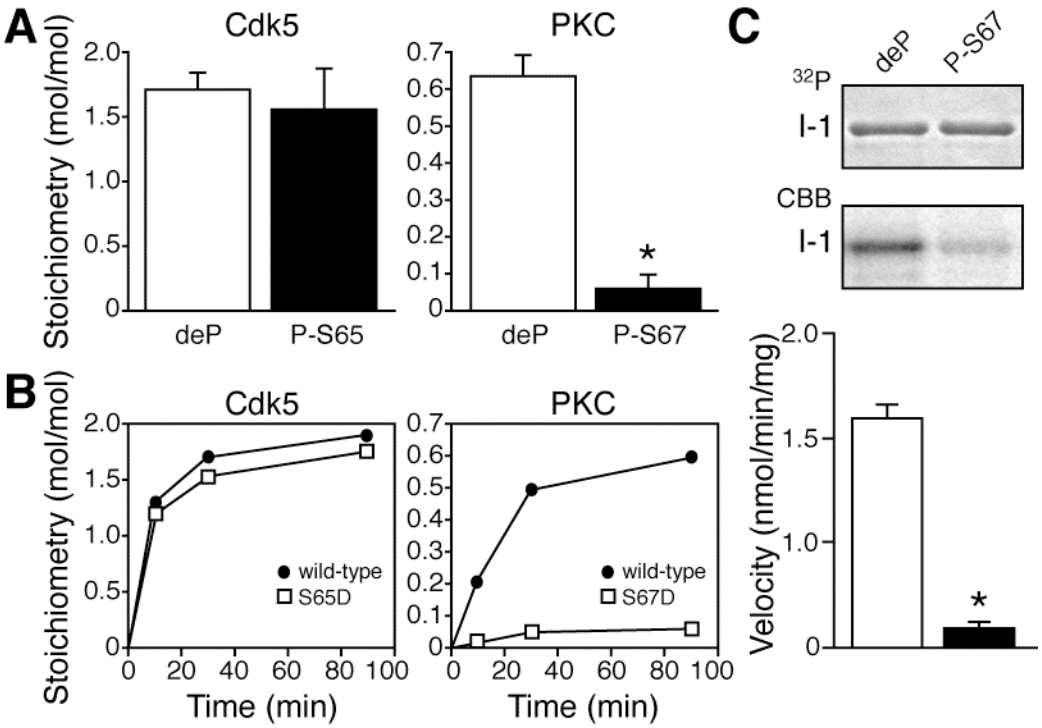
A
Cdk5
PKC
Stoichiometry (mol/mol)
deP
P-S65
P-S67
B
wild-type
S65D
S67D
Time (min)
C
deP
P-S67
32P
I-1
CBB
Velocity (nmol/min/mg)

Figure 4.10: Effect of phospho-Ser65 and phospho-Ser67 on inhibitor-1 phosphorylation by Cdk5 and PKC, respectively. A. Comparison of the Cdk5-dependent phosphorylation of dephospho (*deP*)- and phospho-Ser65 (*P-S65*) inhibitor-1 (left), and the PKC-dependent phosphorylation of dephospho- and phospho-Ser67 (*P-S67*) inhibitor-1 (right) *in vitro*. The histograms depict the final stoichiometry for each 90-min reaction as the mean ± S.E.M. of 4-5 experiments. *, $p < 0.01$, Student's unpaired *t* test. *B.* Time-course analysis of the Cdk5-dependent phosphorylation of wild-type *versus* Ser65→Asp (*S65D*) inhibitor-1 (left), and the PKC-dependent phosphorylation of wild-type *versus* Ser67→Asp (*S67D*) inhibitor-1 (right) *in vitro*. The plots represent phosphate incorporation over time. *C. In vitro* phosphorylation of dephospho (*deP*)- *versus* phospho-Ser67 (*P-S67*) inhibitor-1 (*I-1*) by PKC under linear conditions. The two panels show SDS-PAGE analysis of ^{32}P-labeled (top) and CBB-stained (bottom) dephospho- and phospho-Ser67 inhibitor-1 from 1 of 4 experiments. The initial rate of phosphate incorporation is plotted for each substrate. *, $p < 0.001$, Student's unpaired *t* test.

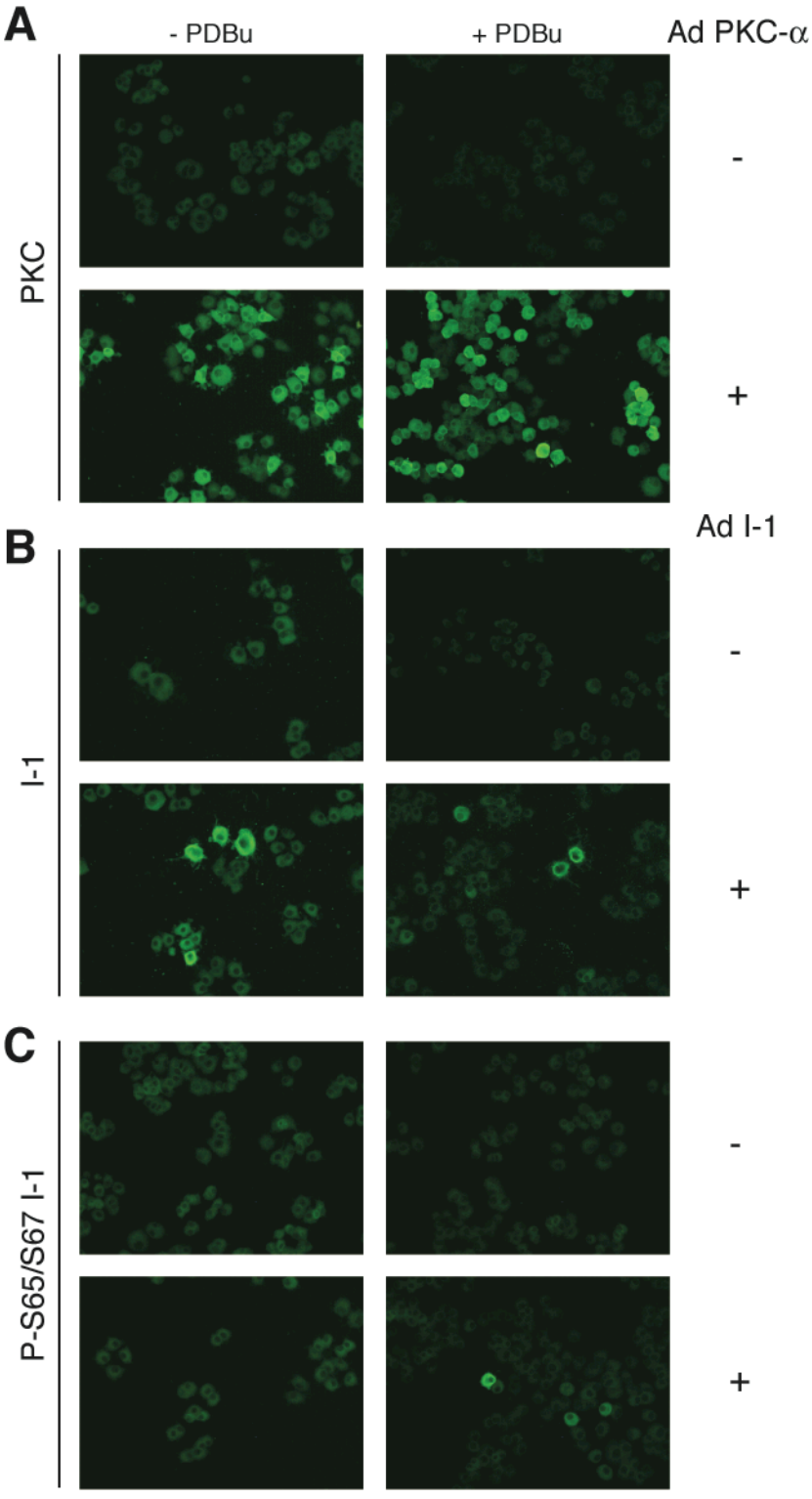
A
- PDBu
+ PDBu
Ad PKC-α
PKC
-
+
B
Ad I-1
I-1
-
+
C
P-S65/S67 I-1
-
+

Figure 4.11: Immunocytochemical analysis of PKC, inhibitor-1, and diphospho-Ser65/Ser67 inhibitor-1 in PC12 cells. *A*. Immunocytochemical stain for PKC (α, β, γ) in naïve PC12 cells (top panels) and PC12 cells acutely infected with Ad PKC-α before incubation in the absence (left panels) or presence (right panels) of PDBu (5 μM, 10 min). *B*. Immunocytochemical stain for total inhibitor-1 (*I-1*) in naïve PC12 cells (top panels) and PC12 cells acutely infected with Ad I-1 before incubation in the absence (left panels) or presence (right panels) of PDBu (5 μM, 10 min). *C*. Immunocytochemical stain for diphospho-Ser65/Ser67 inhibitor-1 in PC12 cells treated as described in *B*.

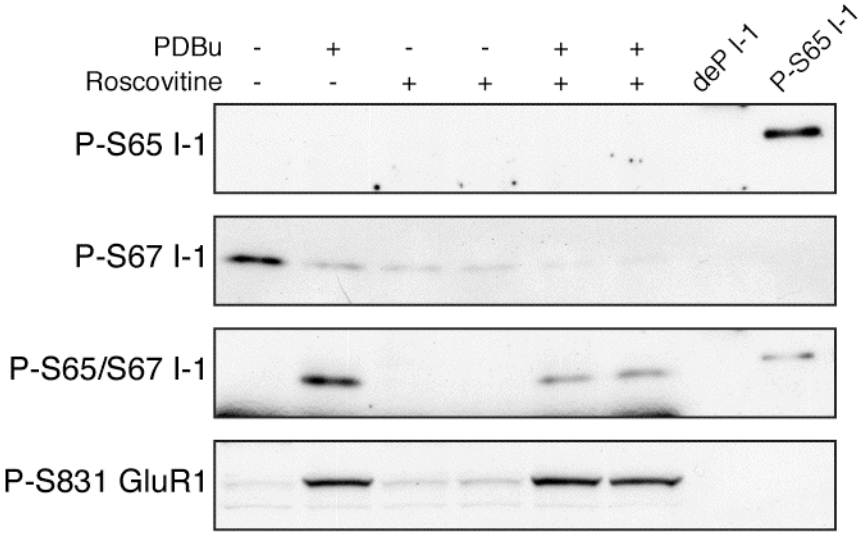

Figure 4.12: Effect of roscovitine on the detection of phospho-Ser65 versus *diphospho-Ser65/Ser67 inhibitor-1 in striatal slices treated with or without PDBu.* Immunoblot analysis of phospho-Ser65, phospho-Ser67, and diphospho-Ser65/Ser67 inhibitor-1 (*I-1*), and phospho-Ser831 GluR1 levels in striatal slices treated with or without PDBu (5 μM, 15 min) following incubation in the absence or presence of the Cdk5 inhibitor, roscovitine (50 μM, 60 min). 5 ng of recombinant dephospho (*deP*)- and phospho-Ser65 inhibitor-1 were also blotted as controls.

CHAPTER 5

REGULATION OF CYCLIN-DEPENDENT KINASE 5 TARGETS BY PROTEIN KINASE C

5.1. Summary

Cyclin-dependent kinase 5 is a proline-directed protein serine/threonine kinase essential for brain development and implicated in synaptic plasticity, dopaminergic neurotransmission, drug addiction, and neurodegenerative disorders. Relatively little is known about the molecular mechanisms that regulate the activity of cyclin-dependent kinase 5 *in vivo*. Studies described in the previous Chapter showed that treatment of striatal slices with the protein kinase C activator, phorbol-12,13-dibutyrate (PDBu), results in a decrease in the phosphorylation of the cyclin-dependent kinase 5 substrate, Ser67 of protein phosphatase inhibitor-1. In order to determine whether PDBu and/or protein kinase C activation can negatively regulate other Cdk5 substrates in the striatum, this analysis was extended in the following studies to Ser6 of inhibitor-1 and Thr75 of the dopamine- and cAMP-regulated phosphoprotein, M_r 32,000, DARPP-32. Treatment of striatal slices with PDBu caused a time- and dose-dependent decrease in the levels of phospho-Ser6 inhibitor-1, phospho-Ser67 inhibitor-1, and phospho-Thr75 DARPP-32, although PDBu had no direct effect on the phosphorylation of inhibitor-1 by cyclin-dependent kinase 5 *in vitro*. In the case of striatal phospho-Ser67 inhibitor-1 and phospho-Thr75 DARPP-32 levels, the decrease due to PDBu was reversed by the protein kinase C inhibitor, Ro-32-0432. Moreover, phospho-Ser6 and phospho-Ser67 inhibitor-1 levels were elevated in striatal tissue from mice lacking protein kinase C-α. Several possible mechanisms by which protein kinase C may regulate cyclin-dependent kinase 5 activity in the striatum were evaluated. Protein kinase C did not phosphorylate cyclin-dependent kinase 5 or its cofactor, p25, *in vitro*. In time-course and dose response

studies, levels of the cyclin-dependent kinase 5 cofactor, p35, did not change in response to PDBu. Moreover, cyclin-dependent kinase 5 immunoprecipitated from striatal slices treated with PDBu did not show altered activity toward a control substrate *in vitro*.

5.2. Introduction

A unique member of the cyclin-dependent kinase family with no apparent role in cell cycle progression, Cdk5 is a proline-directed protein serine/threonine kinase that is highly expressed in post-mitotic, terminally differentiated neurons. To become active, Cdk5 requires association with one of its membrane-bound neuronal activators: p35 (216) or its homolog, p39 (217). Mice lacking Cdk5 (218, 219) or p35 and p39 (220) display abnormal corticogenesis and perinatal lethality, underscoring the critical role of Cdk5 activity in the developing brain. While p35-deficient mice are viable, with less severe signs of disrupted cortical development (221), and mice lacking p39 appear normal (220), the genetic deletion of both cofactors mimics loss of Cdk5, suggesting that p35 and p39 are the only relevant cofactors of Cdk5 in the central nervous system (220). The Ca^{2+}-dependent protease, calpain, cleaves the first ~100 N-terminal residues of p35 or p39, resulting in the soluble proteolytic fragment, p25 or p29, respectively (222, 223). Cdk5 bound to this cleaved cofactor shows prolonged activation, mislocalization, and altered substrate specificity—mechanisms believed to be responsible for aberrant Cdk5-dependent protein phosphorylation in a number of neurodegenerative disorders (224, 225).

Cdk5 levels remain high throughout adulthood in rodents (226). Ischemia (227, 228), excitotoxicity (229), neurotoxicity (230), and chronic cocaine exposure (188) have been reported to elevate these levels. While earlier studies focused on the role of Cdk5 in brain development, more recent work has implicated Cdk5 in synaptic transmission in mature neurons. Presynaptically, Cdk5 has been suggested to regulate neurotransmitter release and synaptic vesicle endocytosis through the phosphorylation of synapsin I (231), the α-subunit of the P/Q-type voltage-dependent Ca^{2+} channel (232), amphiphysin I

(233), dynamin I (234, 235), and synaptojanin I (236). In the postsynaptic compartment, Cdk5 phosphorylates the NR2A subunit of the NMDA-type glutamate receptor (237, 238), the postsynaptic density protein, PSD-95 (239), and the protein phosphatase-1 inhibitors, inhibitor-1 (190) and its striatal homolog, DARPP-32 (188).

In spite of a growing list of physiological substrates, surprisingly little is known about the regulation of Cdk5 activity in neurons, other than the role of cofactor metabolism (240). When phosphorylated by Cdk5, p35 is rapidly turned over by the proteosome (63, 241), a process promoted by physiological levels of glutamatergic stimulation (242). Unphosphorylated, p35 is susceptible to calpain-dependent conversion to its more stable and soluble form, p25 (63, 243). Cleavage of p35 by calpain is stimulated by high intracellular Ca^{2+} levels (222), as may occur in acute neuronal injury (244) and glutamate excitotoxicity (245, 246).

In Chapter 4, it was observed that the PKC-activating phorbol ester, PDBu, decreases the Cdk5-dependent phosphorylation of inhibitor-1 at Ser67 in the striatum. There is currently no other evidence that phorbol esters or PKC act upon Cdk5-dependent pathways. The following studies investigate a possible role for PKC in the regulation of other Cdk5 substrates, and possibly Cdk5 activity, in the brain.

5.3. Experimental Procedures

All reagents were from sources indicated in previous Chapters, unless otherwise specified. Striatal slice pharmacology, quantitative immunoblot analysis, and *in vitro* protein phosphorylation reactions were conducted as described in previous Chapters. The antibody for phospho-Ser6 inhibitor-1 was purified and characterized by Baochan Nguyen (UT Southwestern Medical Center) as described for other phosphorylation state-specific antibodies in Chapter 4. *Prkca*$^{-/-}$ mice and wild-type littermates were provided by Jeffery Molkentin (University of Cincinnati, Children's Hospital Medical Center) (191).

5.3.1. Immunoprecipitation and assay of Cdk5

For Cdk5 immunoprecipitation, acutely prepared mouse striatal slices incubated in the absence or presence of 5 μM PDBu for 30 min were lysed with a Dounce homogenizer in 1 ml of lysis buffer containing 150 mM NaCl, 20 mM Trizma-HCl, pH 7.4, 1 mM EDTA, 0.5% Igepal CA-630, 10 mM NaF, 5 mM sodium orthovanadate, and protease inhibitors. Lysates were centrifuged at 10,000 × *g* for 10 min at 4°C. Supernatants were pre-cleared by incubation with rabbit IgG conjugated to agarose (Santa Cruz) for 30 min at 4°C. Following centrifugation at 1,500 × *g* for 5 min at 4°C, pellets were washed three times with 1 ml of lysis buffer and once with kinase assay buffer containing 50 mM HEPES, pH 7.0, 10 mM $MgCl_2$, and 1 mM DTT, and saved as controls. Pre-cleared supernatants were incubated with 25 μl of anti-Cdk5 antibody conjugated to agarose (Santa Cruz) for 60 min at 4°C and centrifuged at 1,500 × *g* for 4 min at 4°C. Pellets washed three times with 1 ml of lysis buffer and once with kinase assay buffer. Cdk5 assays were performed in a volume of 30 μl containing 2 μg of histone H1, 500 mM ATP, and 0.2 mCi/ml [γ-^{32}P] ATP. Following incubation at 30°C for 60 min, reactions were stopped by the addition of an equal volume of SDS protein sample buffer. Samples were boiled for 5 min, separated by SDS-PAGE, and analyzed by autoradiography, as described in Chapter 2.

5.3.2. Statistical analysis

Differences between data groups were evaluated for significance using a Student's *t* test of unpaired data (± standard error of the mean).

5.4. Results

5.4.1. Effect of PDBu and Ro-32-0432 on the level of phosphorylation of Cdk5 substrates in the striatum

Treatment of striatal slices with the PKC-activating phorbol ester, PDBu, results in a time- and dose-dependent decrease in the level of phosphorylation of at least three Cdk5 targets in this tissue, Ser6 and Ser67 of inhibitor-1 and Thr75 of DARPP-32 (Figure 5.1A-C). Because DARPP-32 is unlikely to serve as a PKC substrate *in vivo* (see Chapter 4, Discussion), this decrease is not adequately explained by an intramolecular effect involving the PKC-dependent phosphorylation of a residue near a Cdk5 site. To evaluate the possibility that PDBu exerts a non-specific, PKC-independent inhibitory effect on Cdk5 activity in the striatum through direct interaction with Cdk5 or one of its cofactors, *in vitro* protein phosphorylation reactions were conducted with Cdk5/p25 and recombinant inhibitor-1 in the absence or presence of PDBu (Figure 5.1D). PDBu had no effect on the ability of Cdk5 to phosphorylate inhibitor-1, arguing against the direct inhibition of Cdk5 by PDBu *in vivo*. The possibility remained, however, that PDBu causes a non-specific suppression of Cdk5 activity by acting indirectly through upstream regulators of Cdk5-mediated signaling.

To determine whether the effect of PDBu on the phosphorylation of Cdk5 substrates in the striatum is PKC-dependent, levels of phospho-Ser67 inhibitor-1 were assessed in striatal slices treated with PDBu following incubation in the absence or presence of the PKC inhibitor, Ro-32-0432 (Figure 5.2A). Pretreatment with Ro-32-0432 reversed the effect of PDBu on Ser67 phosphorylation, indicating that PDBu likely mediates its inhibitory effect through the activation of PKC. Similar results were obtained with phospho-Thr75 DARPP-32 (data not shown).

5.4.2. Effect of Prkca *deletion on the level of phosphorylation of Cdk5 substrates in the striatum*

To complement these pharmacological findings, the phosphorylation state of the same Cdk5 substrates was assessed in brain tissue from wild-type and *Prkca*$^{-/-}$ mice (Figure 5.2B-D). Deletion of the gene encoding PKC-α did not alter total inhibitor-1 or DARPP-32 levels in the brain (data not shown). Relative to controls, cortical tissue from *Prkca*$^{-/-}$ mice had approximately 1.6- and 2.6-fold higher basal levels of phospho-Ser6 and phospho-Ser67 inhibitor-1, respectively (Figure 5.2B and C). Phosphorylation of these Cdk5 sites was also enhanced in striatal, but not cerebellar, tissue from *Prkca*$^{-/-}$ animals. Compared to control levels, *Prkca*$^{-/-}$ striatum showed a 6.1-fold elevation in the basal levels of phospho-Ser6 inhibitor-1 and a 2.6-fold elevation in the basal levels of phospho-Ser67 inhibitor-1. No phospho-Ser6 inhibitor-1 was detected in cerebellar tissue from wild-type or *Prkca*$^{-/-}$ animals. Interestingly, phospho-Ser67 inhibitor-1 levels were up-regulated by the same proportion in *Prkca*$^{-/-}$ cortex and striatum, whereas levels of phospho-Ser6 inhibitor-1 were altered more dramatically in the striatum relative to cortex. These findings suggest that PKC-α differentially regulates these two Cdk5 targets in a tissue-specific manner.

As expected, the striatal inhibitor-1 homolog, DARPP-32, was not detectable in the cortex or cerebellum, but abundantly expressed in the striatum. Compared to the fold-increase in the levels of phospho-Ser6 and phospho-Ser67 inhibitor-1, phospho-Thr75 DARPP-32 levels showed a relatively modest, but significant, increase of 1.7-fold in *Prkca*$^{-/-}$ striatum (Figure 5.2D). This represents a reversal of the pattern observed in wild-type striatal slices treated with PDBu (Figure 5.1A and B), suggesting the possibility that DARPP-32 may be subject to regulation by PKC isoforms in addition to PKC-α. Together with the findings described in the previous subsection, these results point to a role for PKC in the regulation of Cdk5 activity in the striatum.

5.4.3. Evaluation of Cdk5 inhibition by PKC as a mechanism for the PKC-dependent down-regulation of Cdk5 substrate phosphorylation in the striatum

It is possible that PKC decreases the phosphorylation level of Cdk5 substrates *in vivo* by inhibiting Cdk5 activity, perhaps through the direct phosphorylation of Cdk5 or one of its cofactors. Contrary to this notion, the incubation of recombinant Cdk5/p25 with PKC resulted in no detectable change in the phosphorylation of Cdk5 or p25 *in vitro* whereas inhibitor-1 was efficiently phosphorylated by PKC (Figure 5.3A).

Cdk5 activity is regulated *in vivo* by the availability of neuronal cofactors (240). To assess whether PKC activation alters Cdk5 cofactor stability in the striatum, p35 levels were assessed in striatal slices treated with PDBu in time-course and dose response experiments (Figure 5.3B). PDBu had no apparent effect on the levels of striatal p35. Cdk5 levels were likewise unaffected by this treatment (data not shown).

These findings do not support a direct effect of PKC on the phosphorylation or stability of Cdk5 and its cofactors. However, they do not rule out the possibility that PKC alters Cdk5 activity though another mechanism, perhaps by impinging on upstream regulators of Cdk5-mediated signaling. As a more direct test of this possibility, Cdk5 immunoprecipitated from striatal slices treated with or without PDBu was evaluated for its ability to phosphorylate histone H1 *in vitro* (Figure 5.3C). Treatment with PDBu had no apparent effect on Cdk5 activity in this assay.

5.5. Discussion

The results indicate a role for PKC in the regulation of several Cdk5 targets in the brain, suggesting the possibility that PKC regulates Cdk5 activity. Pharmacological activation of PKC caused a time- and dose-dependent decrease in the phosphorylation of Cdk5 substrates in the striatum, an effect that was reversed by a specific PKC inhibitor. Conversely, genetic deletion of PKC-α activity resulted in elevated basal levels of phosphorylation for Cdk5 substrates *in vivo*. Together, these findings provide convincing

evidence that the observed effects on Cdk5 targets are specific to PKC. However, it remains unclear whether PKC mediates these effects by regulating Cdk5.

There is some evidence to suggest that Cdk5 is subject to regulation by phosphorylation (247-249). However, PKC did not phosphorylate recombinant Cdk5 or p25 *in vitro*. Moreover, PKC activation *in vivo* did not result in altered p35 stability, the most commonly accepted determinant of Cdk5 activity and substrate specificity in neurons. Perhaps least expectedly, *in vitro* protein kinase activity toward a control substrate appeared unchanged for Cdk5 isolated by immunoprecipitation from striatal tissue that had been treated with PDBu. This observation is particularly difficult to explain, given the fact that in the same tissue preparation, PDBu causes a 50-85% reduction in the *in vivo* phosphorylation of at least three Cdk5 substrates.

At this point, the possibility needs to be considered that PKC does not regulate Cdk5 activity. It is important to bear in mind that the phosphorylation state of Cdk5 substrates *in vivo* is determined not by Cdk5 alone, but rather by the balance between Cdk5 and protein phosphatase activities. Either side of this equation may be subject to regulation by PKC. The Cdk5 sites on inhibitor-1 (Ser6, Ser67) and DARPP-32 (Thr75) are dephosphorylated by the type 2 protein phosphatases, PP-2A and/or PP-2B (190, 250) (Baochan Nguyen, personal communication). However, although it is reported that PP-2A and PP-2B are involved in the down-regulation of PKC activity in some systems (251-253), there is no evidence in the literature to suggest the regulation of type 2 protein phosphatases by phorbol esters or PKC. Nonetheless, future experiments need to address this issue by evaluating whether specific PP-2A or PP-2B inhibitors can reverse the effect of PDBu on the level of phosphorylation of Cdk5 substrates in the striatum. Presumably, treatment with protein phosphatase inhibitors would not produce a change if PKC were exerting its effects primarily through Cdk5. More indirectly, experiments could be conducted to assess the phosphorylation state of proteins that are PP-2A or PP-2B substrates, but not targets of Cdk5, in tissue from *Prkca*$^{-/-}$ mice as well as wild-type tissue treated with PKC activators or inhibitors.

Although the evidence presented does not support the PKC-dependent down-regulation of Cdk5 activity as an explanation for the effects of pharmacological

manipulation or genetic disruption of PKC activity on the phosphorylation of Cdk5 substrates *in vivo*, it should be noted that these results are only preliminary. The immunoprecipitation/protein kinase assay for Cdk5 activity certainly needs to be repeated, and perhaps extended to *Prkca*$^{-/-}$ tissue and/or wild-type tissue treated with PKC inhibitors. Cdk5 immunoprecipitates as a stable heterodimer with its cofactor. Therefore, this assay has been used successfully to monitor changes in Cdk5 activity due to altered cofactor metabolism (63, 242). However, it remains possible that PKC regulates Cdk5 by a mechanism that is susceptible to disruption by the challenges of tissue lysis and immunoprecipitation. Given that in these experiments PKC had no measurable effect on the levels or phosphorylation state of Cdk5 or its cofactor—presumably the only two tissue components isolated by the immunoprecipitation of Cdk5—perhaps it should not be surprising that PDBu did not detectably alter tissue Cdk5 activity as determined by the subsequent *in vitro* protein kinase assay. There is a growing body of evidence that the Cdk5/p35 heterodimer often occurs within larger protein assemblies inside the cell and these protein-protein interactions are important in the regulation of Cdk5 activity and subcellular localization (254). Thus, PKC may exert its putative effect on Cdk5 indirectly, through its actions on the cellular binding partners of Cdk5 and/or its cofactors.

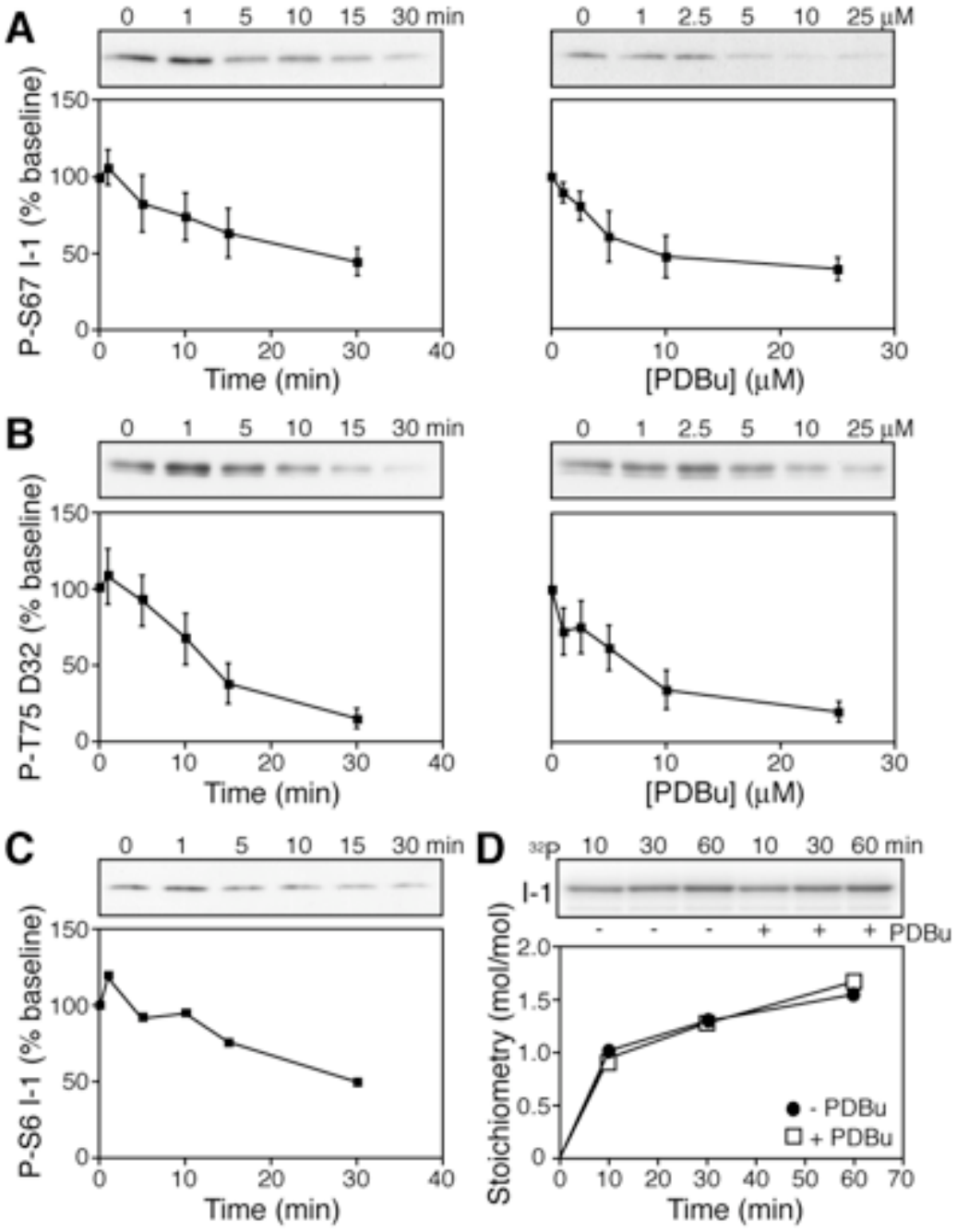
A
0 1 5 10 15 30 min
P-S67 I-1 (% baseline)
Time (min)
0 1 2.5 5 10 25 µM
[PDBu] (µM)
B
0 1 5 10 15 30 min
P-T75 D32 (% baseline)
Time (min)
0 1 2.5 5 10 25 µM
[PDBu] (µM)
C
0 1 5 10 15 30 min
P-S6 I-1 (% baseline)
Time (min)
D
32P 10 30 60 10 30 60 min
I-1
- - - + + + PDBu
Stoichiometry (mol/mol)
- PDBu
+ PDBu
Time (min)

Figure 5.1: The effect of PDBu on the phosphorylation of Cdk5 substrates in the striatum. *A.* Time-course and PDBu dose response curves of phospho-Ser67 inhibitor-1 (*I-1*) levels determined by quantitative immunoblot analysis of striatal slices treated with 5 μM PDBu for 0-30 min (left), or with 0-25 μM PDBu for 15 min (right). Data represent means ± S.E.M. for 4 time-course and 4 dose response experiments. *B.* Time-course and PDBu dose response curves of phospho-Thr75 DARPP-32 (*D32*) levels determined by quantitative immunoblot analysis of striatal slices treated as described in *A*. Data represent means ± S.E.M. for 4 time-course and 4 dose response experiments. *C.* Immunoblot analysis of phospho-Ser6 inhibitor-1 levels in striatal slices treated with 5 μM PDBu for 0-30 min. *D.* Cdk5-dependent phosphorylation of inhibitor-1 in the absence or presence of 5 μM PDBu *in vitro*. The panel shows SDS-PAGE analysis of ^{32}P-labeled inhibitor-1.

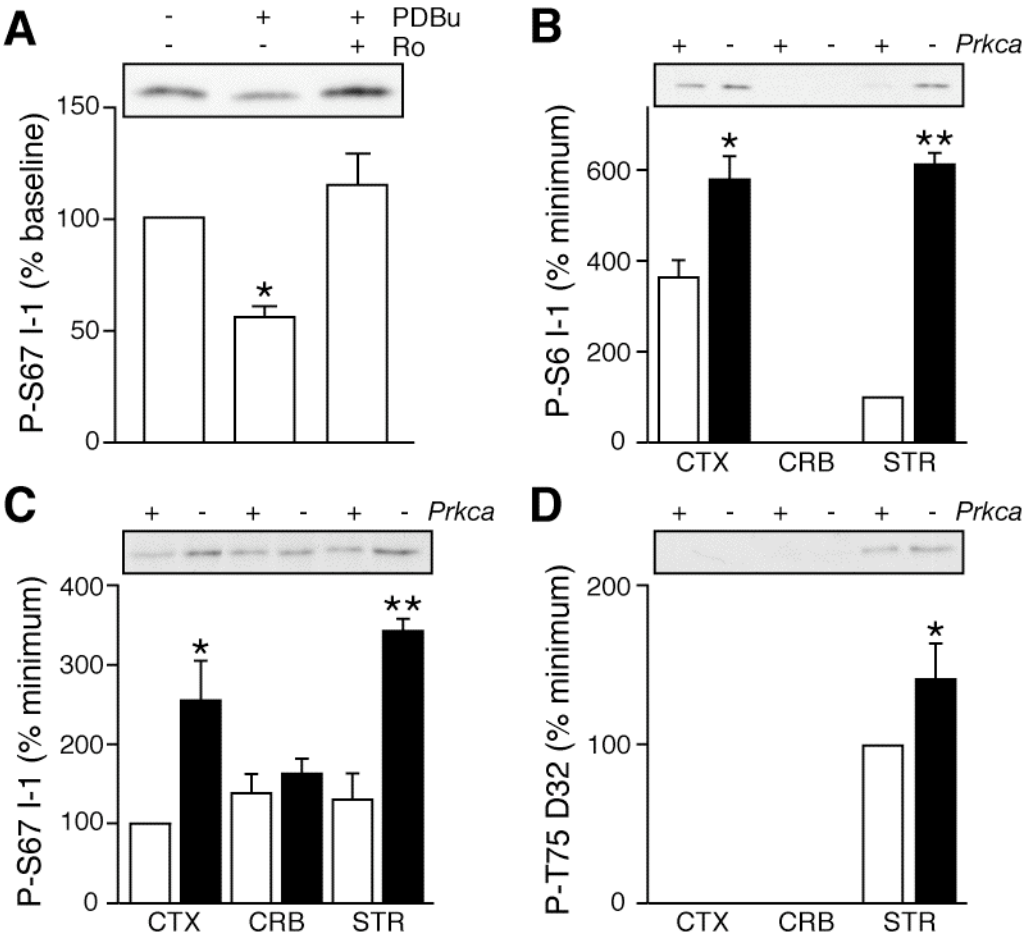
A
- + + PDBu
- - + Ro
P-S67 I-1 (% baseline)
150
100
50
0
*
B
+ - + - + - Prkca
P-S6 I-1 (% minimum)
600
400
200
0
*
**
CTX
CRB
STR
C
+ - + - + - Prkca
P-S67 I-1 (% minimum)
400
300
200
100
0
*
**
CTX
CRB
STR
D
+ - + - + - Prkca
P-T75 D32 (% minimum)
200
100
0
*
CTX
CRB
STR

Figure 5.2: The effect of pharmacological inhibition or genetic deletion of PKC on the phosphorylation of Cdk5 substrates in the brain. *A*. Quantitative immunoblot analysis of phospho-Ser67 inhibitor-1 (*I-1*) levels in striatal slices treated with PDBu (0 or 5 μM, 15 min) following incubation in the absence or presence of the PKC inhibitor, Ro-32-0432 (*Ro*, 5 μM, 60 min). *, $p < 0.001$, Student's unpaired *t* test, n = 4. *B.* Quantitative immunoblot analysis of phospho-Ser6 inhibitor-1 levels in 100 μg of total protein from wild-type (+) and *Prkca*$^{-/-}$ (-) cerebral cortex (*CTX*), cerebellum (*CRB*), and striatum (*STR*). Phospho-Ser6 inhibitor-1 levels are normalized to the mean value obtained from the tissue in which phospho-Ser6 inhibitor-1 was least abundant. *, $p < 0.02$ compared to wild-type cortex, Student's unpaired *t* test, n = 3. **, $p < 0.001$ compared to wild-type striatum, Student's unpaired *t* test, n = 3. *C.* The membranes in *B* immunoblotted and quantified for phospho-Ser67 inhibitor-1. *, $p < 0.01$ compared to wild-type cortex, Student's unpaired *t* test, n = 3. **, $p < 0.01$ compared to wild-type striatum, Student's unpaired *t* test, n = 3. *D.* The membranes in *B* immunoblotted and quantified for phospho-Thr75 DARPP-32 (*D32*). *, $p < 0.05$ compared to wild-type striatum, Student's unpaired *t* test, n = 3.

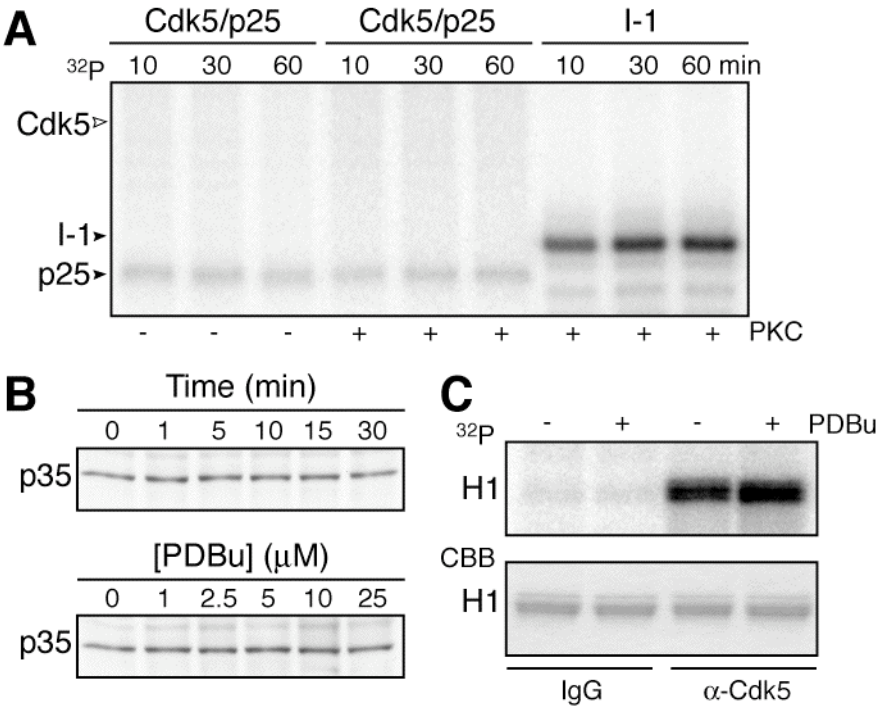

Figure 5.3: Investigation of a possible mechanism of PKC-mediated Cdk5 regulation. A. PKC-dependent phosphorylation of Cdk5/p25 and inhibitor-1 (*I-1*) *in vitro*. The panel shows SDS-PAGE analysis of Cdk5/p25 that was ^{32}P-labeled in the absence and presence of PKC. Inhibitor-1 phosphorylated by PKC was included as a control. *B*. Immunoblot analysis of p35 levels in striatal slices treated with 5 μM PDBu for 0-30 min (top), or 0-25 μM PDBu for 15 min (bottom). *C*. Phosphorylation of histone H1 by Cdk5 immunoprecipitated from the lysates of striatal slices treated with or without 5 μM PDBu for 30 min (α-*Cdk5*). In control experiments, rabbit IgG-conjugated agarose (*IgG*) pellets from the pre-clearing step were used as a source of Cdk5 activity. The panels show SDS-PAGE analysis of ^{32}P-labeled (top) and CBB-stained (bottom) histone H1.

BIBLIOGRAPHY

1. Kennelly, P. J. 1999. In *Introduction to Cellular Signal Transduction*. A. Sitaramayya, ed. Birkhauser, Boston, p. 235.
2. Fischer, E. H., and E. G. Krebs. 1955. Conversion of phosphorylase b to phosphorylase a in muscle extracts. *J Biol Chem 216:121*.
3. Krebs, E. G., and E. H. Fischer. 1956. The phosphorylase b to a converting enzyme of rabbit skeletal muscle. *Biochim Biophys Acta 20:150*.
4. Krebs, E. G., A. B. Kent, and E. H. Fischer. 1958. The muscle phosphorylase b kinase reaction. *J Biol Chem 231:73*.
5. Fischer, E. H., D. J. Graves, E. R. Crittenden, and E. G. Krebs. 1959. Structure of the site phosphorylated in the phosphorylase b to a reaction. *J Biol Chem 234:1698*.
6. Marks, F. 1996. In *Protein Phosphorylation*. F. Marks, ed. VCH Publishers Inc., New York, p. 1.
7. Hunter, T. 1995. Protein kinases and phosphatases: the yin and yang of protein phosphorylation and signaling. *Cell 80:225*.
8. Plowman, G. D., S. Sudarsanam, J. Bingham, D. Whyte, and T. Hunter. 1999. The protein kinases of Caenorhabditis elegans: a model for signal transduction in multicellular organisms. *Proc Natl Acad Sci U S A 96:13603*.
9. Manning, G., D. B. Whyte, R. Martinez, T. Hunter, and S. Sudarsanam. 2002. The protein kinase complement of the human genome. *Science 298:1912*.
10. Girault, J. A. 1993. Protein phosphorylation and dephosphorylation in mammalian central nervous system. *Neurochem Int 23:1*.
11. Tokuda, M., and O. Hatase. 1998. Regulation of neuronal plasticity in the central nervous system by phosphorylation and dephosphorylation. *Mol Neurobiol 17:137*.
12. Vaughan, P. F., J. H. Walker, and C. Peers. 1998. The regulation of neurotransmitter secretion by protein kinase C. *Mol Neurobiol 18:125*.

13. Adams, J. P., E. D. Roberson, J. D. English, J. C. Selcher, and J. D. Sweatt. 2000. MAPK regulation of gene expression in the central nervous system. *Acta Neurobiol Exp (Wars) 60:377*.

14. Selcher, J. C., E. J. Weeber, A. W. Varga, J. D. Sweatt, and M. Swank. 2002. Protein kinase signal transduction cascades in mammalian associative conditioning. *Neuroscientist 8:122*.

15. Shobe, J. 2002. The role of PKA, CaMKII, and PKC in avoidance conditioning: permissive or instructive? *Neurobiol Learn Mem 77:291*.

16. Nguyen, P. V., and N. H. Woo. 2003. Regulation of hippocampal synaptic plasticity by cyclic AMP-dependent protein kinases. *Prog Neurobiol 71:401*.

17. Yamauchi, T. 2005. Neuronal Ca2+/calmodulin-dependent protein kinase II--discovery, progress in a quarter of a century, and perspective: implication for learning and memory. *Biol Pharm Bull 28:1342*.

18. Fredholm, B. B. 1997. Adenosine and neuroprotection. *Int Rev Neurobiol 40:259*.

19. Stone, T. W. 2005. Adenosine, neurodegeneration and neuroprotection. *Neurol Res 27:161*.

20. Dunwiddie, T., V. 1999. Adenosine and suppression of seizures. *Adv Neurol. 79:1001*.

21. Sawynok, J. 1998. Adenosine receptor activation and nociception. *Eur J Pharmacol 347:1*.

22. Basheer, R., R. E. Strecker, M. M. Thakkar, and R. W. McCarley. 2004. Adenosine and sleep-wake regulation. *Prog Neurobiol 73:379*.

23. Dunwiddie, T. V., and S. A. Masino. 2001. The role and regulation of adenosine in the central nervous system. *Annu. Rev. Neurosci. 24:31*.

24. Dunwiddie, T. V. 1985. The physiological role of adenosine in the central nervous system. *Int. Rev. Neurobiol. 27:63*.

25. Fredholm, B. B., M. P. Abbracchio, G. Burnstock, J. W. Daly, T. K. Harden, K. A. Jacobson, P. Leff, and M. Williams. 1994. Nomenclature and classification of purinoceptors. *Pharmacol Rev 46:143*.

26. Fredholm, B. B., J. F. Chen, S. A. Masino, and J. M. Vaugeois. 2005. Actions of adenosine at its receptors in the CNS: insights from knockouts and drugs. *Annu Rev Pharmacol Toxicol 45:385*.

27. Strecker, R. E., S. Morairty, M. M. Thakkar, T. Porkka-Heiskanen, R. Basheer, L. J. Dauphin, D. G. Rainnie, C. M. Portas, R. W. Greene, and R. W. McCarley. 2000. Adenosinergic modulation of basal forebrain and preoptic/anterior hypothalamic neuronal activity in the control of behavioral state. *Behav. Brain Res. 115:183*.

28. Ledent, C., J. M. Vaugeois, S. N. Schiffmann, T. Pedrazzini, M. El Yacoubi, J. J. Vanderhaeghen, J. Constentin, J. K. Heath, G. Vassart, and M. Parmentier. 1997. Aggressiveness, hypoalgesia and high blood pressure in mice lacking the adenosine A2a receptor. *Nature 388:674*.

29. Fredholm, B. B., K. Battig, J. Holmen, A. Nehlig, and E. E. Zvartau. 1999. Actions of caffeine in the brain with special reference to factors that contribute to its widespread use. *Pharmacol. Rev. 51:83*.

30. Daly, J. W., P. Butts-Lamb, and W. Padgett. 1983. Subclasses of adenosine receptors in the central nervous system: interaction with caffeine and related methylxanthines. *Cell Mol Neurobiol 3:69*.

31. Bruns, R. F., G. H. Lu, and T. A. Pugsley. 1986. Characterization of the A2 adenosine receptor labeled by [3H]NECA in rat striatal membranes. *Mol Pharmacol 29:331*.

32. Jacobson, K. A., S. M. Siddiqi, M. E. Olah, X. D. Ji, N. Melman, K. Bellamkonda, Y. Meshulam, G. L. Stiles, and H. O. Kim. 1995. Structure-activity relationships of 9-alkyladenine and ribose-modified adenosine derivatives at rat A3 adenosine receptors. *J Med Chem 38:1720*.

33. Zhou, Q. Y., C. Li, M. E. Olah, R. A. Johnson, G. L. Stiles, and O. Civelli. 1992. Molecular cloning and characterization of an adenosine receptor: the A3 adenosine receptor. *Proc Natl Acad Sci U S A 89:7432*.

34. Zimmerman, H. 1992. 5' Nucleotidase: molecular structure and functional aspects. *Biochem. J. 285:345*.

35. Berne, M., H. R. Winn, and R. Rubio. 1982. The effect of inadequate oxygen supply to the brain on cerebral adenosine levels. In *Cerebral Hypoxia in the Pathogenesis of Migraine*. F. C. Rose, and W. K. Amery, eds. Pitman, London, p. 89.

36. Greene, R. W., and H. L. Haas. 1991. The electrophysiology of adenosine in the mammalian central nervous system. *Prog Neurobiol 36:329*.

37. Basheer, R., T. Porkka-Heiskanen, R. E. Strecker, M. M. Thakkar, and R. W. McCarley. 2000. Adenosine as a biological signal mediating sleepiness following prolonged wakefulness. *Biol Signals Recept 9:319*.

38. Cass, C. E., J. D. Young, and S. A. Baldwin. 1998. Recent advances in the molecular biology of nucleoside transporters of mammalian cells. *Biochem. Cell Biol. 76:761*.

39. Arch, J. R., and E. A. Newsholme. 1978. Activities and some properties of 5'-nucleotidase, adenosine kinase and adenosine deaminase in tissues of vertebrates and invertebrates in relation to the control of the concentration and the physiological role of adenosine. *Biochem. J. 174:965*.

40. Krenitsky, T. A., R. L. Miller, and J. A. Fyfe. 1974. Levels of nucleoside and nucleotide kinases in rhesus monkey tissues. *Biochem Pharmacol 23:70*.

41. Snyder, F. F., and T. Lukey. 1982. Kinetic considerations for the regulation of adenosine and deoxyadenosine metabolism in mouse and human tissues based on a thymocyte model. *Biochim Biophys Acta 696:299*.

42. Kornberg, A., and W. E. Pricer, Jr. 1951. Enzymatic phosphorylation of adenosine and 2,6-diaminopurine riboside. *J Biol Chem 193:481*.

43. Caputto, R. 1951. The enzymatic synthesis of adenylic acid; adenosinekinase. *J Biol Chem 189:801*.

44. Lindberg, B., H. Klenow, and K. Hansen. 1967. Some properties of partially purified mammalian adenosine kinase. *J Biol Chem 242:350*.

45. Spychala, J., N. S. Datta, K. Takabayashi, M. Datta, I. H. Fox, T. Gribbin, and B. S. Mitchell. 1996. Cloning of human adenosine kinase cDNA: sequence

similarity to microbial ribokinases and fructokinases. *Proc. Natl. Acad. Sci. USA 93:1232*.

46. Mathews, I. I., M. D. Erion, and S. E. Ealick. 1998. Structure of human adenosine kinase at 1.5 Å resolution. *Biochemistry 37:15607*.
47. Pak, A. A., H. L. Haas, U. K. Decking, and J. Schrader. 1994. Inhibition of adenosine kinase increases endogenous adenosine and depresses neuronal activity in hippocampal slices. *neuropharmacology 33:1049*.
48. Lloyd, H. G. E., and B. B. Fredholm. 1995. Involvement of adenosine deaminase and adenosine kinase in regulating extracellular adenosine concentration in rat hippocampal slices. *Neurochem. Int. 26:173*.
49. Arrigoni, E., D. G. Rainnie, R. W. McCarley, and R. W. Greene. 2001. Adenosine-mediated presynaptic modulation of glutamatergic transmission in the laterodorsal tegmentum. *J Neurosci. 21:1076*.
50. Brundege, J. M., and T. V. Dunwiddie. 1996. Modulation of excitatory synaptic transmission by adenosine released from single hippocampal pyramidal neurons. *J. Neurosci. 16:5603*.
51. Boison, D., L. Scheurer, V. Zumsteg, T. Rulicke, P. Litynski, B. Fowler, S. Brandner, and H. Mohler. 2002. Neonatal hepatic steatosis by disruption of the adenosine kinase gene. *Proc. Natl. Acad. Sci. USA 99:6985*.
52. Latini, S., and F. Pedata. 2001. Adenosine in the central nervous system: release mechanisms and extracellular concentrations. *J. Neurochem. 79:463*.
53. Miller, L. P., L. A. Jelovich, L. Yao, J. DaRe, B. Ugarkar, and A. C. Foster. 1996. Pre- and peristroke treatment with the adenosine kinase inhibitor, 5'-deoxyiodotubercidin, significantly reduces infarct volume after temporary occlusion of the middle cerebral artery in rats. *Neurosci. Lett. 220:73*.
54. Wiesner, J. B., B. G. Ugarkar, A. J. Castellino, J. Barankiewicz, D. P. Dumas, H. E. Gruber, A. C. Foster, and M. D. Erion. 1999. Adenosine kinase inhibitors as a novel approach to anticonvulsant therapy. *J. Pharmacol. Exp. Ther. 289:1669*.

55. Poon, A., and J. Sawynok. 1999. Antinociceptive and anti-inflammatory properties of an adenosine kinase inhibitor and an adenosine deaminase inhibitor. *Eur. J. Pharmacol. 384:123*.

56. Pawelczyk, T., M. Sakowicz, M. Podgorska, and M. Szczepanska-Konkel. 2003. Insulin induces expression of adenosine kinase gene in rat lymphocytes by signaling through the mitogen-activated protein kinase pathway. *Exp. Cell Res. 286:152*.

57. Mackiewicz, M., E. V. Nikonova, J. E. Zimmerman, R. J. Galante, L. Zhang, J. R. Cater, J. D. Geiger, and A. I. Pack. 2003. Enzymes of adenosine metabolism in the brain: diurnal rhythm and the effect of sleep deprivation. *J. Neurochem. 85:348*.

58. Alanko, L., S. Heiskanen, D. Stenberg, and T. Porkka-Heiskanen. 2003. Adenosine kinase and 5'-nucleotidase activity after prolonged wakefulness in the cortex and the basal forebrain of rat. *Neurochem. Int. 42:449*.

59. Gouder, N., L. Scheurer, J. M. Fritschy, and D. Boison. 2004. Overexpression of adenosine kinase in epileptic hippocampus contributes to epileptogenesis. *J. Neurosci. 24:692*.

60. Fedele, D. E., N. Gouder, M. Guttinger, L. Gabernet, L. Scheurer, T. Rulicke, F. Crestani, and D. Boison. 2005. Astrogliosis in epilepsy leads to overexpression of adenosine kinase, resulting in seizure aggravation. *Brain 128:2383*.

61. Kaczmarek, L. K., K. R. Jennings, F. Strumwasser, A. C. Nairn, U. Walter, F. D. Wilson, and P. Greengard. 1980. Microinjection of catalytic subunit of cyclic AMP-dependent protein kinase enhances calcium action potentials of bag cell neurons in cell culture. *Proc. Natl. Acad. Sci. USA 77:7487*.

62. Woodgett, J. R., and T. Hunter. 1987. Isolation and characterization of two distinct forms of protein kinase C. *J. Biol. Chem. 262:4836*.

63. Saito, T., R. Onuki, Y. Fujita, G. Kusakawa, K. Ishiguro, J. A. Bibb, T. Kishimoto, and S. Hisanaga. 2003. Developmental regulation of the proteolysis of the p35 cyclin-dependent kinase 5 activator by phosphorylation. *J Neurosci 23:1189*.

64. Spychala, J., and B. S. Mitchell. 2002. Cyclosporin A and FK506 decrease adenosine kinase activity and adenosine uptake in T-lymphocytes. *J. Lab. Clin. Med. 140:84*.

65. Huang, F. L., and W. H. Glinsmann. 1976. Separation and characterization of two phosphorylase phosphatase inhibitors from rabbit skeletal muscle. *Eur. J. Biochem. 70:419*.

66. Bibb, J. A., A. Nishi, J. P. O'Callaghan, G. L. Snyder, A. Horiuchi, L. M., J. Ule, S. L. Pelech, L. Meijer, T. Saito, T. Hisanaga, A. J. Czernik, A. C. Nairn, and P. Greengard. 2001. Phosphorylation of Protein Phosphatase Inhibitor-1by Cdk5. *J. Biol. Chem. 276:14490*.

67. de Jonge, H. R., and O. M. Rosen. 1977. Self-phosphorylation of cyclic guanosine 3':5'-monophosphate-dependent protein kinase from bovine lung. Effect of cyclic adenosine 3':5'-monophosphate, cyclic guanosine 3':5'-monophosphate and histone. *J. Biol. Chem. 252:2780*.

68. Schatzman, R. C., R. L. Raynor, R. B. Fritz, and J. F. Kuo. 1983. Purification to homogeneity, characterization and monoclonal antibodies of phospholipid-sensitive Ca2+-dependent protein kinase from spleen. *Biochem. J. 209:435*.

69. Campbell, D. G., D. G. Hardie, and P. R. Vulliet. 1986. Identification of four phosphorylation sites in the N-terminal region of tyrosine hydroxylase. *J. Biol. Chem. 261:10489*.

70. Desdouits, F., J. C. Siciliano, P. Greengard, and J. A. Girault. 1995. Dopamine- and cAMP-regulated phosphoprotein DARPP-32: Phosphorylation of Ser-137 by casein kinase I inhibits dephosphorylation of Thr-34 by calcineurin. *Proc. Natl. Acad. Sci. USA 92:2682*.

71. Girault, J. A., H. C. Hemmings, Jr., K. R. Williams, A. C. Nairn, and P. Greengard. 1989. Phosphorylation of DARPP-32, a dopamine- and cAMP-regulated phosphoprotein, by casein kinase II. *J. Biol. Chem. 264:21748*.

72. Bibb, J. A., G. L. Snyder, A. Nishi, Z. Yan, L. Meijer, A. A. Fienberg, L. H. Tsai, Y. T. Kwon, J. A. Girault, A. J. Czernik, R. L. Huganir, H. C. Hemmings, Jr., A.

C. Nairn, and P. Greengard. 1999. Phosphorylation of DARPP-32 by Cdk5 modulates dopamine signalling in neurons. *Nature 402:669*.

73. Strausberg, R. L., E. A. Feingold, L. H. Grouse, J. G. Derge, R. D. Klausner, F. S. Collins, L. Wagner, C. M. Shenmen, G. D. Schuler, S. F. Altschul, B. Zeeberg, K. H. Buetow, C. F. Schaefer, N. K. Bhat, R. F. Hopkins, H. Jordan, T. Moore, S. I. Max, J. Wang, F. Hsieh, L. Diatchenko, K. Marusina, A. A. Farmer, G. M. Rubin, L. Hong, M. Stapleton, M. B. Soares, M. F. Bonaldo, T. L. Casavant, T. E. Scheetz, M. J. Brownstein, T. B. Usdin, S. Toshiyuki, P. Carninci, C. Prange, S. S. Raha, N. A. Loquellano, G. J. Peters, R. D. Abramson, S. J. Mullahy, S. A. Bosak, P. J. McEwan, K. J. McKernan, J. A. Malek, P. H. Gunaratne, S. Richards, K. C. Worley, S. Hale, A. M. Garcia, L. J. Gay, S. W. Hulyk, D. K. Villalon, D. M. Muzny, E. J. Sodergren, X. Lu, R. A. Gibbs, J. Fahey, E. Helton, M. Ketteman, A. Madan, S. Rodrigues, A. Sanchez, M. Whiting, A. Madan, A. C. Young, Y. Shevchenko, G. G. Bouffard, R. W. Blakesley, J. W. Touchman, E. D. Green, M. C. Dickson, A. C. Rodriguez, J. Grimwood, J. Schmutz, R. M. Myers, Y. S. Butterfield, M. I. Krzywinski, U. Skalska, D. E. Smailus, A. Schnerch, J. E. Schein, S. J. Jones, and M. A. Marra. 2002. Generation and initial analysis of more than 15,000 full-length human and mouse cDNA sequences. *Proc Natl Acad Sci U S A 99:16899*.

74. McNally, T., R. J. Helfrich, M. Cowart, S. A. Dorwin, J. L. Meuth, K. B. Idler, K. A. Klute, R. L. Simmer, E. A. Kowaluk, and D. N. Halbert. 1997. Cloning and expression of the adenosine kinase gene from rat and human tissues. *Biochem. Biophys. Res. Commun. 231:645*.

75. Kishimoto, A., K. Nishiyama, H. Nakanishi, Y. Uratsuji, H. Nomura, Y. Takeyama, and Y. Nishizuka. 1985. Studies on the phosphorylation of myelin basic protein by protein kinase C and adenosine 3':5'-monophosphate-dependent protein kinase. *J. Biol. Chem. 260:12492*.

76. Ackerman, S. H., and A. Tzagoloff. 2005. Function, structure, and biogenesis of mitochondrial ATP synthase. *Prog Nucleic Acid Res Mol Biol 80:95*.

77. Bijur, G. N., and R. S. Jope. 2003. Rapid accumulation of Akt in mitochondria following phosphatidylinositol 3-kinase activation. *J Neurochem 87:1427*.

78. Sakowicz, M., M. Grden, and T. Pawelczyk. 2001. Expression level of adenosine kinase in rat tissues. Lack of phosphate effect on the enzyme activity. *Acta Biochim. Pol. 48:745*.

79. Rodriguez, P., B. Mitton, and E. G. Kranias. 2005. Phosphorylation of glutathione-S-transferase by protein kinase C-alpha implications for affinity-tag purification. *Biotechnol Lett 27:1869*.

80. Sidorova, M. P., L. E. Ermakova, N. E. Kotel'nikova, and N. P. Kudina. 2001. Electrosurface properties of microcrystalline cellulose of different origin in 1:1 electrolyte solutions. *Colloid Journal 63:100*.

81. Snyder, S. H., J. J. Katims, Z. Annau, R. F. Bruns, and J. W. Daly. 1981. Adenosine receptors and behavioral actions of methylxanthines. *Proc Natl Acad Sci U S A 78:3260*.

82. Akbar, M., F. Okajima, H. Tomura, S. Shimegi, and Y. Kondo. 1994. A single species of A1 adenosine receptor expressed in Chinese hamster ovary cells not only inhibits cAMP accumulation but also stimulates phospholipase C and arachidonate release. *Mol Pharmacol 45:1036*.

83. Freund, S., M. Ungerer, and M. J. Lohse. 1994. A1 adenosine receptors expressed in CHO-cells couple to adenylate cyclase and to phospholipase C. *Naunyn Schmiedebergs Arch Pharmacol 350:49*.

84. Jockers, R., M. E. Linder, M. Hohenegger, C. Nanoff, B. Bertin, A. D. Strosberg, S. Marullo, and M. Freissmuth. 1994. Species difference in the G protein selectivity of the human and bovine A1-adenosine receptor. *J Biol Chem 269:32077*.

85. Olah, M. E. 1997. Identification of A2a adenosine receptor domains involved in selective coupling to Gs. Analysis of chimeric A1/A2a adenosine receptors. *J Biol Chem 272:337*.

86. Kull, B., P. Svenningsson, and B. B. Fredholm. 2000. Adenosine A(2A) receptors are colocalized with and activate g(olf) in rat striatum. *Mol Pharmacol 58:771*.

87. Corvol, J. C., J. M. Studler, J. S. Schonn, J. A. Girault, and D. Herve. 2001. Galpha(olf) is necessary for coupling D1 and A2a receptors to adenylate cyclase in the striatum. *J Neurochem 76:1585*.

88. Herve, D., C. Le Moine, J. C. Corvol, L. Belluscio, C. Ledent, A. A. Fienberg, M. Jaber, J. M. Studler, and J. A. Girault. 2001. Galpha(olf) levels are regulated by receptor usage and control dopamine and adenosine action in the striatum. *J Neurosci 21:4390*.

89. Ochiishi, T., L. Chen, A. Yukawa, Y. Saitoh, Y. Sekino, T. Arai, H. Nakata, and H. Miyamoto. 1999. Cellular localization of adenosine A1 receptors in rat forebrain: immunohistochemical analysis using adenosine A1 receptor-specific monoclonal antibody. *J Comp Neurol 411:301*.

90. Okada, M., K. Mizuno, and S. Kaneko. 1996. Adenosine A1 and A2 receptors modulate extracellular dopamine levels in rat striatum. *Neurosci Lett 212:53*.

91. Flagmeyer, I., H. L. Haas, and D. R. Stevens. 1997. Adenosine A1 receptor-mediated depression of corticostriatal and thalamostriatal glutamatergic synaptic potentials in vitro. *Brain Res 778:178*.

92. Brown, S. J., S. James, M. Reddington, and P. J. Richardson. 1990. Both A1 and A2a purine receptors regulate striatal acetylcholine release. *J Neurochem 55:31*.

93. Fredholm, B. B., and T. V. Dunwiddie. 1988. How does adenosine inhibit transmitter release? *Trends Pharmacol Sci 9:130*.

94. Alexander, S. P., and M. Reddington. 1989. The cellular localization of adenosine receptors in rat neostriatum. *Neuroscience 28:645*.

95. Ferre, S., B. B. Fredholm, M. Morelli, P. Popoli, and K. Fuxe. 1997. Adenosine-dopamine receptor-receptor interactions as an integrative mechanism in the basal ganglia. *Trends Neurosci 20:482*.

96. Schiffmann, S. N., F. Libert, G. Vassart, and J. J. Vanderhaeghen. 1991. Distribution of adenosine A2 receptor mRNA in the human brain. *Neurosci Lett 130:177*.

97. Schiffmann, S. N., O. Jacobs, and J. J. Vanderhaeghen. 1991. Striatal restricted adenosine A2 receptor (RDC8) is expressed by enkephalin but not by substance P neurons: an in situ hybridization histochemistry study. *J Neurochem 57:1062*.

98. Fink, J. S., D. R. Weaver, S. A. Rivkees, R. A. Peterfreund, A. E. Pollack, E. M. Adler, and S. M. Reppert. 1992. Molecular cloning of the rat A2 adenosine receptor: selective co-expression with D2 dopamine receptors in rat striatum. *Brain Res Mol Brain Res 14:186*.

99. Hettinger, B. D., A. Lee, J. Linden, and D. L. Rosin. 2001. Ultrastructural localization of adenosine A2A receptors suggests multiple cellular sites for modulation of GABAergic neurons in rat striatum. *J Comp Neurol 431:331*.

100. Rosin, D. L., B. D. Hettinger, A. Lee, and J. Linden. 2003. Anatomy of adenosine A2A receptors in brain: morphological substrates for integration of striatal function. *Neurology 61:S12*.

101. Ferre, S., G. von Euler, B. Johansson, B. B. Fredholm, and K. Fuxe. 1991. Stimulation of high-affinity adenosine A2 receptors decreases the affinity of dopamine D2 receptors in rat striatal membranes. *Proc Natl Acad Sci U S A 88:7238*.

102. Fuxe, K., S. Ferre, M. Zoli, and L. F. Agnati. 1998. Integrated events in central dopamine transmission as analyzed at multiple levels. Evidence for intramembrane adenosine A2A/dopamine D2 and adenosine A1/dopamine D1 receptor interactions in the basal ganglia. *Brain Res Brain Res Rev 26:258*.

103. Fuxe, K., S. Ferre, M. Canals, M. Torvinen, A. Terasmaa, D. Marcellino, S. R. Goldberg, W. Staines, K. X. Jacobsen, C. Lluis, A. S. Woods, L. F. Agnati, and R. Franco. 2005. Adenosine A2A and dopamine D2 heteromeric receptor complexes and their function. *J Mol Neurosci 26:209*.

104. Barraco, R. A., K. A. Martens, M. Parizon, and H. J. Normile. 1993. Adenosine A2a receptors in the nucleus accumbens mediate locomotor depression. *Brain Res Bull 31:397*.

105. Kanda, T., M. J. Jackson, L. A. Smith, R. K. Pearce, J. Nakamura, H. Kase, Y. Kuwana, and P. Jenner. 1998. Adenosine A2A antagonist: a novel antiparkinsonian agent that does not provoke dyskinesia in parkinsonian monkeys. *Ann Neurol 43:507*.

106. El Yacoubi, M., C. Ledent, J. F. Menard, M. Parmentier, J. Costentin, and J. M. Vaugeois. 2000. The stimulant effects of caffeine on locomotor behaviour in mice are mediated through its blockade of adenosine A(2A) receptors. *Br J Pharmacol 129:1465*.

107. Huang, Z. L., W. M. Qu, N. Eguchi, J. F. Chen, M. A. Schwarzschild, B. B. Fredholm, Y. Urade, and O. Hayaishi. 2005. Adenosine A2A, but not A1, receptors mediate the arousal effect of caffeine. *Nat Neurosci 8:858*.

108. Lieberman, H. R., W. J. Tharion, B. Shukitt-Hale, K. L. Speckman, and R. Tulley. 2002. Effects of caffeine, sleep loss, and stress on cognitive performance and mood during U.S. Navy SEAL training. Sea-Air-Land. *Psychopharmacology (Berl) 164:250*.

109. Fredholm, B. B. 1995. Astra Award Lecture. Adenosine, adenosine receptors and the actions of caffeine. *Pharmacol Toxicol 76:93*.

110. Johansson, B., L. Halldner, T. V. Dunwiddie, S. A. Masino, W. Poelchen, L. Gimenez-Llort, R. M. Escorihuela, A. Fernandez-Teruel, Z. Wiesenfeld-Hallin, X. J. Xu, A. Hardemark, C. Betsholtz, E. Herlenius, and B. B. Fredholm. 2001. Hyperalgesia, anxiety, and decreased hypoxic neuroprotection in mice lacking the adenosine A1 receptor. *Proc Natl Acad Sci U S A 98:9407*.

111. Salmi, P., K. Chergui, and B. B. Fredholm. 2005. Adenosine-dopamine interactions revealed in knockout mice. *J Mol Neurosci 26:239*.

112. Nagatsu, T., M. Levitt, and S. Udenfriend. 1964. Tyrosine Hydroxylase. The Initial Step In Norepinephrine Biosynthesis. *J Biol Chem 239:2910*.

113. Ueda, T., and P. Greengard. 1977. Adenosine 3':5'-monophosphate-regulated phosphoprotein system of neuronal membranes. I. Solubilization, purification, and some properties of an endogenous phosphoprotein. *J Biol Chem 252:5155*.

114. De Camilli, P., R. Cameron, and P. Greengard. 1983. Synapsin I (protein I), a nerve terminal-specific phosphoprotein. I. Its general distribution in synapses of the central and peripheral nervous system demonstrated by immunofluorescence in frozen and plastic sections. *J Cell Biol 96:1337*.

115. Moriyoshi, K., M. Masu, T. Ishii, R. Shigemoto, N. Mizuno, and S. Nakanishi. 1991. Molecular cloning and characterization of the rat NMDA receptor. *Nature 354:31*.

116. Monyer, H., R. Sprengel, R. Schoepfer, A. Herb, M. Higuchi, H. Lomeli, N. Burnashev, B. Sakmann, and P. H. Seeburg. 1992. Heteromeric NMDA receptors: molecular and functional distinction of subtypes. *Science 256:1217*.

117. Hollmann, M., A. O'Shea-Greenfield, S. W. Rogers, and S. Heinemann. 1989. Cloning by functional expression of a member of the glutamate receptor family. *Nature 342:643*.

118. Boulter, J., M. Hollmann, A. O'Shea-Greenfield, M. Hartley, E. Deneris, C. Maron, and S. Heinemann. 1990. Molecular cloning and functional expression of glutamate receptor subunit genes. *Science 249:1033*.

119. Allen, P. B., C. C. Ouimet, and P. Greengard. 1997. Spinophilin, a novel protein phosphatase 1 binding protein localized to dendritic spines. *Proc Natl Acad Sci U S A 94:9956*.

120. Walaas, S. I., D. W. Aswad, and P. Greengard. 1983. A dopamine- and cyclic AMP-regulated phosphoprotein enriched in dopamine-innervated brain regions. *Nature 301:69*.

121. Montminy, M. R., and L. M. Bilezikjian. 1987. Binding of a nuclear protein to the cyclic-AMP response element of the somatostatin gene. *Nature 328:175*.

122. Campbell, D. G., D. G. Hardie, and P. R. Vulliet. 1986. Identification of four phosphorylation sites in the N-terminal region of tyrosine hydroxylase. *J Biol Chem 261:10489*.

123. Wu, J., D. Filer, A. J. Friedhoff, and M. Goldstein. 1992. Site-directed mutagenesis of tyrosine hydroxylase. Role of serine 40 in catalysis. *J Biol Chem 267:25754*.

124. Czernik, A. J., D. T. Pang, and P. Greengard. 1987. Amino acid sequences surrounding the cAMP-dependent and calcium/calmodulin-dependent phosphorylation sites in rat and bovine synapsin I. *Proc Natl Acad Sci U S A 84:7518*.

125. Hosaka, M., R. E. Hammer, and T. C. Sudhof. 1999. A phospho-switch controls the dynamic association of synapsins with synaptic vesicles. *Neuron 24:377*.

126. Tingley, W. G., M. D. Ehlers, K. Kameyama, C. Doherty, J. B. Ptak, C. T. Riley, and R. L. Huganir. 1997. Characterization of protein kinase A and protein kinase C phosphorylation of the N-methyl-D-aspartate receptor NR1 subunit using phosphorylation site-specific antibodies. *J Biol Chem 272:5157*.

127. Scott, D. B., T. A. Blanpied, and M. D. Ehlers. 2003. Coordinated PKA and PKC phosphorylation suppresses RXR-mediated ER retention and regulates the surface delivery of NMDA receptors. *Neuropharmacology 45:755*.

128. Roche, K. W., R. J. O'Brien, A. L. Mammen, J. Bernhardt, and R. L. Huganir. 1996. Characterization of multiple phosphorylation sites on the AMPA receptor GluR1 subunit. *Neuron 16:1179*.

129. Hsieh-Wilson, L. C., F. Benfenati, G. L. Snyder, P. B. Allen, A. C. Nairn, and P. Greengard. 2003. Phosphorylation of spinophilin modulates its interaction with actin filaments. *J Biol Chem 278:1186*.

130. Hemmings, H. C., Jr., P. Greengard, H. Y. Tung, and P. Cohen. 1984. DARPP-32, a dopamine-regulated neuronal phosphoprotein, is a potent inhibitor of protein phosphatase-1. *Nature 310:503*.

131. Gonzalez, G. A., and M. R. Montminy. 1989. Cyclic AMP stimulates somatostatin gene transcription by phosphorylation of CREB at serine 133. *Cell 59:675*.

132. Thiel, G., A. J. Czernik, F. Gorelick, A. C. Nairn, and P. Greengard. 1988. Ca2+/calmodulin-dependent protein kinase II: identification of threonine-286 as

the autophosphorylation site in the alpha subunit associated with the generation of Ca2+-independent activity. *Proc Natl Acad Sci U S A 85:6337*.

133. Strack, S., M. A. Barban, B. E. Wadzinski, and R. J. Colbran. 1997. Differential inactivation of postsynaptic density-associated and soluble Ca2+/calmodulin-dependent protein kinase II by protein phosphatases 1 and 2A. *J Neurochem 68:2119*.

134. Blitzer, R. D., J. H. Connor, G. P. Brown, T. Wong, S. Shenolikar, R. Iyengar, and E. M. Landau. 1998. Gating of CaMKII by cAMP-regulated protein phosphatase activity during LTP. *Science 280:1940*.

135. Anderson, N. G., J. L. Maller, N. K. Tonks, and T. W. Sturgill. 1990. Requirement for integration of signals from two distinct phosphorylation pathways for activation of MAP kinase. *Nature 343:651*.

136. Payne, D. M., A. J. Rossomando, P. Martino, A. K. Erickson, J. H. Her, J. Shabanowitz, D. F. Hunt, M. J. Weber, and T. W. Sturgill. 1991. Identification of the regulatory phosphorylation sites in pp42/mitogen-activated protein kinase (MAP kinase). *Embo J 10:885*.

137. Gomez, N., and P. Cohen. 1991. Dissection of the protein kinase cascade by which nerve growth factor activates MAP kinases. *Nature 353:170*.

138. Crews, C. M., A. Alessandrini, and R. L. Erikson. 1992. The primary structure of MEK, a protein kinase that phosphorylates the ERK gene product. *Science 258:478*.

139. Charest, D. L., G. Mordret, K. W. Harder, F. Jirik, and S. L. Pelech. 1993. Molecular cloning, expression, and characterization of the human mitogen-activated protein kinase p44erk1. *Mol Cell Biol 13:4679*.

140. Roberson, E. D., J. D. English, J. P. Adams, J. C. Selcher, C. Kondratick, and J. D. Sweatt. 1999. The mitogen-activated protein kinase cascade couples PKA and PKC to cAMP response element binding protein phosphorylation in area CA1 of hippocampus. *J Neurosci 19:4337*.

141. Kanterewicz, B. I., N. N. Urban, D. B. McMahon, E. D. Norman, L. J. Giffen, M. F. Favata, P. A. Scherle, J. M. Trzskos, G. Barrionuevo, and E. Klann. 2000. The

extracellular signal-regulated kinase cascade is required for NMDA receptor-independent LTP in area CA1 but not area CA3 of the hippocampus. *J Neurosci 20:3057*.

142. Yuan, L. L., J. P. Adams, M. Swank, J. D. Sweatt, and D. Johnston. 2002. Protein kinase modulation of dendritic K+ channels in hippocampus involves a mitogen-activated protein kinase pathway. *J Neurosci 22:4860*.

143. Snyder, G. L., J. A. Girault, J. Y. Chen, A. J. Czernik, J. W. Kebabian, J. A. Nathanson, and P. Greengard. 1992. Phosphorylation of DARPP-32 and protein phosphatase inhibitor-1 in rat choroid plexus: regulation by factors other than dopamine. *J Neurosci 12:3071*.

144. Ouimet, C. C., P. E. Miller, H. C. Hemmings, Jr., S. I. Walaas, and P. Greengard. 1984. DARPP-32, a dopamine- and adenosine 3':5'-monophosphate-regulated phosphoprotein enriched in dopamine-innervated brain regions. III. Immunocytochemical localization. *J Neurosci 4:111*.

145. Hayashi, K., Y. Pan, H. Shu, J. W. Kansy, C. L. White, C. A. Tamminga, A. Sobel, P. A. Curmi, and J. A. Bibb. 2006. Phosphorylation of the tubulin binding protein stathmin by Cdk5 and MAP kinases in the brain. *J Neurochem, in final revision*.

146. Svenningsson, P., C. Le Moine, G. Fisone, and B. B. Fredholm. 1999. Distribution, biochemistry and function of striatal adenosine A2A receptors. *Prog Neurobiol 59:355*.

147. Wirkner, K., Z. Gerevich, T. Krause, A. Gunther, L. Koles, D. Schneider, W. Norenberg, and P. Illes. 2004. Adenosine A2A receptor-induced inhibition of NMDA and GABAA receptor-mediated synaptic currents in a subpopulation of rat striatal neurons. *Neuropharmacology 46:994*.

148. Gerevich, Z., K. Wirkner, and P. Illes. 2002. Adenosine A2A receptors inhibit the N-methyl-D-aspartate component of excitatory synaptic currents in rat striatal neurons. *Eur J Pharmacol 451:161*.

149. Svenningsson, P., M. Lindskog, F. Rognoni, B. B. Fredholm, P. Greengard, and G. Fisone. 1998. Activation of adenosine A2A and dopamine D1 receptors

stimulates cyclic AMP-dependent phosphorylation of DARPP-32 in distinct populations of striatal projection neurons. *Neuroscience 84:223*.

150. Uematsu, K., M. Futter, L. C. Hsieh-Wilson, H. Higashi, H. Maeda, A. C. Nairn, P. Greengard, and A. Nishi. 2005. Regulation of spinophilin Ser94 phosphorylation in neostriatal neurons involves both DARPP-32-dependent and independent pathways. *J Neurochem 95:1642*.

151. Norenberg, W., K. Wirkner, and P. Illes. 1997. Effect of adenosine and some of its structural analogues on the conductance of NMDA receptor channels in a subset of rat neostriatal neurones. *Br J Pharmacol 122:71*.

152. Norenberg, W., K. Wirkner, H. Assmann, M. Richter, and P. Illes. 1998. Adenosine A2A receptors inhibit the conductance of NMDA receptor channels in rat neostriatal neurons. *Amino Acids 14:33*.

153. Popoli, P., A. Pintor, M. R. Domenici, C. Frank, M. T. Tebano, A. Pezzola, L. Scarchilli, D. Quarta, R. Reggio, F. Malchiodi-Albedi, M. Falchi, and M. Massotti. 2002. Blockade of striatal adenosine A2A receptor reduces, through a presynaptic mechanism, quinolinic acid-induced excitotoxicity: possible relevance to neuroprotective interventions in neurodegenerative diseases of the striatum. *J Neurosci 22:1967*.

154. Popoli, P., C. Frank, M. T. Tebano, R. L. Potenza, A. Pintor, M. R. Domenici, V. Nazzicone, A. Pezzola, and R. Reggio. 2003. Modulation of glutamate release and excitotoxicity by adenosine A2A receptors. *Neurology 61:S69*.

155. Tebano, M. T., A. Pintor, C. Frank, M. R. Domenici, A. Martire, R. Pepponi, R. L. Potenza, R. Grieco, and P. Popoli. 2004. Adenosine A2A receptor blockade differentially influences excitotoxic mechanisms at pre- and postsynaptic sites in the rat striatum. *J Neurosci Res 77:100*.

156. Domenici, M. R., R. Pepponi, A. Martire, M. T. Tebano, R. L. Potenza, and P. Popoli. 2004. Permissive role of adenosine A2A receptors on metabotropic glutamate receptor 5 (mGluR5)-mediated effects in the striatum. *J Neurochem 90:1276*.

157. Choe, E. S., E. H. Shin, and J. Q. Wang. 2006. Regulation of phosphorylation of NMDA receptor NR1 subunits in the rat neostriatum by group I metabotropic glutamate receptors in vivo. *Neurosci Lett 394:246*.

158. Hakansson, K., S. Galdi, J. Hendrick, G. Snyder, P. Greengard, and G. Fisone. 2006. Regulation of phosphorylation of the GluR1 AMPA receptor by dopamine D2 receptors. *J Neurochem 96:482*.

159. Chiang, M. C., Y. C. Lee, C. L. Huang, and Y. Chern. 2005. cAMP-response element-binding protein contributes to suppression of the A2A adenosine receptor promoter by mutant Huntingtin with expanded polyglutamine residues. *J Biol Chem 280:14331*.

160. Sexl, V., G. Mancusi, C. Holler, E. Gloria-Maercker, W. Schutz, and M. Freissmuth. 1997. Stimulation of the mitogen-activated protein kinase via the A2A-adenosine receptor in primary human endothelial cells. *J Biol Chem 272:5792*.

161. Seidel, M. G., M. Klinger, M. Freissmuth, and C. Holler. 1999. Activation of mitogen-activated protein kinase by the A(2A)-adenosine receptor via a rap1-dependent and via a p21(ras)-dependent pathway. *J Biol Chem 274:25833*.

162. Schulte, G., and B. B. Fredholm. 2000. Human adenosine A(1), A(2A), A(2B), and A(3) receptors expressed in Chinese hamster ovary cells all mediate the phosphorylation of extracellular-regulated kinase 1/2. *Mol Pharmacol 58:477*.

163. Canals, M., E. Angulo, V. Casado, E. I. Canela, J. Mallol, F. Vinals, W. Staines, B. Tinner, J. Hillion, L. Agnati, K. Fuxe, S. Ferre, C. Lluis, and R. Franco. 2005. Molecular mechanisms involved in the adenosine A1 and A2A receptor-induced neuronal differentiation in neuroblastoma cells and striatal primary cultures. *J Neurochem 92:337*.

164. Kennelly, P. J. 2001. Protein phosphatases--a phylogenetic perspective. *Chem Rev 101:2291*.

165. Fauman, E. B., and M. A. Saper. 1996. Structure and function of the protein tyrosine phosphatases. *Trends Biochem Sci 21:413*.

166. Barford, D. 1996. Molecular mechanisms of the protein serine/threonine phosphatases. *Trends Biochem Sci 21:407*.

167. Morrison, D. K., M. S. Murakami, and V. Cleghon. 2000. Protein kinases and phosphatases in the Drosophila genome. *J Cell Biol 150:F57*.

168. Cohen, P. T. 2002. Protein phosphatase 1--targeted in many directions. *J Cell Sci 115:241*.

169. Ceulemans, H., W. Stalmans, and M. Bollen. 2002. Regulator-driven functional diversification of protein phosphatase-1 in eukaryotic evolution. *Bioessays 24:371*.

170. Huang, F. L., and W. H. Glinsmann. 1976. Separation and characterization of two phosphorylase phosphatase inhibitors from rabbit skeletal muscle. *Eur J Biochem 70:419*.

171. Elbrecht, A., J. DiRenzo, R. G. Smith, and S. Shenolikar. 1990. Molecular cloning of protein phosphatase inhibitor-1 and its expression in rat and rabbit tissues. *J Biol Chem 265:13415*.

172. Sikes, S., and S. Shenolikar. 2005. Protein phosphatase inhibitor-1, an amplifier of cAMP signals. *Cellsci Rev 2:175*.

173. Cohen, P., G. A. Nimmo, S. Shenolikar, and J. G. Foulkes. 1978. *FEBS Symp 54:161*.

174. Nimmo, G. A., and P. Cohen. 1978. The regulation of glycogen metabolism. Purification and characterisation of protein phosphatase inhibitor-1 from rabbit skeletal muscle. *Eur J Biochem 87:341*.

175. Foulkes, J. G., S. J. Strada, P. J. Henderson, and P. Cohen. 1983. A kinetic analysis of the effects of inhibitor-1 and inhibitor-2 on the activity of protein phosphatase-1. *Eur J Biochem 132:309*.

176. Cohen, P. 1989. The structure and regulation of protein phosphatases. *Annu Rev Biochem 58:453*.

177. Shenolikar, S., and A. C. Nairn. 1991. Protein phosphatases: recent progress. *Adv Second Messenger Phosphoprotein Res 23:1*.

178. Mulkey, R. M., S. Endo, S. Shenolikar, and R. C. Malenka. 1994. Involvement of a calcineurin/inhibitor-1 phosphatase cascade in hippocampal long-term depression. *Nature 369:486*.

179. MacDougall, L. K., D. G. Campbell, M. J. Hubbard, and P. Cohen. 1989. Partial structure and hormonal regulation of rabbit liver inhibitor-1; distribution of inhibitor-1 and inhibitor-2 in rabbit and rat tissues. *Biochim Biophys Acta 1010:218*.

180. Allen, P. B., O. Hvalby, V. Jensen, M. L. Errington, M. Ramsay, F. A. Chaudhry, T. V. Bliss, J. Storm-Mathisen, R. G. Morris, P. Andersen, and P. Greengard. 2000. Protein phosphatase-1 regulation in the induction of long-term potentiation: heterogeneous molecular mechanisms. *J Neurosci 20:3537*.

181. Carr, A. N., A. G. Schmidt, Y. Suzuki, F. del Monte, Y. Sato, C. Lanner, K. Breeden, S. L. Jing, P. B. Allen, P. Greengard, A. Yatani, B. D. Hoit, I. L. Grupp, R. J. Hajjar, A. A. DePaoli-Roach, and E. G. Kranias. 2002. Type 1 phosphatase, a negative regulator of cardiac function. *Mol Cell Biol 22:4124*.

182. El-Armouche, A., T. Rau, O. Zolk, D. Ditz, T. Pamminger, W. H. Zimmermann, E. Jackel, S. E. Harding, P. Boknik, J. Neumann, and T. Eschenhagen. 2003. Evidence for protein phosphatase inhibitor-1 playing an amplifier role in beta-adrenergic signaling in cardiac myocytes. *Faseb J 17:437*.

183. Pathak, A., F. del Monte, W. Zhao, J. E. Schultz, J. N. Lorenz, I. Bodi, D. Weiser, H. Hahn, A. N. Carr, F. Syed, N. Mavila, L. Jha, J. Qian, Y. Marreez, G. Chen, D. W. McGraw, E. K. Heist, J. L. Guerrero, A. A. DePaoli-Roach, R. J. Hajjar, and E. G. Kranias. 2005. Enhancement of cardiac function and suppression of heart failure progression by inhibition of protein phosphatase 1. *Circ Res 96:756*.

184. Gustafson, E. L., J. A. Girault, H. C. Hemmings, Jr., A. C. Nairn, and P. Greengard. 1991. Immunocytochemical localization of phosphatase inhibitor-1 in rat brain. *J Comp Neurol 310:170*.

185. Gupta, R. C., S. Mishra, S. Rastogi, M. Imai, O. Habib, and H. N. Sabbah. 2003. Cardiac SR-coupled PP1 activity and expression are increased and inhibitor 1

protein expression is decreased in failing hearts. *Am J Physiol Heart Circ Physiol 285:H2373*.

186. Desdouits, F., D. Cohen, A. C. Nairn, P. Greengard, and J. A. Girault. 1995. Phosphorylation of DARPP-32, a dopamine- and cAMP-regulated phosphoprotein, by casein kinase I in vitro and in vivo. *J Biol Chem 270:8772*.

187. Girault, J. A., H. C. Hemmings, Jr., K. R. Williams, A. C. Nairn, and P. Greengard. 1989. Phosphorylation of DARPP-32, a dopamine- and cAMP-regulated phosphoprotein, by casein kinase II. *J Biol Chem 264:21748*.

188. Bibb, J. A., G. L. Snyder, A. Nishi, Z. Yan, L. Meijer, A. A. Fienberg, L. H. Tsai, Y. T. Kwon, J. A. Girault, A. J. Czernik, R. L. Huganir, H. C. Hemmings, Jr., A. C. Nairn, and P. Greengard. 1999. Phosphorylation of DARPP-32 by Cdk5 modulates dopamine signalling in neurons. *Nature 402:669*.

189. Aitken, A., T. Bilham, and P. Cohen. 1982. Complete primary structure of protein phosphatase inhibitor-1 from rabbit skeletal muscle. *Eur J Biochem 126:235*.

190. Bibb, J. A., A. Nishi, J. P. O'Callaghan, J. Ule, M. Lan, G. L. Snyder, A. Horiuchi, T. Saito, S. Hisanaga, A. J. Czernik, A. C. Nairn, and P. Greengard. 2001. Phosphorylation of protein phosphatase inhibitor-1 by Cdk5. *J Biol Chem 276:14490*.

191. Braz, J. C., K. Gregory, A. Pathak, W. Zhao, B. Sahin, R. Klevitsky, T. F. Kimball, J. N. Lorenz, A. C. Nairn, S. B. Liggett, I. Bodi, S. Wang, A. Schwartz, E. G. Lakatta, A. A. DePaoli-Roach, J. Robbins, T. E. Hewett, J. A. Bibb, M. V. Westfall, E. G. Kranias, and J. D. Molkentin. 2004. PKC-alpha regulates cardiac contractility and propensity toward heart failure. *Nat Med 10:248*.

192. Czernik, A. J., J. Mathers, K. Tsou, P. Greengard, and S. M. Mische. 1997. Phosphorylation state-specific antibodies: Preparation and application. In *Regulatory Protein Modification*, Vol. Neuromethods vol. 30. H. C. H. Jr., ed. Humana, Totowa, NJ, p. 219.

193. Braz, J. C., O. F. Bueno, L. J. De Windt, and J. D. Molkentin. 2002. PKC alpha regulates the hypertrophic growth of cardiomyocytes through extracellular signal-regulated kinase1/2 (ERK1/2). *J Cell Biol 156:905*.

194. Nishi, A., G. L. Snyder, A. C. Nairn, and P. Greengard. 1999. Role of calcineurin and protein phosphatase-2A in the regulation of DARPP-32 dephosphorylation in neostriatal neurons. *J Neurochem 72:2015*.

195. Lovinger, D. M., and E. Tyler. 1996. Synaptic transmission and modulation in the neostriatum. *Int Rev Neurobiol 39:77*.

196. Pi, Y., D. Zhang, K. R. Kemnitz, H. Wang, and J. W. Walker. 2003. Protein kinase C and A sites on troponin I regulate myofilament Ca2+ sensitivity and ATPase activity in the mouse myocardium. *J Physiol 552:845*.

197. Coe, I. R., L. Yao, I. Diamond, and A. S. Gordon. 1996. The role of protein kinase C in cellular tolerance to ethanol. *J Biol Chem 271:29468*.

198. Francesconi, A., and R. M. Duvoisin. 2000. Opposing effects of protein kinase C and protein kinase A on metabotropic glutamate receptor signaling: selective desensitization of the inositol trisphosphate/Ca2+ pathway by phosphorylation of the receptor-G protein-coupling domain. *Proc Natl Acad Sci U S A 97:6185*.

199. Shea, T. B., M. L. Beermann, U. Leli, and R. A. Nixon. 1992. Opposing influences of protein kinase activities on neurite outgrowth in human neuroblastoma cells: initiation by kinase A and restriction by kinase C. *J Neurosci Res 33:398*.

200. Li, M. X., M. Jia, H. Jiang, V. Dunlap, and P. G. Nelson. 2001. Opposing actions of protein kinase A and C mediate Hebbian synaptic plasticity. *Nat Neurosci 4:871*.

201. Miles, K., D. T. Anthony, L. L. Rubin, P. Greengard, and R. L. Huganir. 1987. Regulation of nicotinic acetylcholine receptor phosphorylation in rat myotubes by forskolin and cAMP. *Proc Natl Acad Sci U S A 84:6591*.

202. Safran, A., C. Provenzano, R. Sagi-Eisenberg, and S. Fuchs. 1990. Phosphorylation of membrane-bound acetylcholine receptor by protein kinase C: characterization and subunit specificity. *Biochemistry 29:6730*.

203. Nelson, P. G., M. A. Lanuza, M. Jia, M. X. Li, and J. Tomas. 2003. Phosphorylation reactions in activity-dependent synapse modification at the neuromuscular junction during development. *J Neurocytol 32:803*.

204. Moss, S. J., C. A. Doherty, and R. L. Huganir. 1992. Identification of the cAMP-dependent protein kinase and protein kinase C phosphorylation sites within the major intracellular domains of the beta 1, gamma 2S, and gamma 2L subunits of the gamma-aminobutyric acid type A receptor. *J Biol Chem 267:14470*.

205. Poisbeau, P., M. C. Cheney, M. D. Browning, and I. Mody. 1999. Modulation of synaptic GABAA receptor function by PKA and PKC in adult hippocampal neurons. *J Neurosci 19:674*.

206. Liu, Q. R., P. W. Zhang, Z. Lin, Q. F. Li, A. S. Woods, J. Troncoso, and G. R. Uhl. 2004. GBPI, a novel gastrointestinal- and brain-specific PP1-inhibitory protein, is activated by PKC and inactivated by PKA. *Biochem J 377:171*.

207. Liu, Q. R., J. P. Gong, and G. R. Uhl. 2005. Families of protein phosphatase 1 modulators activated by protein kinases a and C: focus on brain. *Prog Nucleic Acid Res Mol Biol 79:371*.

208. Zachariou, V., M. Benoit-Marand, P. B. Allen, P. Ingrassia, A. A. Fienberg, F. Gonon, P. Greengard, and M. R. Picciotto. 2002. Reduction of cocaine place preference in mice lacking the protein phosphatase 1 inhibitors DARPP 32 or Inhibitor 1. *Biol Psychiatry 51:612*.

209. Genoux, D., U. Haditsch, M. Knobloch, A. Michalon, D. Storm, and I. M. Mansuy. 2002. Protein phosphatase 1 is a molecular constraint on learning and memory. *Nature 418:970*.

210. Weiser, D. C., S. Sikes, S. Li, and S. Shenolikar. 2004. The inhibitor-1 C terminus facilitates hormonal regulation of cellular protein phosphatase-1: functional implications for inhibitor-1 isoforms. *J Biol Chem 279:48904*.

211. Ikebe, M., D. J. Hartshorne, and M. Elzinga. 1986. Identification, phosphorylation, and dephosphorylation of a second site for myosin light chain kinase on the 20,000-dalton light chain of smooth muscle myosin. *J Biol Chem 261:36*.

212. Ikebe, M., and D. J. Hartshorne. 1985. Phosphorylation of smooth muscle myosin at two distinct sites by myosin light chain kinase. *J Biol Chem 260:10027*.

213. White, M. F., S. E. Shoelson, H. Keutmann, and C. R. Kahn. 1988. A cascade of tyrosine autophosphorylation in the beta-subunit activates the phosphotransferase of the insulin receptor. *J Biol Chem 263:2969*.

214. Simmerman, H. K., J. H. Collins, J. L. Theibert, A. D. Wegener, and L. R. Jones. 1986. Sequence analysis of phospholamban. Identification of phosphorylation sites and two major structural domains. *J Biol Chem 261:13333*.

215. Mayer, E. J., W. Huckle, R. G. Johnson, Jr., and E. McKenna. 2000. Characterization and quantitation of phospholamban and its phosphorylation state using antibodies. *Biochem Biophys Res Commun 267:40*.

216. Tsai, L.-H., I. Delalle, V. S. Caviness Jr., T. Chae, and E. Harlow. 1994. p35 is a neural-specific regulatory subunit of cyclin-dependent kinase 5. *Nature 371:419*.

217. Tang, D., J. Yeung, K. Y. Lee, M. Matsushita, H. Matsui, K. Tomizawa, O. Hatase, and J. H. Wang. 1995. An isoform of the neuronal cyclin-dependent kinase 5 (Cdk5) activator. *J Biol Chem 270:26897*.

218. Ohshima, T., J. M. Ward, C.-G. Huh, G. Longenecker, Veeranna, H. C. Pant, R. O. Brady, L. J. Martin, and A. B. Kulkarni. 1996. Targeted disruption of the cyclin-dependent kinase 5 gene results in abnormal corticogenesis, neuronal pathology and perinatal death. *Proc. Natl. Acad. Sci. USA 93:11173*.

219. Gilmore, E. C., T. Ohshima, A. M. Goffinet, A. B. Kulkarni, and K. Herrup. 1998. Cyclin-dependent kinase 5-deficient mice demonstrate novel developmental arrest in cerebral cortex. *J Neurosci 18:6370*.

220. Ko, J., S. Humbert, R. T. Bronson, S. Takahashi, A. B. Kulkarni, E. Li, and L. H. Tsai. 2001. p35 and p39 are essential for cyclin-dependent kinase 5 function during neurodevelopment. *J Neurosci 21:6758*.

221. Chae, T., Y. T. Kwon, R. Bronson, P. Dikkes, E. Li, and L. H. Tsai. 1997. Mice lacking p35, a neuronal specific activator of Cdk5, display cortical lamination defects, seizures, and adult lethality. *Neuron 18:29*.

222. Kusakawa, G., T. Saito, R. Onuki, K. Ishiguro, T. Kishimoto, and S. Hisanaga. 2000. Calpain-dependent proteolytic cleavage of the p35 cyclin-dependent kinase 5 activator to p25. *J Biol Chem 275:17166*.

223. Patzke, H., and L. H. Tsai. 2002. Calpain-mediated cleavage of the cyclin-dependent kinase-5 activator p39 to p29. *J Biol Chem 277:8054*.

224. Patrick, G. N., L. Zukerberg, M. Nikolic, S. de la Monte, P. Dikkes, and L. H. Tsai. 1999. Conversion of p35 to p25 deregulates Cdk5 activity and promotes neurodegeneration. *Nature 402:615*.

225. Hashiguchi, M., T. Saito, S. Hisanaga, and T. Hashiguchi. 2002. Truncation of CDK5 activator p35 induces intensive phosphorylation of Ser202/Thr205 of human tau. *J Biol Chem 277:44525*.

226. Zheng, M., C. L. Leung, and R. K. Liem. 1998. Region-specific expression of cyclin-dependent kinase 5 (cdk5) and its activators, p35 and p39, in the developing and adult rat central nervous system. *J Neurobiol 35:141*.

227. Green, S. L., K. S. Kulp, and R. Vulliet. 1997. Cyclin-dependent protein kinase 5 activity increases in rat brain following ischemia. *Neurochem Int 31:617*.

228. Hayashi, T., H. Warita, K. Abe, and Y. Itoyama. 1999. Expression of cyclin-dependent kinase 5 and its activator p35 in rat brain after middle cerebral artery occlusion. *Neurosci Lett 265:37*.

229. Henchcliffe, C., and R. E. Burke. 1997. Increased expression of cyclin-dependent kinase 5 in induced apoptotic neuron death in rat substantia nigra. *Neurosci Lett 230:41*.

230. Neystat, M., M. Rzhetskaya, T. F. Oo, N. Kholodilov, O. Yarygina, A. Wilson, B. F. El-Khodor, and R. E. Burke. 2001. Expression of cyclin-dependent kinase 5 and its activator p35 in models of induced apoptotic death in neurons of the substantia nigra in vivo. *J Neurochem 77:1611*.

231. Matsubara, M., M. Kusubata, K. Ishiguro, T. Uchida, K. Titani, and H. Taniguchi. 1996. Site-specific phosphorylation of synapsin I by mitogen-activated protein kinase and Cdk5 and its effects on physiological functions. *J Biol Chem 271:21108*.

232. Tomizawa, K., J. Ohta, M. Matsushita, A. Moriwaki, S. T. Li, K. Takei, and H. Matsui. 2002. Cdk5/p35 regulates neurotransmitter release through phosphorylation and downregulation of P/Q-type voltage-dependent calcium channel activity. *J Neurosci 22:2590*.

233. Floyd, S. R., E. B. Porro, V. I. Slepnev, G. C. Ochoa, L. H. Tsai, and P. De Camilli. 2001. Amphiphysin 1 binds the cyclin-dependent kinase (cdk) 5 regulatory subunit p35 and is phosphorylated by cdk5 and cdc2. *J Biol Chem 276:8104*.

234. Tan, T. C., V. A. Valova, C. S. Malladi, M. E. Graham, L. A. Berven, O. J. Jupp, G. Hansra, S. J. McClure, B. Sarcevic, R. A. Boadle, M. R. Larsen, M. A. Cousin, and P. J. Robinson. 2003. Cdk5 is essential for synaptic vesicle endocytosis. *Nat Cell Biol 5:701*.

235. Tomizawa, K., S. Sunada, Y. F. Lu, Y. Oda, M. Kinuta, T. Ohshima, T. Saito, F. Y. Wei, M. Matsushita, S. T. Li, K. Tsutsui, S. Hisanaga, K. Mikoshiba, K. Takei, and H. Matsui. 2003. Cophosphorylation of amphiphysin I and dynamin I by Cdk5 regulates clathrin-mediated endocytosis of synaptic vesicles. *J Cell Biol 163:813*.

236. Lee, S. Y., M. R. Wenk, Y. Kim, A. C. Nairn, and P. De Camilli. 2004. Regulation of synaptojanin 1 by cyclin-dependent kinase 5 at synapses. *Proc Natl Acad Sci U S A 101:546*.

237. Li, B. S., M. K. Sun, L. Zhang, S. Takahashi, W. Ma, L. Vinade, A. B. Kulkarni, R. O. Brady, and H. C. Pant. 2001. Regulation of NMDA receptors by cyclin-dependent kinase-5. *Proc Natl Acad Sci U S A 98:12742*.

238. Wang, J., S. Liu, Y. Fu, J. H. Wang, and Y. Lu. 2003. Cdk5 activation induces hippocampal CA1 cell death by directly phosphorylating NMDA receptors. *Nat Neurosci 6:1039*.

239. Morabito, M. A., M. Sheng, and L. H. Tsai. 2004. Cyclin-dependent kinase 5 phosphorylates the N-terminal domain of the postsynaptic density protein PSD-95 in neurons. *J Neurosci 24:865*.

240. Hisanaga, S., and T. Saito. 2003. The regulation of cyclin-dependent kinase 5 activity through the metabolism of p35 or p39 Cdk5 activator. *Neurosignals 12:221*.

241. Patrick, G. N., P. Zhou, Y. T. Kwon, P. M. Howley, and L. H. Tsai. 1998. p35, the neuronal-specific activator of cyclin-dependent kinase 5 (Cdk5) is degraded by the ubiquitin-proteasome pathway. *J Biol Chem 273:24057*.

242. Wei, F. Y., K. Tomizawa, T. Ohshima, A. Asada, T. Saito, C. Nguyen, J. A. Bibb, K. Ishiguro, A. B. Kulkarni, H. C. Pant, K. Mikoshiba, H. Matsui, and S. Hisanaga. 2005. Control of cyclin-dependent kinase 5 (Cdk5) activity by glutamatergic regulation of p35 stability. *J Neurochem 93:502*.

243. Kerokoski, P., T. Suuronen, A. Salminen, H. Soininen, and T. Pirttila. 2002. Influence of phosphorylation of p35, an activator of cyclin-dependent kinase 5 (cdk5), on the proteolysis of p35. *Brain Res Mol Brain Res 106:50*.

244. Nath, R., M. Davis, A. W. Probert, N. C. Kupina, X. Ren, G. P. Schielke, and K. K. Wang. 2000. Processing of cdk5 activator p35 to its truncated form (p25) by calpain in acutely injured neuronal cells. *Biochem Biophys Res Commun 274:16*.

245. Lee, M. S., Y. T. Kwon, M. Li, J. Peng, R. M. Friedlander, and L. H. Tsai. 2000. Neurotoxicity induces cleavage of p35 to p25 by calpain. *Nature 405:360*.

246. Kerokoski, P., T. Suuronen, A. Salminen, H. Soininen, and T. Pirttila. 2004. Both N-methyl-D-aspartate (NMDA) and non-NMDA receptors mediate glutamate-induced cleavage of the cyclin-dependent kinase 5 (cdk5) activator p35 in cultured rat hippocampal neurons. *Neurosci Lett 368:181*.

247. Sharma, P., M. Sharma, N. D. Amin, R. W. Albers, and H. C. Pant. 1999. Regulation of cyclin-dependent kinase 5 catalytic activity by phosphorylation. *Proc Natl Acad Sci U S A 96:11156*.

248. Zukerberg, L. R., G. N. Patrick, M. Nikolic, S. Humbert, C. L. Wu, L. M. Lanier, F. B. Gertler, M. Vidal, R. A. Van Etten, and L. H. Tsai. 2000. Cables links Cdk5 and c-Abl and facilitates Cdk5 tyrosine phosphorylation, kinase upregulation, and neurite outgrowth. *Neuron 26:633*.

249. Liu, F., X. H. Ma, J. Ule, J. A. Bibb, A. Nishi, A. J. DeMaggio, Z. Yan, A. C. Nairn, and P. Greengard. 2001. Regulation of cyclin-dependent kinase 5 and casein kinase 1 by metabotropic glutamate receptors. *Proc Natl Acad Sci U S A 98:11062*.

250. Nishi, A., J. A. Bibb, G. L. Snyder, H. Higashi, A. C. Nairn, and P. Greengard. 2000. Amplification of dopaminergic signalling by a novel positive feedback loop. *Submitted*.

251. Hansra, G., F. Bornancin, R. Whelan, B. A. Hemmings, and P. J. Parker. 1996. 12-O-Tetradecanoylphorbol-13-acetate-induced dephosphorylation of protein kinase Calpha correlates with the presence of a membrane-associated protein phosphatase 2A heterotrimer. *J Biol Chem 271:32785*.

252. Ricciarelli, R., and A. Azzi. 1998. Regulation of recombinant PKC alpha activity by protein phosphatase 1 and protein phosphatase 2A. *Arch Biochem Biophys 355:197*.

253. Lum, H., J. L. Podolski, M. E. Gurnack, I. T. Schulz, F. Huang, and O. Holian. 2001. Protein phosphatase 2B inhibitor potentiates endothelial PKC activity and barrier dysfunction. *Am J Physiol Lung Cell Mol Physiol 281:L546*.

254. Lim, A. C., D. Qu, and R. Z. Qi. 2003. Protein-protein interactions in Cdk5 regulation and function. *Neurosignals 12:230*.

VITAE

Bogachan Sahin was born in Birmingham, England, on June 5, 1976, the son of Fusun Sahin and Hasan Sahin. After completing his secondary education at Robert College of Istanbul, Turkey in 1994, he entered Princeton University, Princeton, New Jersey. He received the degree of Bachelor of Arts in Molecular Biology from Princeton University in June, 1998. While an undergraduate, he had the opportunity to work with Arnold J. Levine at Princeton University. In July, 1998, he entered the Medical Scientist Training Program at the University of Texas Southwestern Medical Center at Dallas, Texas. After completing two years of medical school, he began his graduate work in the laboratory of James A. Bibb, Ph.D. and defended his dissertation in May, 2006. He was awarded the degrees of Doctor of Medicine and Doctor of Philosophy in May, 2008.

Permanent Address: Kartaltepe Mah., Terakki Cad.
Esenova Apt. No. 23/5
Bakirkoy, Istanbul 34740
Turkey